

Notes on Quantum Field Theory II

Marco Serone

SISSA, via Bonomea 265, I-34136 Trieste, Italy

Last update: September 8, 2025

Contents

1	Introduction	4
2	Quantum field theory and critical phenomena	6
2.1	Phase transitions	7
2.2	Mean field theory	10
2.3	QFT description of critical phenomena	15
3	Large N in QFT	19
3.1	Matrix models	19
3.2	Vector models	27
4	Kinks, vortices, and monopoles	34
4.1	Homotopy groups and topological invariants	35
4.2	General considerations and a scaling argument for field configurations	38
4.3	Kinks in 1+1 dimensions	41
4.4	The 3d vortex	47
4.5	Monopoles in $4d$	50
4.6	Charge fractionalization in presence of fermions	54
4.7	Chiral fermions from magnetic flux on S^2	56
4.7.1	Spinors in curved space-times: vielbein formalism	57
4.7.2	Fermions on S^2	58
5	Instantons	62
5.1	Quantum mechanics	63
5.1.1	Harmonic oscillator	63
5.1.2	Symmetric double wells	67
5.1.3	Periodic potentials	71
5.2	Instantons in $4d$ non-abelian gauge theories	72
5.2.1	Theta vacua	78
5.2.2	Fermions in instanton background and a non-perturbative anomaly	80
5.2.3	Witten effect and dyons	82

5.2.4	Topologically non-trivial configurations in the Higgs phase	84
5.3	Bounces and vacuum decay	85
5.3.1	Metastability of the Standard Model	89
6	Phases of gauge theories	93
6.1	Wilson and 't Hooft Lines	94
6.2	Symmetries as topological operators	97
6.2.1	Higher-form symmetries	100
6.3	Phases of abelian and non-abelian gauge theories	105
6.3.1	Abelian gauge theories	106
6.3.2	Yang-Mills theory	107
6.3.3	Yang-Mills theory with fundamental matter	108
6.3.4	Yang-Mills theory with adjoint matter	109
6.4	Generalized 't Hooft anomaly matching conditions	109
6.4.1	A mixed $U(1)^{(1)} \times U(1)^{(1)}$ 't Hooft anomaly in Maxwell theory	111
6.4.2	A \mathbb{Z}_2 anomaly in quantum mechanics	112
6.4.3	't Hooft anomalies and charge fractionalization	114
6.4.4	$SU(N)$ Yang-Mills theory at $\theta = \pi$	115

Chapter 1

Introduction

These are the lecture notes for the SISSA Quantum Field Theory II (QFT II) course which follows after QFT I. The notes *do assume* that the reader has a good knowledge of the topics covered in the QFT I course.

While QFT I is mostly devoted to the study of fields which are weakly interacting, QFT II focus mostly on non-perturbative phenomena, which are invisible in ordinary perturbation theory. Needless to say, it is much harder to describe non-perturbative phenomena than perturbative ones. For this reason it is useful to also study QFTs in $d < 4$ space-time dimensions, where analytic results are more often available. QFTs in $d < 4$ are interesting for a variety of reasons. First, they can be seen as toy models of $4d$ models of which they share some common phenomenon. Understanding the phenomenon in the $d < 4$ model can be useful for its understanding in the $4d$ model. Notable examples are $2d$ QFTs which undergo a chiral symmetry breaking and a dynamical mass generation, like $4d$ QCD, but are amenable of an analytic treatment. Second, $4d$ theories can have defects, strings, domain walls, etc, whose dynamics is described by an effective QFT in $d < 4$. Last, but not least, QFT is a basic tool to describe not only phenomena in particle physics, but also in statistical and condensed matter physics. In particular, critical phenomena in statistical physics are described by Euclidean QFTs. In this case, d is the dimension of space (and not of space-time), and hence $d = 3$ is the most interesting case.

These notes are structured as follows.

We start in chapter 2 by discussing the relation between QFT and critical phenomena. We define phase transitions, discuss the mean field theory approximation, and see how a QFT arises as a universal effective, long distance, description of some statistical theory. The focus is mostly on explaining how QFT can be used in statistical physics, but no concrete model is studied. In Chapter 3 we introduce the large N expansion. This is a tremendously useful perturbative expansion, which in certain cases allows us to get results which are non-perturbative when expressed in terms of the ordinary coupling expansion. We discuss large N for so called matrix and vector QFTs. Chapter 4 is devoted to the study of extended field configurations which are not ordinary particles, i.e. are not small fluctuations around the vacuum. We discuss the relevance

of topology for their stability and focus on three classes of configurations: kinks in $2d$, vortices in $3d$, and monopoles in $4d$. Some other effects when fermions are present are also discussed. In chapter 5 we discuss instantons and bounces, extended Euclidean field configurations with finite action. Instantons give rise to tunneling between degenerate vacua, while bounces govern the decay amplitude of a meta-stable vacuum in QFT. We consider instantons in quantum mechanics and in $4d$ gauge theories. Chapter 6 is dedicated to a description of the possible phases of $4d$ gauge theories. Some attention is paid to the global structure of the gauge group, exemplified in a comparison between $SU(N)$ and $PSU(N)$ gauge theories. At the cost of being a bit more abstract, we introduce a modern classification in terms of higher-form symmetries and discuss generalized 't Hooft anomaly matching conditions. This is motivated by the recent intense activity and development in the subject which is bringing to an extension of the notion of symmetries (and anomalies) in QFT.

Mathematical background necessary to follow the lectures will be sprinkled through the course, but some basic knowledge of differential geometry and group theory (at the level of the SISSA “Differential Geometry and Group theory” course) is assumed.

Three assignments, essential parts of the QFT II course, are *included* in the notes in a boxed text. Some other comments are also boxed. The notes are far from being comprehensive. Due to lack of time, several important topics are not covered (notably lattice gauge theories) and applications to low dimensional QFTs are minimal.

We recommend [1] for readers that want to deepen the connection between statistical physics and QFT, in particular regarding the RG flow. For large N an old but evergreen reference is the paper [2]. There is by now an impressive number of more or less advanced QFT textbooks describing perturbative phenomena, less so for textbook focusing on non-perturbative phenomena. A classic reference for instantons in quantum mechanics and bounces are the lectures by Coleman [3], which include also a nice discussion of the $1/N$ expansion. We recommend [4] for a nice and pedagogical discussion of kinks, vortices, monopoles and instantons, with an emphasis on their coupling to fermions. A nice overview on solitons and instantons, which emphasizes their physical consequences and also includes a discussion of gauge theory phases, can be found in [5]. For a more in-depth and technical discussion of kinks, vortices, monopoles and instantons we refer to [6]. The perspective of considering gauge theory phases by looking at global higher-form global symmetries is relatively recent [7]. See e.g. [8] for a recent review on generalized global symmetries which, in addition to higher-form symmetries, discusses also so called non-invertible symmetries.

These notes are *preliminary* and surely contain many typos, imprecisions, etc. We hope that the students will help us in improving the notes and in spotting the many mistakes in there.

Chapter 2

Quantum field theory and critical phenomena

Quantum field theory is the fundamental tool we use today to understand and describe high energy physics. It evolved over decades in the effort to unify special relativity and quantum mechanics. As a matter of fact, QFT over the years turned out to be also a fundamental tool in statistical physics to describe second-order classical thermal phase transitions. More than that, important developments in QFT occurred in that context, notably the development of the renormalization group by K. Wilson.

Aim of this chapter is show how QFT can be used to describe second-order phase transitions and how several familiar concepts we learned in the context of high energy physics acquire a new perspective in this context. A key important difference between the two frameworks is that in the study of classical thermal phase transitions we assume that thermal equilibrium is achieved, and hence we study static quantities. The QFTs in question are naturally defined in Euclidean space (ordinary space, no time), in contrast to the Lorentzian QFTs in high energy physics. Most of the techniques we use in high energy physics can be recycled, with almost no effort, in statistical physics. In the study of critical phenomena the QFT often arises as an approximate description at large distances, the underlying UV theory being e.g. defined on a lattice. The focus is mostly on IR properties of the system and their universalities, typical of second-order phase transition. Close to the transition, the QFT becomes scale invariant and approaches a conformal field theory (CFT). Due to lack of time, we only touch upon this wide and interesting topic, which deserves an entire course on its own.

We start in section 2.1 by reviewing basic notions such as phase transitions, order parameters, and critical exponents. In section 2.2 we introduce the mean field approximation and discuss it within the context of the Ising model. In section 2.3 we show how the Ising model at large distances is well approximated by a scalar field theory. We then comment on how RG flow techniques in QFT are useful to determine the critical exponents.

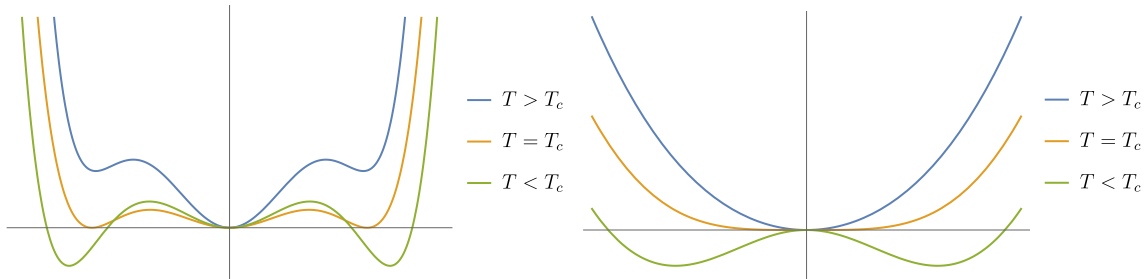


Figure 2.1: Cartoon of a generic first-order (left) and second-order (right) phase transition as the temperature T varies. The horizontal and vertical axis represents an unspecified order parameter and thermodynamic quantity.

2.1 Phase transitions

Phase transitions refer to a qualitative change of matter as one (or more) parameters are varied. They generally arise because of collective phenomena which occur at scales much larger than the microscopic scales defining the material, usually of atomic size. The emergent scale close to a phase transition is denoted correlation length ξ . A notable parameter governing the transition is the temperature T of the system. Examples of phase transitions are the liquid to vapour or the ferromagnetic to paramagnetic transition, as T increases. The phase transition occurs at a critical temperature T_c . Phase transitions as T varies arise because of a competing effect of energy minimization, which typically favors ordered phases, and entropy maximization, which favours disordered phases. An important characterization of phase transitions is their order. We denote by first order the phase transitions where at $T = T_c$ the two phases of matter may coexist together. In this case several thermodynamical quantities are discontinuous and a latent heat is present. Importantly, the correlation length ξ remains finite during a first-order phase transition. Phase transitions with no latent heat and coexistence of phases are of second order. See figure 2.1 for an artistic view of the difference between a first and a second order phase transition. Crucially, as T approaches the critical temperature T_c , the correlation length ξ diverges and collective phenomena occur at very large scales. The system becomes scale invariant at $T = T_c$, in fact conformal invariant. In addition of being the starting and ending points of renormalization group flows in QFTs,

- Conformal Field Theories describe second-order phase transitions in critical phenomena.

We are mostly interested in second-order phase transitions because they show the phenomenon of universality. In this case the two phases can generally be distinguished by looking at the global symmetries of the system, according to the Landau-Ginzburg criterion. We define an *order parameter*, a quantity which usually vanishes in the unbroken phase (also denoted disordered phase) and is non-zero in the broken one (also denoted ordered phase).

Phase transitions occurring in changes of states of matter (from solid to liquid, etc.) are generally of first order. We report as example the phase diagram of water in figure 2.2 as a

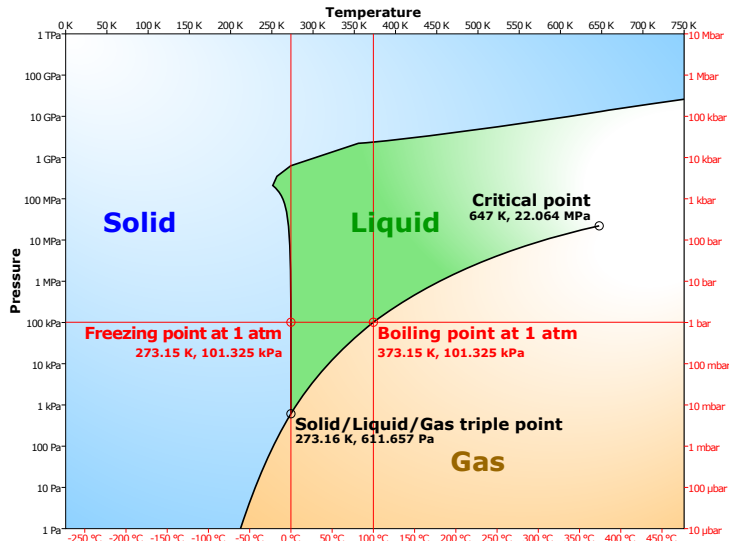


Figure 2.2: Phase diagram of water as a function of temperature and pressure. Picture taken from Wikipedia.

function of T and pressure P . The black lines indicate where the (first order) phase transition occurs in the $T - P$ plane. Note that the line of first-order, liquid to vapor, phase transitions end at a point (denoted as critical point in the figure). At that point the transition becomes of second-order. We see that past the critical point the liquid to vapor phases are continuously connected to each other. Whenever two phases are connected in this way, the transition is called a cross-over. A notable example of second-order phase transition is the ferromagnetic to paramagnetic transition.

Second-order phase transitions of different physical systems turn out to be related and described by a few parameters, which depend only on basic properties, such as the global symmetries involved in the transition or the dimensionality of space. The universality in question is understood in terms of RG evolution. Different physical systems can flow to the same CFT. An example of universality is provided by the critical point of the water-to-vapor and the uniaxial paramagnetic to ferromagnetic transitions. Despite the two phenomena are manifestly distinct, close to the critical point they are both described by the CFT of the three dimensional Ising model. In modern terms, the relevant parameters governing the transition correspond to the anomalous dimensions of certain operators in the CFT. Historically, empirical parameters denoted critical exponents were introduced to describe the leading singular behaviour of various quantities as T approaches T_c . For simplicity, we introduce critical exponents in the context of ferromagnets, indicating with m the magnetization (the order parameter) and with h the external magnetic field. The six critical exponents α , β , γ , δ , ν , η govern the behaviour of the component of a thermodynamical quantity which is singular at $T = T_c$, neglecting possibly

regular terms. They are defined as

$$\begin{aligned}
C(t) &\sim |t|^{-\alpha}, & (h = 0) \\
m(t) &\sim (-t)^\beta, & (t < 0, h = 0) \\
\chi(t) &\sim |t|^{-\gamma}, & (h = 0) \\
h(m) &\sim |m|^\delta, & (t = 0) \\
\xi(t) &\sim |t|^{-\nu}, & (h = 0) \\
G_2(r) &\sim r^{2-d-\eta}, & (h = t = 0).
\end{aligned} \tag{2.1.1}$$

In (2.1.1)

$$t = \frac{T - T_c}{T_c} \tag{2.1.2}$$

represents the relative deviation from the critical temperature T_c , $C = \partial E / \partial T$ is the specific heat, $\chi = \partial m / \partial h$ is the susceptibility, and G_2 is the connected two-point function of the magnetization, which represents the local fluctuations of m between two points separated by a distance r . In the last relation, d is the dimension of space. Only two out of these six exponents are independent. Using dimensional analysis and scaling symmetry, one can show that

$$\begin{aligned}
\alpha + 2\beta + \gamma &= 2, & \gamma &= \beta(\delta - 1), \\
\gamma &= \nu(2 - \eta), & \nu d &= 2 - \alpha.
\end{aligned} \tag{2.1.3}$$

Macroscopic objects are composed of a large number of particles which interact in a non-trivial way. Of course, we do not need to keep track of such interactions, as the key properties are governed by thermodynamics and statistical physics. In particular, for ergodic systems in thermal equilibrium, we sum over all possible microscopic configurations \mathcal{C} weighting each configuration with the Boltzmann factor $\exp(-\beta E(\mathcal{C}))$, where $\beta = 1/T$ and $E(\mathcal{C})$ is the energy of the configuration:

$$Z(\beta) = \sum_{\{\mathcal{C}\}} e^{-\beta E(\mathcal{C})} = e^{-\beta F(\beta)}, \tag{2.1.4}$$

where F is the free energy of the system. Given an observable O (magnetization, correlations among spins, etc.), we define its thermodynamical average as

$$\langle O \rangle = \frac{\sum_{\{\mathcal{C}\}} O e^{-\beta E(\mathcal{C})}}{Z(\beta)}. \tag{2.1.5}$$

When T approaches T_c and ξ becomes much bigger than the microscopic scale of the system we can take the continuum limit and replace the possibly discrete variables such as spins, etc. with a continuum field. In this way the sum over configurations becomes effectively a path integral and we land on a QFT.

As anticipated before, the QFT in question is a d -dimensional Euclidean QFT, where d

denote spatial directions only. The Boltzmann factor βH , where H is the Hamiltonian of the QFT, replaces the iS factor in Lorentzian QFTs, where S is the action. The sum over trajectories in space-time in Lorentzian QFTs turn into a sum over the phase space of configurations in the Euclidean QFT.

Before discussing in more detail how critical exponents are computed in QFT, it is useful to introduce a notable approximation in studying critical phenomena, mean field theory, subject of the next section.

2.2 Mean field theory

Mean field theory is essentially the analogue of a classical approximation, where fluctuations are neglected. We discuss it in the context of the Ising model, one of the simplest and most famous model in statistical physics. The Ising model consists of a d -dimensional lattice of points where a spin variable S_i can take two values, $S_i = \pm 1$, where $i = 1, \dots, N$, N being the total number of lattice points. The Hamiltonian of the system in presence of an external magnetic field h is

$$H_I = -\frac{1}{2} \sum_{i,j=1}^N J_{ij} S_i S_j - \sum_{i=1}^N h_i S_i. \quad (2.2.1)$$

The coupling J_{ij} (sometimes called bond coupling) determines the kind of forces between the spins. We take it to only depend on the distance between site i and site j and symmetric: $J_{ij} = J_{ji}$. The “proper” Ising model corresponds to $J_{ij} \neq 0$ for nearest-neighbour interactions only, also called the short-range Ising model. We can also consider long-range Ising models by taking $J_{ij} \neq 0$, possibly decreasing in some way as the distance between the lattice points increase. For $h_i = 0$, the model enjoys a global \mathbb{Z}_2 symmetry under which $S_i \rightarrow -S_i$.

For $J_{ij} > 0$ the interaction is ferromagnetic, as spins tend to align to minimize the energy. The lowest energy configuration is the one where all spins are $+1$ or -1 (for $h = 0$). This configuration is however unique and is entropically disfavoured. So, a phase transition can occur as T varies. The order parameter of the transition is the average magnetization defined as the spin thermal average:

$$m = \frac{1}{N} \sum_{i=1}^N m_i, \quad m_i \equiv \langle S_i \rangle. \quad (2.2.2)$$

Indeed, a phase transition does occur for $d \geq 2$. For $d = 1$ phase transitions are generally forbidden because fluctuations are stronger and stronger as d decreases.¹ Aside from the $d = 1$ and $d = 2$ cases, we do not know how to analytically solve the model.

As we anticipated, mean field theory consists in neglecting the quadratic spin fluctuations

¹The absence of phase transitions in $d = 1$ is the analogue of the generic absence of spontaneous symmetry breaking in quantum mechanics (we say “generic” because there can be situations where the breaking can occur, see section 6.4.2).

from their average value m . We write

$$\begin{aligned}
S_i S_j &= (S_i - m_i + m_i)(S_j - m_j + m_j) \\
&= m_i m_j + (S_i - m_i)m_j + (S_j - m_j)m_i + (S_i - m_i)(S_j - m_j) \\
&\approx m_i m_j + (S_i - \bar{m}_i)m_j + (S_j - m_j)m_i \\
&= -m_i m_j + m_i S_j + m_j S_i,
\end{aligned} \tag{2.2.3}$$

where in the third row we neglected the $(S_i - m)(S_j - m)$ term. The mean field theory Ising Hamiltonian reads

$$H_1^{\text{MFT}} = \frac{1}{2} \sum_{i,j} J_{ij} m_i m_j - \sum_i (V_i + h_i) S_i, \quad V_i \equiv \sum_j J_{ij} m_j. \tag{2.2.4}$$

Computing $\langle S_i \rangle$ is now trivial, since all spins are decoupled and simplify in the ratio (2.1.5):

$$m_k = \langle S_k \rangle = \frac{\sum_{S_k=\pm 1} e^{\beta(V_k+h_k)S_k} S_k}{\sum_{S_k=\pm 1} e^{\beta(V_k+h_k)S_k}} = \tanh \left[\beta \left(\sum_j J_{kj} m_j + h_k \right) \right]. \tag{2.2.5}$$

The free energy is easily computed to be

$$F = \frac{1}{2} \sum_{i,j} J_{ij} m_i m_j - \beta^{-1} \sum_k \log \left[2 \cosh \left(\beta \left(\sum_j J_{kj} m_j + h_k \right) \right) \right]. \tag{2.2.6}$$

Consider now for simplicity an homogeneous configuration in which $h_i = h$ and $m_i = m$ to each site. We also set

$$J_{ij} = \begin{cases} \frac{J}{n}, & i, j \text{ nearest-neighbor,} \\ 0, & \text{otherwise,} \end{cases} \tag{2.2.7}$$

where n is the number of nearest-neighbor lattice points at each site. This number depends on the lattice topology (triangular, square, etc.) and by d . For square lattices, $n = 2d$. The free-energy (2.2.6) simplifies to

$$\frac{F}{N} = \frac{Jm^2}{2} - \beta^{-1} \log \left[2 \cosh \left(\beta(Jm + h) \right) \right]. \tag{2.2.8}$$

A spontaneous magnetization occurs when F is minimized for $m \neq 0$ at $h = 0$. The condition for an extremum of F gives

$$m = \tanh \left[(Jm + h)\beta \right] \tag{2.2.9}$$

and coincides with (2.2.5) for homogeneous configurations. Depending on β this equation has either one or more solutions: $m = 0$ is always a solution. We can see when more solutions can appear by expanding F for small m . Up to irrelevant constants

$$\frac{F}{N} \approx \frac{1}{2} m^2 J (1 - J\beta) + \frac{J^4 \beta^3}{12} m^4 + \mathcal{O}(m^6). \tag{2.2.10}$$

For $\beta > 1/J$ two other solutions $\pm m_0$ appear, which are two degenerate minima of F . The behaviour of F as a function of m , as T varies is qualitatively as the one in figure 2.1 for second-order phase transitions. We conclude that at

$$T_c = J \tag{2.2.11}$$

the system undergoes a second-order phase transition where the \mathbb{Z}_2 symmetry spontaneously breaks. We can select one of the two vacua $\pm m_0$ by turning on an external magnetic field. Close to T_c , an arbitrarily small magnetic field will be enough to orient all spins in one or the other direction depending on the sign of h .

In mean field approximation the critical exponents are easily calculable. Close to T_c , we expand F in terms of the variable (2.1.2). From (2.2.10) we have

$$m_0(t) \approx \sqrt{-3t} + \dots \quad \implies \quad \beta = \frac{1}{2}. \tag{2.2.12}$$

We compute the magnetic susceptibility by rewriting (2.2.9) as

$$m = -\frac{h}{J} + (1+t) \operatorname{arctanh}(m). \tag{2.2.13}$$

Deriving with respect to h gives

$$\chi = -J^{-1} + \frac{1+t}{1-m^2} \chi \tag{2.2.14}$$

and hence

$$\chi \sim t^{-1} \quad \implies \quad \gamma = 1. \tag{2.2.15}$$

Note that we get the same γ if we approach T_c from $t < 0$ (when $m \neq 0$) or $t > 0$ (when $m = 0$). The exponent δ is extracted setting $t = 0$ in (2.2.13) and expanding from small m :

$$m \approx -\frac{h}{J} + m + \frac{m^3}{3} + \dots, \tag{2.2.16}$$

from which we read

$$h \sim m^3 \quad \implies \quad \delta = 3. \tag{2.2.17}$$

The critical exponent α is computed by recalling the thermodynamical relations

$$E = \frac{\partial(\beta F)}{\partial \beta}, \quad C = -\beta^2 \frac{\partial E}{\partial \beta}. \tag{2.2.18}$$

Setting $h = 0$ and expanding for small t , we get $C \approx m^2(1 - 2t)$. Since $m^2 \sim (-t)$, we see that the specific heat is analytic and hence

$$\alpha = 0. \tag{2.2.19}$$

The determination of ν and η is less trivial, because they are related to the spin fluctuations

which have been neglected from the beginning. We determine the connected spin-spin correlation function as

$$\langle S_i S_j \rangle = -\beta^{-1} \frac{\partial^2 F}{\partial h_i \partial h_j} \Big|_{h_k=0} \equiv G_{ij}. \quad (2.2.20)$$

Close to T_c , the local magnetizations m_i are small for small h_i and we can reliably expand the tanh function in (2.2.5) to first order:

$$m_k \approx \beta h_k + \beta \sum_j J_{kj} m_j. \quad (2.2.21)$$

Since $m_i = -\partial_{h_i} F$, we determine G_{ij} by solving (2.2.21) with $m_i = \beta G_{ij} h_j$. We have

$$G_{ij}(\delta_{jk} - \beta J_{jk}) = \delta_{ik}, \quad (2.2.22)$$

which is conveniently solved in Fourier space. To this purpose we now consider square lattices. Consider a function f_k defined on a one-dimensional chain with sites parametrized by $k \in \mathbb{Z}$ and let a be the distance between two near-by sites. We define the Fourier transform of f_k and its inverse as

$$\hat{f}(p) = \sum_{k=-\infty}^{\infty} f_k e^{-ikap}, \quad f_k = \frac{a}{2\pi} \int_{-\frac{\pi}{a}}^{\frac{\pi}{a}} dp e^{ikap} \hat{f}(p). \quad (2.2.23)$$

The generalization to hyper-cubic lattices in d dimensions is trivial. In Fourier space (2.2.22) turns into

$$\hat{G}(p_\alpha) = \frac{1}{1 - \beta \hat{J}(p_\alpha)}, \quad \alpha = 1, \dots, d. \quad (2.2.24)$$

For nearest-neighbour interactions (2.2.7) we have

$$\hat{J}(p_\alpha) = \sum_{k_\alpha} J_{k_\alpha,0} e^{-iak_\alpha p_\alpha} = \frac{2J}{n} \sum_{\alpha=1}^d \cos(ap_\alpha). \quad (2.2.25)$$

The correlator at large distances is obtained by expanding for small momenta $p_\alpha \ll 1/a$:

$$\hat{G}(p_\alpha) \approx \frac{2d}{J\beta a^2} \frac{1}{p^2 + \mu^2}, \quad p^2 \equiv \sum_{\alpha} p_\alpha p_\alpha, \quad \mu^2 \equiv \frac{2d}{a^2} \left(\frac{1}{\beta J} - 1 \right). \quad (2.2.26)$$

We recognize (2.2.26) as the propagator of a particle of mass m in d dimensions. The correlation length ξ is identified as the inverse of the mass:

$$\xi = \frac{1}{\mu}. \quad (2.2.27)$$

We see that as we approach the critical temperature (2.2.11) the correlation length ξ becomes much bigger than the lattice spacing a . In particular, at $T = T_c$ we have $\mu = 0$ and $\xi = \infty$, signal of a second-order phase transition. At the critical point we get a propagator of a massless

particle which goes as

$$G(r) \sim r^{2-d}. \quad (2.2.28)$$

in d dimensions. Comparing with (2.1.1) we get

$$\eta = 0. \quad (2.2.29)$$

The critical exponent ν is derived from (2.2.26):

$$\xi \sim |t|^{-\frac{1}{2}}, \quad \implies \quad \nu = \frac{1}{2}. \quad (2.2.30)$$

Summarizing, we have in mean field theory

$$\alpha = 0, \quad \beta = \frac{1}{2}, \quad \gamma = 1, \quad \delta = 3, \quad \eta = 0, \quad \nu = \frac{1}{2} \quad (\text{MFT}). \quad (2.2.31)$$

Note that they satisfy the scaling laws (2.1.3), with the exception of the last one, which is satisfied only for $d = 4$. The exponents (2.2.31) predict a larger universality than expected, since they do not even depend on the dimension d of space. The mean field theory approximations is qualitatively and quantitatively correct for $d > 4$, where quantum fluctuations are generally negligible. However it breaks down for the (most interesting) low d cases. In $d = 1$ it qualitatively fails, predicting a phase transition which actually does not occur. In $d \leq 4$ it is qualitatively correct, but quantitatively incorrect, predicting the wrong critical exponents. The renormalization group in QFT is the way to go beyond mean field theory, as we will see in the next section. We will also see how the mean field theory results are naturally explained in terms of QFT.

Note that mean field theory becomes *exact* for weakly coupled (very) long-range Ising models, where we take

$$J_{ij} = \frac{J}{N}, \quad (2.2.32)$$

namely all spins are coupled together with the same strength, independently of their distance. For a constant magnetic field $h_i = h$, we have

$$H_I^{\text{MFT}} = -\frac{J}{2N} \left(\sum_{i=1}^N S_i \right)^2 - h \sum_{i=1}^N S_i. \quad (2.2.33)$$

Introduce a Lagrange multiplier λ so that we can rewrite

$$Z[h] = \sum_{\{S_i\}} \sqrt{\frac{\beta N}{2\pi J}} \int_{-\infty}^{+\infty} d\lambda e^{-\frac{\beta N}{2J} \lambda^2 + \beta(h+\lambda) \sum_i S_i}. \quad (2.2.34)$$

The sum over the 2^N configurations is now trivial, being all the spins decoupled:

$$Z[h] = \sqrt{\frac{\beta N}{2\pi J}} \int_{-\infty}^{+\infty} d\lambda e^{-\frac{\beta N}{2J} \lambda^2} \left[2 \cosh(\beta(\lambda + h)) \right]^N = \sqrt{\frac{\beta N}{2\pi J}} \int_{-\infty}^{+\infty} d\lambda e^{-Nf(\lambda)}, \quad (2.2.35)$$

where

$$f(\lambda) = \frac{\beta}{2J} \lambda^2 - \log \left[2 \cosh (\beta(\lambda + h)) \right]. \quad (2.2.36)$$

In the limit $N \rightarrow \infty$ the integral over λ can be performed using a saddle point approximation. The extrema of f occurs when

$$\lambda = J \tanh [\beta(h + \lambda)]. \quad (2.2.37)$$

We recognize (2.2.37) to be the MFT condition (2.2.9) with the identification $\lambda = Jm$.

2.3 QFT description of critical phenomena

Close to a second-order phase transition $\xi \gg a$ and we can consider an effective description in terms of a continuum theory. Let us then work out how the Ising model (2.2.1) can be recast in terms of a continuum field theory. Since what enters in the partition function is βH and not H , it is convenient to rescale

$$J_{ij} \rightarrow \beta^{-1} J_{ij}, \quad h_i \rightarrow \beta^{-1} h_i, \quad (2.3.1)$$

so that not explicit factors of β enter and both rescaled parameters J_{ij} and h_i are dimensionless. We introduce variables ϕ_i by the identity

$$e^{\frac{1}{2} \sum_{i,j} S_i J_{ij} S_j} = c \prod_i^{\infty} d\phi_i e^{-\frac{1}{2} \sum_{k,l} \phi_k J_{k,l}^{-1} \phi_l + \sum_i \phi_i S_i}, \quad (2.3.2)$$

where c is an irrelevant constant. Thanks to (2.3.2) we can perform the sum over the spin configurations in the partition function. Up to overall constants, we have

$$\begin{aligned} Z &= \int_{-\infty}^{+\infty} \prod_i d\phi_i e^{-\frac{1}{2} \sum_{k,l} \phi_k J_{k,l}^{-1} \phi_l + \sum_k \log \cosh(h_k + \phi_k)} \\ &\sim \int_{-\infty}^{+\infty} \prod_i d\phi_i e^{-\frac{1}{2} \sum_{k,l} \phi_k J_{k,l} \phi_l + \sum_k \log \cosh(h_k + \sum_l J_{kl} \phi_l)}, \end{aligned} \quad (2.3.3)$$

where in the last line we changed variables in the integral $\phi_i \rightarrow \sum_j J_{ij} \phi_j$ and again neglected constant factors coming from the Jacobian. We define

$$x_\mu = a k_\mu, \quad (2.3.4)$$

where $k_\mu \in \mathbb{Z}^d$ are coordinates in the d -dimensional lattice. We also rewrite ϕ_i and J_{ij} as

$$\phi_i = a^{\frac{d-2}{2}} \phi(x), \quad J_{ij} = a^\gamma J(x-y), \quad (2.3.5)$$

where γ is a real parameter. We set $\gamma = d$ so that the Fourier transform of $J(x-y)$ is dimensionless. We take the continuum limit as $a \rightarrow 0$, i.e. assuming that a is the shortest scale in the

theory with a parametric separation of scales. This assumption is expected to be verified close to the critical temperature, where $a \ll \xi$. In this limit the variable x_μ becomes continuous, and the sums over lattice points k are replaced by integrals:

$$a^d \sum_k \rightarrow \int d^d x. \quad (2.3.6)$$

We also take the infinite volume limit by sending the number of lattice sites to infinity, $N \rightarrow \infty$, so that the integral over x is over all space. Close to the critical temperature and for infinitesimal external fields h_i , the field ϕ_i is small, being related to the magnetization, which is infinitesimally small when $T \approx T_c$. We can then set $h_i = 0$, expand the $\log \cosh x$ term and keep only the leading term $x^2/2$. In this approximation and in the continuum limit the exponent of (2.3.3) becomes

$$\begin{aligned} & \frac{a^{-2}}{2} \left(- \int d^d x d^d y \phi(x) \phi(y) J(x-y) + \int d^d x d^d y d^d z \phi(y) \phi(z) J(x-y) J(x-z) \right) + \dots \\ & = - \frac{a^{-2}}{2} \int \frac{d^d p}{(2\pi)^d} \left(|\widehat{\phi}(p)|^2 \widehat{J}(p) - |\widehat{\phi}(p)|^2 |\widehat{J}(p)|^2 \right) + \dots \end{aligned} \quad (2.3.7)$$

We now focus on short-range interactions, limit of nearest neighbour interactions in the underlying lattice model. The form of $\widehat{J}(p)$ in this case has been already determined in (2.2.25). For square lattices, in particular,

$$\widehat{J}(p) \approx \beta J \left(1 - \frac{1}{2d} a^2 p^2 + \mathcal{O}(p^4) \right), \quad (2.3.8)$$

where the factor β comes from (2.3.1). Plugging (2.3.8) in (2.3.7) and going back to configuration space gives

$$- \int d^d x \left[\frac{Z}{2} (\partial_\alpha \phi)^2 + \frac{1}{2} \mu^2 \phi^2 + \dots \right] \quad (2.3.9)$$

where

$$Z = \frac{\beta J}{d} \left(\beta J - \frac{1}{2} \right), \quad \mu^2 = a^{-2} \beta J (1 - \beta J). \quad (2.3.10)$$

The large distance, leading order, approximation of the short-range Ising model is given by a free scalar QFT in d dimensions. Up to an irrelevant overall factor, we recognize the mass term μ^2 in (2.3.10) to correspond to the correlation length (2.2.27) we got in mean field theory. In that approximation $T_c = J$ and hence

$$a^2 \mu^2 \propto \frac{T - T_c}{T_c}. \quad (2.3.11)$$

The next order terms appearing in (2.3.9) are of two kinds: higher-order derivative terms arising from the p expansion of $\widehat{J}(p)$ and higher order x^{2n} terms coming from the expansion of $\log \cosh x$. The next to leading term to consider is the ϕ^4 term coming from the latter expansion. Keeping this term into account and rescaling the field ϕ , we finally get that the partition function of the

Ising model, in the continuum limit, becomes

$$Z = \int \mathcal{D}\phi e^{-S[\phi]}, \quad (2.3.12)$$

with

$$S[\phi] = \int d^d x \left[\frac{1}{2} (\partial_\alpha \phi)^2 + \frac{1}{2} M^2 \phi^2 + \frac{\lambda}{4!} \phi^4 \right], \quad (2.3.13)$$

and

$$M^2 \propto a^{-2} \frac{T - T_c}{T_c}, \quad \lambda \propto a^{d-4}. \quad (2.3.14)$$

Several comments are in order.

- At low energies an emergent $SO(d)$ rotation symmetry emerges, so that the QFT in question is the same as the Euclidean version of a *relativistic* QFT in Minkowski space-time.
- The inverse lattice spacing a^{-1} plays the role of the UV cut-off Λ of the bare action S . Dimensionful parameters are all expressed in terms of this quantity. However, we are not really interested in the short-distance behaviour of this scalar theory, which indeed is seen here as an effective theory, the underlying microscopic theory being a lattice theory. We are instead interested in its long-distance behaviour.
- From the point of view of the QFT (2.3.14) the mean field theory approximation corresponds to take the classical limit and to neglect loop corrections. In particular, spontaneous magnetization corresponds to the classical spontaneous symmetry breaking of the \mathbb{Z}_2 symmetry $\phi \rightarrow -\phi$. For $T > T_c$ the mass term is positive and we are in the unbroken configuration, while for $T < T_c$ the scalar develops a vacuum expectation value and we are in the broken phase. The divergence of the correlation length is manifest as $M = 0$ at the transition point corresponds to $\xi = \infty$.
- The universality of critical phenomena corresponds to the universality of (super-) renormalizable theories in QFT. Independently of the detailed interactions and fields, any microscopic theory which at large distances can be written as (2.3.14) can be tuned to a second-order phase transition in the Ising universality class.
- In high energy physics, the smallness of M with respect to the cut-off scale Λ is what we call a hierarchy problem (related to the Higgs particle). In statistical physics, the hierarchy problem is rephrased as the fact that (second-order) phase transitions are not generic. We have to tune the temperature T to be close to a phase transition. This tuning can be performed for critical phenomena, but it is clearly out of reach in high energy physics.
- Usual QFT scaling and RG arguments naturally explain the range of validity of mean field theory. First of all, it makes sense to expand the action in local operators and keep only the first ones because all others are irrelevant (in the RG sense) in the IR. For $d > 4$ the ϕ^4 term is irrelevant as well, and hence the IR behaviour of the theory is governed by a free,

almost massless, scalar close to the transition. In contrast, for $d < 4$, the theory (2.3.14) is strongly coupled in the IR. In particular, the dimensionless coupling constant is given by

$$g = \frac{\lambda}{M^{4-d}}, \quad (2.3.15)$$

and it blows up at the phase transition. The long distance behaviour of the theory (2.3.14) at the critical temperature is expected to be given by a strongly coupled CFT for $d < 4$.

- The critical exponents should be determined in terms of the fundamental parameters of the CFT, notably the scaling dimensions of its lowest dimensional scalar operators. Since the theory undergoes a non-trivial RG flow, they differ from their classical values determined from the theory (2.3.14).

The considerations made above for the specific case of the Ising model generalize to other kind of models, which also have a continuum description in terms of a QFT. The program of determining critical exponents by studying the RG flow of QFTs like (2.3.14) has been the subject of an intense study in the past by means of various methods. The discussion of these methods, as well as of the large arena of QFTs describing critical phenomena, is beyond the content of this course.

Chapter 3

Large N in QFT

The large N expansion is a very useful perturbative expansion in QFT. It consists in expanding observables in powers of $1/N$, where N is generally an integer related to the number of fields or to the rank of a global or gauge symmetry group of the theory.

It is useful to classify QFTs at large N according to how the fields scale with N . We have *vector models* if the fields are at most in representations of $\mathcal{O}(N)$, like fundamentals, *matrix models* if the fields are at most in representations of $\mathcal{O}(N^2)$, like the adjoint representation, or *tensor models* if representations with higher powers of N are present.¹ For example, 4d QED with N charged particles and $SU(N)$ Yang-Mills theory are examples of a vector and matrix models, respectively.

It is difficult to overestimate the importance of the large N expansion in theoretical physics. It plays an essential role in the AdS/CFT correspondence [9–11], it allows us to analytically understand the generation of a non-perturbative mass gap in certain vector models in 2d, it allows us to have a qualitative understanding of several phenomena in 4d non-abelian gauge theories, etc.

An important general point to keep in mind is the following. Large N techniques in matrix models typically lead to *qualitative* results while in vector models we can have *quantitative* results. We consider the large N limit of matrix and vector models in sections 3.1 and 3.2, respectively.

3.1 Matrix models

The large N limit in non-abelian gauge theories has been introduced by 't Hooft in the seminal paper [12]. An excellent overview can be found in [2], which we follow here.² We start by considering Yang-Mills theories with gauge group $SU(N)$ and no charged matter.

¹Sometimes by matrix models it is meant a model of constant $N \times N$ matrices. Here by matrix models we mean QFTs where the quantum fields are $N \times N$ matrix fields.

²The paper is about baryons in the large N description, which are more complicated than mesons. However, sections 2 ÷ 4 give a crystal clear overview of meson physics at large N . We refer the reader to [2] for further details. We focus in the following on mesons only.

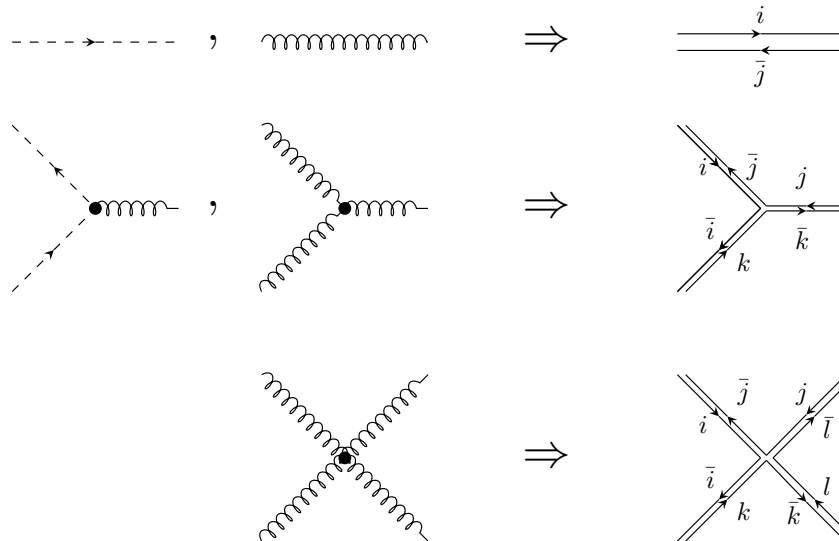


Figure 3.1: Feynman diagrams for gluon and ghost propagators and vertices in double line notation.

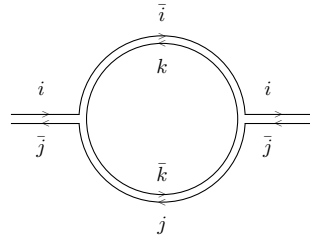
The Lagrangian density is

$$\mathcal{L} = -\frac{1}{4} \sum_{\alpha=1}^{N^2-1} F_{\mu\nu}^{\alpha} F_{\alpha}^{\mu\nu}, \quad F_{\mu\nu}^{\alpha} = \partial_{\mu} A_{\nu}^{\alpha} - \partial_{\nu} A_{\mu}^{\alpha} + g C_{\beta\gamma}^{\alpha} A_{\mu}^{\beta} A_{\nu}^{\gamma}, \quad (3.1.1)$$

with g the gauge coupling constant and $C_{\beta\gamma}^{\alpha}$ the structure constant of the associated Lie algebra. Ghosts and gauge-fixing terms have been omitted.

Since we will get qualitative and not quantitative results, there is no need to keep track of numerical factors, Lorentz tensor structures, indices, etc., with the exception of the color factors. In order to emphasize the color structure of Feynman diagrams, it is useful to introduce 't Hooft double line notation for gluons. We will be working only at leading order in the large N limit. In this limit $N^2 - 1 \approx N^2$ and $SU(N) \approx U(N)$. The adjoint index α can then be rewritten as $\alpha = (i, \bar{j})$, where $i = 1, \dots, N$ and $\bar{j} = 1, \dots, N$ are indices in the fundamental and anti-fundamental of $U(N)$, according to the decomposition $N^2 = N \otimes \bar{N}$. Dropping Lorentz indices, the ordinary Feynman rules for propagators and vertices in the theory can be replaced by a double-line as in figure 3.1. We note that as far as color structure is concerned, ghosts propagators and vertices behave as gluon propagators and cubic vertices, so we do not need to consider them separately. The double line notation is a useful way to detect the powers of N in a given Feynman diagram. Each closed loop gives a power of N . Consider for instance the one-loop contribution to the gluon vacuum polarization. The presence of the closed k index loop

immediately tells us that the graph is proportional to $g^2 N$:



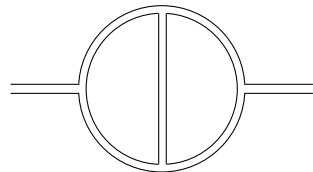
$$\propto g^2 N. \quad (3.1.2)$$

We learn from this example that a well-defined $N \rightarrow \infty$ limit requires

$$g \rightarrow 0, \quad N \rightarrow \infty, \quad \text{with } \lambda \equiv g^2 N = \text{fixed}. \quad (3.1.3)$$

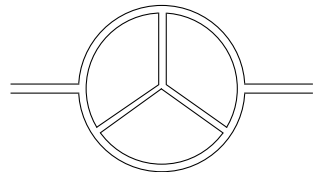
The above relation defines what is called the 't Hooft limit. Large N means that we consider an expansion of observables at finite λ as a series (in general asymptotic) in $1/N$.

We check that higher order diagrams are well-defined in the limit (3.1.3). For further simplicity, we omit from now on to write the color indices and arrows in the diagrams. For example, the two-loop correction



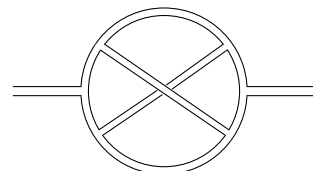
$$\propto g^4 N^2 = \lambda^2, \quad (3.1.4)$$

the three-loop correction



$$\propto g^6 N^3 = \lambda^3. \quad (3.1.5)$$

In the large N limit and for generic values of λ , both graphs (3.1.4) and (3.1.5) are of the same order, i.e. leading in $1/N$. Consider now the three-loop graph



$$\propto g^6 N = \frac{\lambda^3}{N^2}. \quad (3.1.6)$$

The graph is three-loop order (there is no quartic vertex in the middle) and proportional to g^6 . However, the internal loop is given by a single closed line, and hence the graph is proportional to $g^6 N = \lambda^3/N^2$, suppressed by a factor $1/N^2$ with respect to the graph (3.1.5).

The difference between the $\mathcal{O}(1/N^2)$ Feynman diagram (3.1.6) and the previous $\mathcal{O}(1)$ ones

is topological. We denote by *planar* all diagrams that can be drawn on a plane, and *non-planar* all the others. We see that the leading diagrams are all planar, while the one in (3.1.6) is not, as evident from the figure due to the overlapping lines. It is easy to convince ourselves that this is a general phenomenon. At leading order in $1/N$, planar diagrams are the only ones that survive.

Consider now the vacuum energy. In non-canonical normalization of the fields, propagators are proportional to g^2 and vertices (both trilinear and quartic) to $1/g^2$. A diagram with I propagators and V vertices goes like $(g^2)^{I-V} N^C = \lambda^{I-C} N^{V-I+C}$, where C represents the total number of closed lines of the diagram in 't Hooft double line notation. It is very useful to have a geometric interpretation of the diagram. A closed line delimits a face of a two-dimensional surface, with propagators edges of the faces. So we have

$$V - I + C = \# \text{ of vertices} - \# \text{ of edges} + \# \text{ of faces} = \chi = 2 - 2g, \quad (3.1.7)$$

where χ is the Euler character of a surface of genus g . For example, consider the three-loop vacuum planar graph



$$(3.1.8)$$

We have $V = 4$, $I = 6$ and $C = 4$, and correspondingly we get $\chi = 2$, which is the Euler characteristic of a two-sphere. Note that in counting the number of faces, we have to also consider the outer face, the one delimited by the external closed line in (3.1.8). This is infinite on \mathbb{R}^2 , but finite on a compact space. All vacuum planar diagrams have $\chi = 2$. As pointed out already in [12], the large N expansion can be interpreted as a genus expansion, which is the expansion parameter in perturbative string theory. In particular, we expect that the string theory description emerges when the 't Hooft coupling is large and we have to sum over all planar diagrams, giving rise in this way to the string world-sheet. This deep connection between gauge theories and string theory has been made sharp in the AdS/CFT correspondence [9–11].

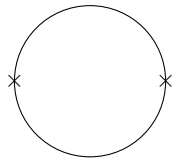
Let us now consider the effect of adding matter, for concreteness fermions in the fundamental representation. The one-loop contribution of fermions to the gluon vacuum polarization is given by

$$\propto g^2 = \frac{\lambda}{N}. \quad (3.1.9)$$

Fermions, being fundamental fields, have propagators with a single line. Using the by now familiar counting rules, we see that graph (3.1.9) is proportional to $g^2 = \lambda/N$, and hence is suppressed by a factor of $1/N$ with respect to the pure gluon contribution in (3.1.2). The matter

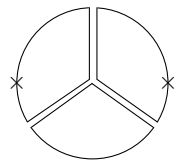
suppression is intuitively obvious, given the different scaling in N of adjoint and fundamental fields. From a geometric point of view, matter loops give rise to edges, but no faces, since we lack the second closed line in 't Hooft double line notation. They give rise to boundaries of the $2d$ surface. In presence of boundaries, the Euler characteristic of a Riemann surface equals $\chi = 2 - 2g - h$, where h represents the number of boundaries.

It is useful to consider the two-point function of gauge-invariant quark bilinears of the form $J_\Gamma(x) = \bar{q}(x)\Gamma q(x)$, where q are quarks in the fundamental and Γ a product of gamma matrices. Depending on Γ , the operator J_Γ can be a space-time scalar, pseudo-scalar, vector, etc. We will not specify the precise structure of Γ , as the considerations that follow are independent of that. The free theory contribution to the two-point function is given by



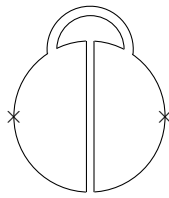
$$\propto N, \tag{3.1.10}$$

and is proportional to N . Another contribution of the same order is given by e.g. the three-loop order graph



$$\propto g^4 N^3 = \lambda^2 N. \tag{3.1.11}$$

The graph



$$\propto g^4 N = \frac{\lambda^2}{N}, \tag{3.1.12}$$

is instead suppressed with respect to (3.1.10) and (3.1.11) by a factor $1/N^2$. If we bring the external gluon line inside the circle delimited by the quark loop, we get a non-planar graph, which we know is $1/N^2$ suppressed with respect to the leading contribution. It is simple to convince ourselves that the leading order result is given by planar diagrams where the only quark line represents the edge (boundary) of the diagram.

Despite planar diagrams are a small fraction of the multitude of all diagrams, they are still infinite in number and summing them is a difficult task. However, several important qualitative properties on the theory can be deduced, assuming that the theory confines when $N \rightarrow \infty$.

In a general interacting theory, from the Källén-Lehmann representation, we expect that the two point-function $\langle J_\Gamma(x)J_\Gamma(0) \rangle$ has a spectral density with poles in correspondence of the stable 1-particle states which can be created out of the vacuum from the operator J_Γ , followed by a continuum of multi-particle states. In a confining gauge theory, the stable 1-particle states

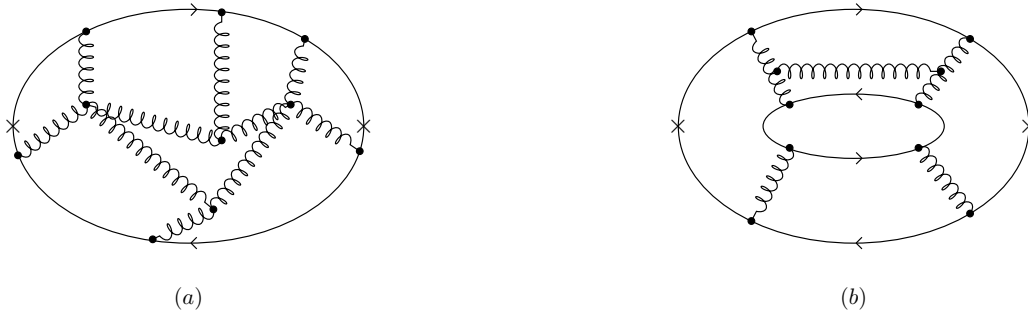


Figure 3.2: Generic multi-loop contribution to the quark bilinear two-point function, in ordinary line notation: (a) Leading planar and (b) $1/N$ suppressed by a fermion loop. The crosses denote the insertion of the quark bilinear operators.

created from J_Γ are mesons, bound states of two valence quarks, whose quantum numbers depend on the choice of Γ . For example, parity even scalars and vector mesons are associated to $\Gamma = 1, \gamma^\mu$, respectively. The number of stable 1-particle states appearing in $\langle J_\Gamma(x)J_\Gamma(0) \rangle$ is generally finite and small, as no symmetry generally prevent higher massive mesons to decay into the lightest ones with the appropriate quantum numbers. Confinement means in particular that the large distance behaviour of any of these two-point functions is exponentially damped:

$$\lim_{|x-y| \rightarrow \infty} \langle J_\Gamma(x)J_\Gamma(0) \rangle \propto e^{-m_\Gamma|x-y|}, \quad (3.1.13)$$

where m_Γ is the mass of the lightest meson created from J_Γ .

In contrast, at leading order in $1/N$, the current J_Γ creates only *single* particle states. This is understood diagrammatically as follows. In perturbation theory, the appearance of multi-particle states in the spectral density is detected by cutting a Feynman diagram and looking at the intermediate states which can propagate, because

$$\text{Im} G(p) \propto \rho(p^2), \quad (3.1.14)$$

where $G(p)$ is a generic two-point function and ρ the associated spectral density, in momentum space. In the case a hand, we have $G(p) = \langle J(-p)J(p) \rangle$. For simplicity we omit from now on the subscript Γ and we have denoted the Fourier transform of the bilinear operator $J(x)$ with the same symbol $J = J(p)$. The absence of quarks loops immediately implies that we can have one-meson states only, see (a) in figure 3.2. Independently of how we cut the diagram, at the planar level two and only two quark lines always emerge, the ones of the external valence quarks. Two-meson states would appear, e.g., at sub-leading order in $1/N$ from a diagram like (b) in figure 3.2. Planarity also forbids multi-particle states with one meson and additional glueballs. Multi-particle states of this kind would arise if, when cutting a diagram, we would get more than one gauge-invariant combination of operators. However, planarity of the diagram guarantees that we always get one and only one gauge-invariant combination. More gauge-invariant combinations

can only appear at sub-leading orders in $1/N$.

The Källén-Lehmann representation of G_2 reduces then to a sum of one-particle states:

$$\langle J(-p) J(p) \rangle = \sum_n \frac{a_n^2}{p^2 - m_n^2}. \quad (3.1.15)$$

The sum runs over all stable meson states with mass $m_n^2 = \mathcal{O}(N^0)$. The expression (3.1.15) is exact at leading order in $1/N$, meaning that it is expected to hold for any value of p . For large values of p , corresponding at short distances $x \rightarrow y$, due to asymptotic freedom, the theory is weakly coupled and the two-point function can be reliably computed in perturbation theory. For massless quarks, the correlator approaches in the UV the two-point function of a conformal field theory operator with classical scaling dimensions $\Delta_J = 3$. However, for large but finite p , we have $\log p^2$ corrections coming from the interactions, which can be reliably computed using the UV description in terms of gluons and quarks. These terms are non-analytic, and should be reproduced from the right hand side of (3.1.15). But for any finite sum, this is manifestly analytic at $p = 0$. We then conclude that the sum over n has to be necessarily infinite. It is remarkable to have a theory which present an infinite number of stable single-particle states. As we will soon see, there is a simple explanation for this peculiar behaviour, as mesons at leading order in $1/N$ are simply free.³

We can also determine the scaling in N of the 1-meson exchange. Since $\langle JJ \rangle \sim \mathcal{O}(N)$, then $a_n^2 \sim \mathcal{O}(N)$, which implies that

$$\langle 0|J(0)|1\text{-meson} \rangle \sim \mathcal{O}(\sqrt{N}). \quad (3.1.16)$$

The N -dependence of the cubic meson coupling is similarly obtained by looking at the three-point function $\langle JJJ \rangle$. Again, at leading order in N , the correlator is order N . Only planar diagrams contribute and in any channel we get only 1-meson exchange. Since $a_n \sim \mathcal{O}(\sqrt{N})$, the three-point function, in terms of meson fields, describes the cubic coupling g_{3M} among mesons as in figure 3.3. We have

$$g_{3M} N^{3/2} \sim N \implies g_{3M} \sim \mathcal{O}(N^{-\frac{1}{2}}). \quad (3.1.17)$$

The three-point function $\langle JJJ \rangle$ allows us to also determine the scaling in N of the amplitude $a_{2M} \sim \langle 0|J(0)|2\text{-meson} \rangle$. This is the contribution to $\langle JJJ \rangle$ where a single current emits two meson states, each one absorbed by the other two currents:

$$\begin{array}{c} \sqrt{N} \times \\ \diagdown \\ \diagup \\ \sqrt{N} \times \end{array} \rightarrow a_{2M} = \mathcal{O}(N) \rightarrow a_{2M} = \mathcal{O}(1). \quad (3.1.18)$$

³Baryons, in contrast, remain interacting in this limit.

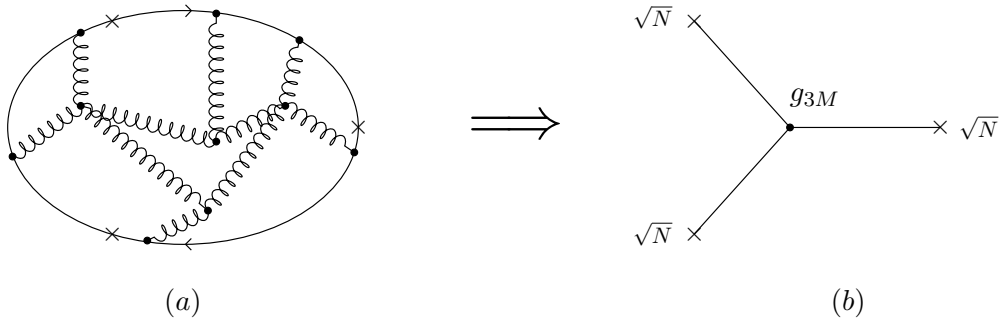


Figure 3.3: (a) Generic multi-loop leading planar contribution to the three-point function of quark bilinears. (b) Resulting effective three-point coupling g_{3M} in the meson effective theory. The crosses denote the insertion of the quark bilinear (a) and meson (b) operators.

Looking at higher-point functions, we can easily get the scaling in N of the M^n meson coupling: $g_{nM} \sim \mathcal{O}(N^{1-\frac{n}{2}})$. A similar analysis can be applied to glueballs by looking at gauge-invariant operators built out only from gauge fields, such as $S = \text{Tr}F^2$. By analogous steps, and recalling that $\langle SS \rangle \sim \mathcal{O}(N^2)$, we get

$$\langle S(-k)S(k) \rangle = \sum_{n=1}^{\infty} \frac{b_n^2}{k^2 - \tilde{m}_n^2}, \quad b_n \sim \mathcal{O}(N), \quad \tilde{m}_n^2 \sim \mathcal{O}(N^0), \quad (3.1.19)$$

where \tilde{m}_n are the masses of the stable glueball states. The coupling g_{nG} between n glueball states scales as $g_{nG} \sim \mathcal{O}(N^{2-n})$. We can also combine the two analysis to get the scaling in N of the coupling $g_{lG,kM}$ between l glueballs and k mesons. For $k > 0$, we have

$$g_{lG,kM} \sim \mathcal{O}(N^{1-l-\frac{k}{2}}). \quad (3.1.20)$$

All couplings are suppressed at large N . In particular, we see that at $N = \infty$, QCD is a theory of an infinite number of free mesons and glueballs!

The operators J or S are particular examples of *single trace* operators, namely gauge-invariant composite operators involving a single trace in color indices. Given the importance of color indices, composite operators in large N are classified as single-trace, double-trace, and so on. Depending on the number of independent color traces we have $\Phi_1 \equiv \text{tr} \mathcal{O}$, $\Phi_2 \equiv \text{tr} \mathcal{O}_1 \text{tr} \mathcal{O}_2$, etc. An important property of correlation functions of general single trace operators is their *factorization*. At leading order at large N , n -point correlation functions of single-trace operators are dominated by their disconnected components. For example, for 4 identical operators Φ_1 of the kind J or S , we have

$$\langle \Phi_1 \Phi_1 \Phi_1 \Phi_1 \rangle \sim \langle \Phi_1 \Phi_1 \rangle \langle \Phi_1 \Phi_1 \rangle + \mathcal{O}(N^{-1}). \quad (3.1.21)$$

The factorization follows from the observation that for any correlation function the *connected*

part of the amplitude scales as N (J) or N^2 (S). Schematically we have

$$\frac{\overbrace{\langle \Phi_1 \dots \Phi_1 \rangle}^n}{\langle \Phi_1 \Phi_1 \rangle^{\frac{n}{2}}} \xrightarrow{N \rightarrow \infty} 1, \quad (3.1.22)$$

while for the connected component of the correlator

$$\frac{\overbrace{\langle \Phi_1 \dots \Phi_1 \rangle_c}^n}{\langle \Phi_1 \Phi_1 \rangle^{\frac{n}{2}}} \xrightarrow{N \rightarrow \infty} \begin{cases} \mathcal{O}(N^{2-n}), & \text{glueball operators} \\ \mathcal{O}(N^{1-\frac{n}{2}}), & \text{meson operators} \end{cases}. \quad (3.1.23)$$

Disconnected terms dominate over connected ones.

Large N factorization implies that for a n multi-trace operator of the form $\Phi_n = \psi_1 \dots \psi_n$, where $\psi_k = \text{tr } \mathcal{O}_k$, we have

$$\gamma_{\Phi_n} = \sum_{k=1}^n \gamma_{\psi_k} + \mathcal{O}(N^{-1}). \quad (3.1.24)$$

There are several properties of real-world QCD which are qualitatively explained from large N considerations. In QCD, $N = 3$, and we can hope that this is large enough for large N considerations to apply. Among others, i) the dominance of pure glue vs sea quarks, ii) the suppression of $\bar{q}q\bar{q}q$ tetraquark states with respect to meson states (explained by large N factorization), iii) appearance of meson states in Regge trajectories, iv) mass splitting between (non-GB) mesons and baryons (baryons at large N have a mass of order N). See e.g. [2] for further properties and details.

3.2 Vector models

In the context of large N physics, vector models refer to theories where fields have up to $\mathcal{O}(N)$ components. The absence of adjoint matrix fields dramatically simplifies the situation. In vector models the parameter N typically refers to the number of matter, or flavour, fields in the theory. The “planar dominance” is generically replaced by a more controllable “bubble dominance”. At each order in $1/N$ there are a finite number of diagrams and quantitative studies are possible.

As an illustrative example, let us consider $4d$ QED with N massless Dirac fields:

$$\mathcal{L} = -\frac{1}{4}F_{\mu\nu}F^{\mu\nu} + \sum_{k=1}^N \bar{\psi}_k i \not{D} \psi_k. \quad (3.2.12)$$

Assignment n.1: CFT phase of QED

(2/2)

(d) Consider the vertex given by the fermion bilinear operator $\sum_i \bar{\psi}_i \psi_i$ at zero momentum:

$$= -\delta Z_m . \quad (3.2.9)$$

Integrate as before the virtual momentum q over a shell $b\Lambda \leq q \leq \Lambda$ to determine the $\log(b)$ term in δZ_m .

Use δZ_ψ and δZ_m found above to determine the exact form of the anomalous dimension of the fermion bilinear at order $1/N$ for any $2 < d < 4$ given by

$$\gamma_{\bar{\psi}\psi} = b \frac{d}{db} (-\delta Z_m + \delta Z_\psi) . \quad (3.2.10)$$

Useful formulas:

$$\int \frac{d^d k}{(2\pi)^d} \frac{1}{(k^2 + \Delta)^2} = \frac{\Gamma(2 - \frac{d}{2})}{(4\pi)^{d/2}} \Delta^{\frac{d}{2}-2}, \quad \int \frac{d^d k}{(2\pi)^d} \frac{k^2}{(k^2 + \Delta)^2} = \frac{d}{2} \frac{\Gamma(1 - \frac{d}{2})}{(4\pi)^{d/2}} \Delta^{\frac{d}{2}-1} \quad (3.2.11)$$

$$\int_0^1 dx [x(1-x)]^{a-1} = \frac{\Gamma^2(a)}{\Gamma(2a)}, \quad a > 0$$

we see that the large N limit requires

$$e \rightarrow 0, \quad N \rightarrow \infty, \quad \text{with } \lambda \equiv e^2 N = \text{fixed}, \quad (3.2.14)$$

similarly to (3.1.3). Since we have no adjoint fields, no double-line notation is necessary. It is immediate to see that (3.2.13) is the only 1PI contribution to the photon propagator, at leading order in $1/N$. More strikingly, it turns out that the graph (3.2.13) is the only 1PI loop diagram at order $1/N$ in general. Vertex and fermion propagator corrections, in particular, are $1/N$ suppressed. For example, we have

$$\propto e^3 = \frac{e\lambda}{N}, \quad \propto e^2 = \frac{\lambda}{N} . \quad (3.2.15)$$

This tremendous simplification makes possible to compute with little effort quantities at the

lowest orders in $1/N$. Consider for example the beta-function β at leading order. Recall that in QED, to all orders in perturbation theory (both at finite and large N), we have

$$\beta(e) = e\gamma_A(e), \quad (3.2.16)$$

where γ_A is the anomalous dimension of the photon. Its leading order contribution at large N is given by the photon bubble (3.2.13), which also equals the one-loop contribution in ordinary perturbation theory, given by $\gamma_A = e^2 N / (12\pi^2)$ (see e.g. section 5.7 of [13]). Together with (3.2.16) it gives

$$\beta(\lambda) = 2Ne\beta(e) = \frac{1}{6\pi^2}\lambda^2 + \mathcal{O}(N^{-1}), \quad (3.2.17)$$

to all orders in λ . As a consequence of (3.2.17) we can rigorously establish that QED in $d = 4 - \epsilon$ dimensions has a weakly coupled fixed:

$$\beta(\lambda) = -\epsilon\lambda + \frac{\lambda^2}{6\pi^2} + \mathcal{O}(N^{-1}) \longrightarrow \lambda^* = 6\pi^2\epsilon + \mathcal{O}(N^{-1}). \quad (3.2.18)$$

We can also compute quantities at sub-leading orders by taking into account the only $\mathcal{O}(1)$ effect given by the bubble diagram (3.2.13). Resummations of bubbles give rise to an effective photon propagator, *exact* in λ at leading order in $1/N$. We denote it by a double wavy line (do not confuse this double line with 't Hooft double line used in matrix models!):

$$\text{resummed wavy line} = \text{wavy line} + \text{wavy line} \text{ with one bubble} + \text{wavy line} \text{ with two bubbles} + \dots \quad (3.2.19)$$

Replacing in Feynman diagrams the ordinary propagator with its resummed version takes into account of all possible higher loop, but same order in $1/N$, diagrams.

Non-abelian gauge theories in $4d$ are no longer UV free when we take a large number of matter field. For this reason the vector large N limit is not as interesting as its matrix version in $d = 4$. Probably the most interesting applications of large N vector models are in $d = 2$ dimensions, where they allow us to have an analytic understanding of several non-perturbative phenomena. As an illustrative example we consider here two notable models, the Gross-Neveu [14] and the non-linear sigma model. The 2d Gross-Neveu model is described by the Lagrangian density

$$\mathcal{L} = \sum_{k=1}^N \bar{\psi}_k i \not{\partial} \psi_k + \frac{g^2}{2} \left(\sum_{k=1}^N \bar{\psi}_k \psi_k \right)^2. \quad (3.2.20)$$

We can introduce an auxiliary field σ to write the equivalent Lagrangian

$$\mathcal{L}' = \sum_{k=1}^N \bar{\psi}_k i \not{\partial} \psi_k - \frac{N}{2} \sigma^2 + g\sqrt{N}\sigma \sum_{k=1}^N \bar{\psi}_k \psi_k, \quad (3.2.21)$$

and take the large N limit

$$g \rightarrow 0, \quad N \rightarrow \infty, \quad \text{with } \lambda \equiv g^2 N = \text{fixed}. \quad (3.2.22)$$

Note that with the normalizations taken in (3.2.21) the trilinear vertex coupling is finite in the limit. We see that all correlation functions of σ , at leading order in $1/N$, are governed by a single fermion loop and are of order N , all other contributions being sub-leading. For example, the only diagrams contributing at leading order to the two-point and four-point functions $\langle \sigma \sigma \rangle$ and $\langle \sigma \sigma \sigma \sigma \rangle$ are

$$\begin{array}{c} \text{---} \circ \text{---} \\ \propto (g\sqrt{N})^2 N = \lambda N, \end{array} \quad \begin{array}{c} \text{---} \circ \text{---} \\ \text{---} \circ \text{---} \\ \propto (g\sqrt{N})^4 N = \lambda^2 N. \end{array} \quad (3.2.23)$$

Fluctuations of σ are suppressed. In the normalizations of (3.2.21) we do not pay factors of N in inserting trilinear vertices, but we pay a factor $1/N$ for each σ propagator. For example,

$$\begin{array}{c} \text{---} \circ \text{---} \\ \text{---} \circ \text{---} \\ \text{---} \circ \text{---} \\ \propto (g\sqrt{N})^6 N \times N^{-1} = \lambda^3. \end{array} \quad (3.2.24)$$

Integrating out the fermions, we see that the full Coleman-Weinberg potential for σ is of order N and is determined from the one loop fermion determinant only. We do not discuss the details of this computation, which were worked out in an assignment in the QFT I course. We just point out that large N in the Gross-Neveu model allows us to rigorously establish the spontaneous breaking of a \mathbb{Z}_2 chiral symmetry and the generation of a non-perturbatively generated mass scale.

Another interesting application of large N occurs in the study of the non-linear sigma model. This is a theory of N scalars ϕ_i . The Lagrangian is that of free fields, but the ϕ_i are coordinates on a S^{N-1} sphere and are subject to a constraint

$$\sum_{i=1}^N \phi_i^2 = \frac{1}{g^2}, \quad (3.2.25)$$

where g^2 is a constant. The theory has a manifest $O(N)$ symmetry under which the ϕ_i transform in the fundamental representation. Because of the constraint, the theory is interacting and g^2 acts as a coupling constant. This can be seen by classically solving the constraint in terms of a field, say ϕ_N . We have $\phi_N = \pm \sqrt{1 - g^2 \sum_a \phi_a^2} / g$, where $a = 1, \dots, N-1$. Plugging this in the scalar kinetic term for ϕ_N would give rise to an infinite number of derivative interactions weighted by g^2 . From a naive analysis of the model along these lines, we would conclude that

the constraint forces ϕ_N to develop a vacuum expectation value. Then the $O(N)$ symmetry is spontaneously broken to $O(N - 1)$, giving rise to an interacting theory of $N - 1$ massless Goldstone bosons. This expectation turns out to be wrong. No spontaneous symmetry breaking occurs, and all scalars get a common non-perturbatively generated mass for $N > 2$.

This is in fact a general phenomenon, for which it is worth to make a short digression. Quantum fluctuations in two-dimensions are generally too strong to allow for a ordered phase with a continuous symmetry [15,16]. A way to understand what goes wrong in relativistic systems in $d = 2$ is by recalling Goldstone theorem. According to this theorem, whenever a global internal symmetry is spontaneously broken in a generic QFT, massless scalars should appear for each broken generator. In $d = 2$, however, the propagator of a free massless scalar is not well-defined, as it grows logarithmically with the distance and it has IR divergences. So Goldstone theorem applies only for $d \geq 3$ and no *continuous* global symmetry can spontaneously break in $d = 2$ [17]. In contrast, *discrete* global symmetries can spontaneously break, an example being the \mathbb{Z}_2 chiral symmetry of the Gross-Neveu model discussed before.

Coming back to the non-linear sigma model, the absence of the $O(N)$ breaking can be seen analytically at large N as follows. We implement the constraint (3.2.25) by introducing an auxiliary field σ , which acts as a Lagrange multiplier. The Lagrangian of the non-linear sigma model reads

$$\mathcal{L} = \frac{1}{2} \sum_{i=1}^N (\partial\phi_i)^2 - \sigma \left(\sum_{i=1}^N \phi_i^2 - \frac{N}{\lambda} \right), \quad (3.2.26)$$

where $\lambda = g^2 N$ is the 't Hooft-like coupling kept fixed in the large N limit. The auxiliary field σ has no quadratic term to start with, but this is generated by quantum corrections. The leading order 1PI term is given by the bubble in the first diagram in (3.2.23), which scales as N . Resumming all bubbles give rise to an effective propagator for σ which goes like $1/N$. Hence, fluctuations of σ are suppressed, as in the Gross-Neveu models. In order to understand the vacuum structure of the theory, we compute the effective potential at leading order in $1/N$. We have $\phi_i = \sqrt{N}\phi_{i,0} + \phi_i^q$, where $\phi_{i,0}$ and ϕ_i^q are respectively the vacuum expectation value and the quantum fluctuations of the scalar fields. Since the σ fluctuations are suppressed, at leading order in $1/N$ the ϕ_0 -dependent part of the scalar potential arises only from the $\sigma\phi^2$ term in the Lagrangian (3.2.26):

$$V \supset N\sigma \sum_{i=1}^N \phi_{i,0}^2, \quad (3.2.27)$$

which is minimized by either $\phi_{i,0} = 0$ or $\sigma = 0$. Determining the extrema of σ is less trivial and requires a loop computation. In order to keep the analysis as simple as possible, we introduce the only counterterm which is needed to renormalize the effective potential, a tadpole for σ of the form $N\sigma\delta Z$. We use dimensional regularization and $\overline{\text{MS}}$ scheme. Integrating out the N scalar

fields, we have (see e.g. section 5.11 of [13])

$$V_{\text{eff},B}(\sigma) = \mu^{2-d} \frac{N}{2} \int \frac{d^d p_E}{(2\pi)^d} \log(p_E^2 + \sigma) = \frac{N}{d(4\pi)^{d/2}} \mu^\epsilon \sigma^{d/2} \Gamma(1 - d/2), \quad (3.2.28)$$

where $\epsilon = 2 - d$ and the RG scale μ has been introduced in such a way that the effective potential remains of dimension 2 for any d . Demanding finiteness of $V_{\text{eff},B} + N\sigma\delta Z$ fixes

$$\delta Z = -\frac{1}{8\pi} \left(\frac{2}{\epsilon} - \gamma_E + \log(4\pi) \right), \quad (3.2.29)$$

and hence, including the tree-level term in (3.2.26), we get the leading $\mathcal{O}(N)$ effective potential

$$V_N(\sigma) = N \frac{\sigma}{8\pi} \left[1 - 8\pi \left(\lambda^{-1}(\mu) - \sum_{i=1}^N \phi_{i,0}^2 \right) + \log \left(\frac{\sigma}{\mu^2} \right) \right]. \quad (3.2.30)$$

The potential V_N does not have extrema at $\sigma = 0$, so we conclude that

$$\phi_{i,0} = 0, \quad (3.2.31)$$

and

$$\sigma = \mu^2 e^{-\frac{8\pi}{\lambda(\mu)}}, \quad (3.2.32)$$

which is a non-perturbatively generated RG invariant scale. We see from (3.2.26) that the VEV (3.2.32) induces a mass for all scalars

$$m^2 = 2\mu^2 e^{-\frac{8\pi}{\lambda(\mu)}}. \quad (3.2.33)$$

In contrast to the naive expectation, the model is trivially gapped in the IR. The spectrum at low energy consists of N “meson” states which transform as vectors of the unbroken $O(N)$ symmetry.

Chapter 4

Kinks, vortices, and monopoles

In perturbative QFT we define particles as the small fluctuations of a quantum field and an Hilbert space as the collection of all possible multi-particle states. However, not all physical states in a QFT are of this form. There are a variety of dynamical objects associated to extended field configurations which are not small fluctuations. For example, when a discrete symmetry spontaneously breaks, domain walls separate regions of space with different ground states. When a continuous symmetry spontaneously breaks, we can have vortices and strings, dynamical one-dimensional configurations. We can also have point-like objects like magnetic monopoles. All such configurations are non-trivial field configurations with finite energy. They can be stable or unstable. In the former case, stability is generally guaranteed by the conservation of a so called topological quantum number. Among the various extended field configurations, we focus in this chapter on the kink in 2d theories where a \mathbb{Z}_2 symmetry is spontaneously broken, the vortex in 3d where a $U(1)$ symmetry is spontaneously broken, and the 't Hooft-Polyakov magnetic monopole in a 4d gauge theory where $SU(2)$ is spontaneously broken to $U(1)$. We will then discuss some physical implications when fermions are present, like charge fractionalization and the appearance of fermion zero modes.

We can also have non-trivial stable field configurations with finite *action* in an Euclidean QFT. Such configurations are denoted instantons and will be discussed in chapter 5.

Configurations such as kinks, vortices and monopoles on one side, and instantons on the other side, are not unrelated as the Hamiltonian of a $d+1$ -dimensional Lorentzian theory and the action of an Euclidean d -dimensional theory formally coincide. Static finite energy configurations in $d+1$ dimensions (such as kinks and monopoles) can be interpreted as finite action configurations in d dimensions (instantons). We will comment from time to time about this correspondence in the next chapters.

We start in section 4.1 with a brief recap of homotopy theory and topological invariants, relevant to understand the topological nature of vortices and monopoles. In section 4.2 we use a scaling argument to classify possibly stable field configurations in various dimensions in presence of scalars and gauge fields. The considerations in these first two sections apply also to instantons. We discuss kinks in 2d in section 4.3 and vortices in 3d in section 4.4. In section 4.5 we discuss

monopoles. The detailed analysis of the 't Hooft-Polyakov monopole is left as an exercise for the reader, so in this section we provide a more general picture of monopoles and show how to classify magnetic charges in $4d$ gauge theories. In sections 4.6 and 4.7 we consider fermions in non-trivial backgrounds. We discuss the phenomenon of charge fractionalization for kinks in section 4.6 and the appearance of (chiral) zero modes in section 4.7. The last section includes a subsection with a brief review of the vielbein formalism, useful to study fermions in non-trivial backgrounds.

4.1 Homotopy groups and topological invariants

Topologically stable field configurations in asymptotically flat space are classified by homotopy theory. For this reason, it is useful to start this chapter with a brief review of this topic. The discussion will be heuristic, basic, and only a few essential aspects of homotopy necessary for the understanding of what follows will be addressed. See e.g. [18] for more details.

A connected d -dimensional manifold M is said to be multiply connected if there exists a closed path $p(t)$, with $p(0) = p(1)$, which cannot be contracted on M . The point $p_0 = p(0) = p(1)$ is called the base point. We say that the closed curve p_1 is homotopically equivalent to p_2 if they can be deformed to each other, namely if there exists a family of paths $p(t, y)$ such that $p(t, 0) = p_1(t)$, $p(t, 1) = p_2(t)$, $p(0, y) = p(1, y) = p_0$, for $0 \leq y \leq 1$. Homotopic equivalence is an equivalence relation: two closed curves are in the same class if and only if they are homotopically equivalent. The set of equivalence class forms a group known as the first homotopy group of the manifold and is denoted by $\pi_1(M)$. The group structure is defined as follows. If $p_1(t)$ and $p_2(t)$ are in the equivalence classes C_1 and C_2 , then

$$p_{12}(t) = \begin{cases} p_1(2t), & 0 \leq t \leq \frac{1}{2}, \\ p_2(2t - 1), & \frac{1}{2} \leq t \leq 1, \end{cases} \quad (4.1.1)$$

is in $C_1 \times C_2$. One can check that this product defines a group structure (associativity, unit element, inverse). For example, for $M = S^1$, the closed paths $\theta(t)$ with $\theta(0) = \theta_0$, $\theta(1) = \theta_0 + 2\pi n$ define the homotopy class n , namely how many times we wrap around the circle. Two closed curves with different values of n cannot be deformed to each other and hence cannot be homotopically equivalent. We then have

$$\pi_1(S^1) = \mathbb{Z}. \quad (4.1.2)$$

For manifolds M which can be written as direct products of manifolds, $M = M_1 \times M_2$, we have

$$\pi_1(M_1 \times M_2) = \pi_1(M_1) \times \pi_1(M_2). \quad (4.1.3)$$

A manifold M with $\pi_1(M) = \emptyset$ is called *simply connected*. Examples of notable simply connected manifolds are S^d , with $d > 1$, and the $SU(N)$ group manifolds. The global structure of the group

does matter. For example, $\pi_1(SO(N)) = \mathbb{Z}_2$ for $N \geq 3$, so $\pi_1(SO(3)) = \pi_1(SU(2)/\mathbb{Z}_2) \neq \emptyset$, while $\pi_1(SU(2)) = \emptyset$.

We can generalize homotopy groups by replacing closed curves, namely circles, by k -dimensional spheres S^k , with $k > 1$. In this case we have the homotopy groups $\pi_k(M)$. Consider S^k as the hypercube with boundaries identified, and base point p_0 a point at the boundary. The product of two mappings $p_1(t_i)$ and $p_2(t_i)$, $i = 1, \dots, k$, is defined as

$$p_{12}(t_i) = \begin{cases} p_1(2t_1, t_2, \dots, t_k), & 0 \leq t_1 \leq \frac{1}{2}, \\ p_2(2t_1 - 1, t_2, \dots, t_k), & \frac{1}{2} \leq t_1 \leq 1. \end{cases} \quad (4.1.4)$$

For all compact simple Lie groups G (not necessarily simply connected), we have

$$\pi_2(G) = \emptyset, \quad \pi_3(G) = \mathbb{Z}. \quad (4.1.5)$$

We also have

$$\pi_k(S^k) = \mathbb{Z}, \quad k \geq 1. \quad (4.1.6)$$

Given the coset G/H , if G is simple, compact, and simply connected ($\pi_1(G) = \emptyset$), we have

$$\pi_2(G/H) = \pi_1(H), \quad (4.1.7)$$

where H is a subgroup of G . The relation (4.1.7) will be important in the discussion of monopoles.

Kinks, vortices and monopoles are topologically stable configurations because they are charged under a so called topological current. In contrast to ordinary Noether currents, topological currents J_T^μ do not arise from an invariance of the action. They are so denoted because they are conserved for *any* field configuration, not necessarily on-shell. Moreover, the time component J_T^0 , whose integral over space gives the charge Q_T of the field configuration, turns out to be a total derivative, so that Q_T can be expressed as an integral over the boundary of space. We then get

$$Q_T = \int_{B_{d-1}} J_T^0 = \int_{S_\infty^{d-2}} \tilde{J}_T, \quad (4.1.8)$$

where the whole space is parametrized by the B_{d-1} ball, whose boundary is the $d-2$ sphere at infinity S_∞^{d-2} . In (4.1.8) $J_T^0 = \partial_r \tilde{J}_T$, r being a radial coordinate, and \tilde{J}_T is a function of the fields of the theory.¹ The integral (4.1.8) is topological invariant and measures the homotopy class of the homotopy group $\pi_{d-2}(G/H)$, where G/H is a coset space associated to a spontaneous symmetry breaking $G \rightarrow H$. The relation (4.1.8) can also be used in $d = 2$, recalling that $\pi_0(M)$ is the set of connected components of a manifold M . We cannot pass from a field configuration in one topological sector to another one without passing field configurations with infinite energy.

In many cases the topological charge (4.1.8), or equivalently the homotopy class of $\pi_{d-2}(G/H)$, is computed as the degree of the map $\Psi : X \rightarrow Y$, where $X = S_\infty^{d-2}$ and $Y = G/H$. This requires

¹This is the case for $d > 2$. In $d = 2$, $J_T^0 = \partial_x \tilde{J}_T$ and the last integral in (4.1.8) is replaced by two points, the contributions at $x = \pm\infty$.

that $\dim X = \dim Y$ and that both X and Y be orientable and closed. Let Ω be the volume form on Y , normalized so that

$$\int_Y \Omega = 1. \quad (4.1.9)$$

Then the degree \deg of a map Ψ is defined to be

$$\deg \Psi = \int_X \Psi^*(\Omega), \quad (4.1.10)$$

where Ψ^* is the pull-back of Ψ . The degree $\deg \Psi$ is a topological invariant. Under small deformations of $\Psi \rightarrow \Psi + \delta\Psi$, $\delta\Psi^*$ is an exact form on X and integrates to zero by the Stokes theorem. We can show the exactness of $\delta\Psi^*$ by an explicit computation. Let $y^i(x^j)$ be the functions representing the map Ψ and

$$\Omega = \beta(y) dy^1 \wedge \dots \wedge dy^d \quad (4.1.11)$$

the volume form on Y . Then

$$\Psi^*(\Omega) = \frac{\beta(y)}{d!} \epsilon_{i_1 \dots i_d} \partial_{j_1} y^{i_1} \dots \partial_{j_d} y^{i_d} dx^{j_1} \wedge \dots \wedge dx^{j_d}. \quad (4.1.12)$$

A small map deformation $\delta\Psi$ is represented by deformation functions δy^i . We have

$$\delta\Psi^*(\Omega) = \frac{\epsilon_{i_1 \dots i_d}}{d!} dx^{j_1} \wedge \dots \wedge dx^{j_d} \left(\frac{\partial \beta}{\partial y^k} \delta y^k \partial_{j_1} y^{i_1} \dots \partial_{j_d} y^{i_d} + \beta \sum_{k=1}^d \partial_{j_1} y^{i_1} \dots \partial_{j_k} \delta y^{i_k} \dots \partial_{j_d} y^{i_d} \right). \quad (4.1.13)$$

The quantities entering the sum in the second term of (4.1.13) can be written as

$$\begin{aligned} \beta \partial_{j_1} y^{i_1} \dots \partial_{j_k} \delta y^{i_k} \dots \partial_{j_d} y^{i_d} &= \partial_{j_k} \left(\beta \partial_{j_1} y^{i_1} \dots \delta y^{i_k} \dots \partial_{j_d} y^{i_d} \right) - (\partial_{j_k} \beta) \partial_{j_1} y^{i_1} \dots \delta y^{i_k} \dots \partial_{j_d} y^{i_d} \\ &= \partial_{j_k} (\dots) - \sum_{l=1}^d \frac{\partial \beta}{\partial y^l} \partial_{j_k} y^l \partial_{j_1} y^{i_1} \dots \delta y^{i_k} \dots \partial_{j_d} y^{i_d} \\ &= \partial_{j_k} (\dots) - \frac{\partial \beta}{\partial y^{i_k}} \delta y^{i_k} \partial_{j_1} y^{i_1} \dots \partial_{j_d} y^{i_d}, \end{aligned} \quad (4.1.14)$$

with the equalities valid when we antisymmetry in both j_1, \dots, j_d and i_1, \dots, i_d . Plugging (4.1.14) in (4.1.13) gives

$$\delta\Psi^*(\Omega) = \frac{\epsilon_{i_1 \dots i_d}}{d!} dx^{j_1} \wedge \dots \wedge dx^{j_d} \frac{\partial (\beta \partial_{j_1} y^{i_1} \dots \delta y^{i_k} \dots \partial_{j_d} y^{i_d})}{\partial x^{j_k}}, \quad (4.1.15)$$

proving the claim.

Whenever \tilde{J}_T can be interpreted as the pull back of a map Ψ , the topological charge Q_T equals the degree of the map Ψ . For example, the homotopy class of $\pi_1(S^1)$ is computed starting from the S^1 volume form $\Omega = d\theta/(2\pi)$, with $0 \leq \theta \leq 2\pi$. A map Ψ is given by functions $f(\theta)$

which take values on S^1 , namely $f(\theta) \sim f(\theta) + 2\pi n$, $n \in \mathbb{Z}$. We have

$$\deg \Psi = \frac{1}{2\pi} \int_0^{2\pi} \frac{df}{d\theta} d\theta = \frac{1}{2\pi} (f(2\pi) - f(0)) = n. \quad (4.1.16)$$

A particularly important class of maps are those where Y is a group manifold G . A volume form for a group manifold can be expressed in terms of the left-invariant Maurer-Cartan form $\theta_L = g dg^{-1}$, where $g \in G$:

$$\Omega = c \operatorname{Tr} \left(\theta_L \wedge \theta_L \wedge \dots \wedge \theta_L \right), \quad (4.1.17)$$

where c is a constant to be fixed to ensure the correct normalization of Ω . The map Ψ is given by $g = g(\theta^a)$, where θ^a are the angular variables of S_∞^{d-2} . Cyclicity of the trace implies that the degree of Ψ vanishes trivially for even d , so (4.1.17) is mostly useful when G is odd-dimensional. Since $S^1 \cong U(1)$, the map $S^1 \rightarrow S^1$ in (4.1.16) can be recast in terms of (4.1.17) with $G = U(1)$, taking $g = \exp(i\theta)$ and $c = i/(2\pi)$. A less trivial and particularly important case is $G = SU(2)$ where, as we will see in chapter 5, $\deg \Psi$ gives the instanton number. When X is a general closed manifold, not necessarily a sphere, $\deg \Psi$ measures the non-triviality of certain topological quantities denoted Chern classes.

The simplest symmetries and breaking patterns which give rise to topologically non-trivial configurations in d dimensions are given by those G and H such that $\pi_{d-2}(G/H) \neq \emptyset$. In $d = 2$ it is enough to have a discrete group, such as $G = \mathbb{Z}$, broken to nothing ($H = \emptyset$). In this case $\pi_0(G/H) = \pi_0(G) = G$. In $d = 3$, given (4.1.2), a simple choice is given by $G = U(1)$ broken again to nothing ($H = \emptyset$). In $d = 4$, using (4.1.7), a simple choice is given by $G = SU(2)$ and $H = U(1)$. Kinks, vortices, and monopoles are respectively an example of topologically stable field configurations in each of the above cases.

As we will see, for $d > 2$ gauge fields are necessary to get stable configurations with finite energy. In both $d = 3$ and $d = 4$, we work in the gauge

$$A_0^a = 0, \quad a = 1, \dots, \dim G. \quad (4.1.18)$$

For static, time-independent, field configurations the Hamiltonian density in the gauge (4.1.18) is proportional to $\operatorname{Tr} F_{ij}^2$, where $i, j = 1, \dots, d-1$ run over the spatial directions.

4.2 General considerations and a scaling argument for field configurations

Stable and static field configurations with finite energy are not generic features of QFTs in any dimension. In fact, a simple scaling argument (sometimes called Derrick theorem [19]) is enough to rule out their existence in various cases. Let us start by considering a theory with p scalar fields in $d = n + 1$ space-time dimensions (sums over i and a understood). The Hamiltonian reads

$$H = \int_{-\infty}^{\infty} d^n x \left(\frac{1}{2} (\partial_i \phi_a)^2 + V(\phi_a) \right), \quad i = 1, \dots, n, \quad a = 1, \dots, p. \quad (4.2.1)$$

The scalar potential is taken to be non-negative definite and vanishing on the global minimum of the theory (typically given by the trivial constant field configurations). Let $\bar{\phi}_a(x)$ be a putative static solution of the equations of motion of the fields ϕ_a with finite energy. We define

$$\begin{aligned} I_1 &\equiv \int_{-\infty}^{\infty} d^n x \frac{1}{2} (\partial_i \bar{\phi}_a)^2, \\ I_2 &\equiv \int_{-\infty}^{\infty} d^n x V(\bar{\phi}_a). \end{aligned} \tag{4.2.2}$$

Consider the rescaled configuration

$$\bar{\phi}_{\lambda,a}(x) = \bar{\phi}_a(\lambda x). \tag{4.2.3}$$

In terms of I_1 and I_2 defined above, its energy reads

$$\bar{H}_\lambda = \lambda^{2-n} I_1 + \lambda^{-n} I_2. \tag{4.2.4}$$

Since $\bar{\phi}_a$ is a static solution of the equations of motion, it should be an extremum of H . In particular

$$\left. \frac{d\bar{H}_\lambda}{d\lambda} \right|_{\lambda=1} = (2-n)I_1 - nI_2 = 0. \tag{4.2.5}$$

Since I_1 and I_2 are positive definite, (4.2.5) immediately implies that static, finite energy configurations involving scalar fields are possible only in $d = n + 1 \leq 3$ space-time dimensions. For $d = 3$, (4.2.5) implies $I_2 = 0$, hence non-trivial configurations require to have a continuous degeneracy of the potential. We check the stability of the configurations by computing the second derivative with respect to λ and ensure that it is not negative definite²

$$\left. \frac{d^2 \bar{H}_\lambda}{d\lambda^2} \right|_{\lambda=1} = (2-n)(1-n)I_1 + n(n+1)I_2 = 2(2-n)I_1, \tag{4.2.6}$$

where in the last step we plugged (4.2.5). We see that this is non-negative for $d \leq 3$.

Consider now a pure non-abelian gauge theory. Static configurations in the gauge (4.1.18) have Hamiltonian

$$H = \frac{1}{2g^2} \int d^n x \text{tr} F_{ij}^2, \tag{4.2.7}$$

with $F = dA - iA \wedge A$, in differential form notation and in a non-canonically normalized basis. Let $\bar{A}(x)$ be a solution to the equations of motion with finite energy and define

$$I_3 \equiv \int_{-\infty}^{\infty} d^n x \frac{1}{2g^2} \text{tr} \bar{F}_{ij}^2. \tag{4.2.8}$$

²This is only a necessary, but not sufficient, condition for stability, as an instability could arise in other directions in field space.

Then the rescaled configuration

$$\bar{A}_\lambda(x) = \lambda \bar{A}(\lambda x), \quad (4.2.9)$$

will have an action

$$H_\lambda = \lambda^{4-n} I_3, \quad (4.2.10)$$

and hence

$$\left. \frac{d\bar{H}_\lambda}{d\lambda} \right|_{\lambda=1} = (4-n)I_3. \quad (4.2.11)$$

For $n \neq 4$ we can have an extremum only if $I_3 = 0$. But the Hamiltonian (4.2.7) is positive definite, so $I_3 = 0$ implies $F_{ij} = 0$, the trivial solution. We conclude that pure gauge theories can admit static finite energy configurations only in $d = 5$ space-time dimensions.

Let us now consider the more general situations where we have both scalar and gauge fields together, with Hamiltonian

$$H = \int_{-\infty}^{\infty} d^n x \left(\frac{1}{2} (D_i \phi_a)^2 + V(\phi_a) + \frac{1}{2g^2} \text{tr} F_{ij}^2 \right). \quad (4.2.12)$$

Let again $\bar{\phi}_a, \bar{A}$ be finite energy solutions and $\bar{\phi}_\lambda, \bar{A}_\lambda$ their associated rescaled configurations like in (4.2.3) and (4.2.8). Similarly to before, we get

$$\left. \frac{d\bar{H}_\lambda}{d\lambda} \right|_{\lambda=1} = (2-n)I_1 - nI_2 + (4-n)I_3 = 0. \quad (4.2.13)$$

We can have non-trivial extended configurations only when the coefficients multiplying $I_{1,2,3}$ can have different signs, which fix $n \leq 3$. We check the stability

$$\left. \frac{d^2 \bar{H}_\lambda}{d\lambda^2} \right|_{\lambda=1} = (2-n)(1-n)I_1 + n(n+1)I_2 + (4-n)(3-n)I_3 = 2I_1(2-n) + 4I_3(4-n), \quad (4.2.14)$$

which is also verified.

The considerations above apply also for Euclidean finite action configurations (instantons) by replacing the Hamiltonian (4.2.1) with the action and identifying n with the total space-time dimensions. Summarizing, we have the following important results:

Static finite energy configurations are possible

1. in $d = 2$, and $d = 3$ if and only if the potential vanishes (scalar fields only).
2. in $d = 5$ (gauge fields only).
3. in $d = 2, 3, 4$ (gauge and scalar fields).

Finite action Euclidean configurations (instantons) are possible

1. in $d = 1$, and $d = 2$ if and only if the potential vanishes (scalar fields only).
2. in $d = 4$ (gauge fields only).

3. in $d = 1, 2, 3$ (gauge and scalar fields).

There are various way to circumvent the above no-go theorem. For example, one could consider time-dependent configurations, derivative interactions in scalar theories which would invalidate the above scaling argument, or simply be satisfied with a configuration which satisfies the equation of motion to a good approximation, but not exactly. The theorem does not apply to field configurations with infinite total energy but finite *energy density*, such as domain walls or strings, or in cases in which the potential is normalized differently, as it occurs for the bounces (see section 5.3).

We will discuss in these notes only field configurations which are topologically stable, but it is important to point out that there also exist topologically trivial field configurations which are stable for other reasons. A notable example are so called Q -balls. These are solitons charged under a global symmetry whose decay is kinematically forbidden. See e.g. [4] for an overview.

4.3 Kinks in 1+1 dimensions

Consider a scalar field theory in 1+1 dimensions with Lagrangian density

$$\mathcal{L} = \frac{1}{2}(\partial\phi)^2 - V(\phi), \quad (4.3.1)$$

where $V(\phi)$ is normalized such that $V = 0$ at the global minimum (or minima, in case of a degeneration). We want to look for classical *time-independent* field configurations $\bar{\phi}(x)$ which are solutions of the equation of motion

$$-\partial_x^2 \bar{\phi} + V'(\bar{\phi}) = 0, \quad (4.3.2)$$

where $V' = \partial_\phi V$, and for which the Hamiltonian

$$H = \int_{-\infty}^{\infty} dx \left(\frac{1}{2}(\partial_x \phi)^2 + V(\phi) \right) \quad (4.3.3)$$

is *finite*. Finiteness of the energy requires that for $x \rightarrow \pm\infty$, $\bar{\phi}(x)$ approaches one of the global minima of V , and moreover $\partial_x \bar{\phi}(x) \rightarrow 0$. If we replace x with time and V by $-V$, the problem reduces to a particle subject to a classical potential. If V has a unique global minimum at $\phi = \phi_0$, we immediately see that the only solution with finite energy is $\bar{\phi} = \phi_0$ for any x , i.e. the trivial solution with vanishing energy, see the upper panels of figure 4.1. On the other hand, if we have degenerate minima, we can have solutions that start from one minimum and monotonically move to another one. For large “times”, the “particle” will stay half of its time at $\phi = -\phi_0$ and then quickly move at $\phi = \phi_0$, where it will stay for the other half-time. See the lower panels of figure 4.1 for a two-fold degenerate potential. Such solutions are easily found by noticing that the energy

$$\frac{1}{2}(\partial_x \bar{\phi})^2 - V = E = 0 \quad (4.3.4)$$

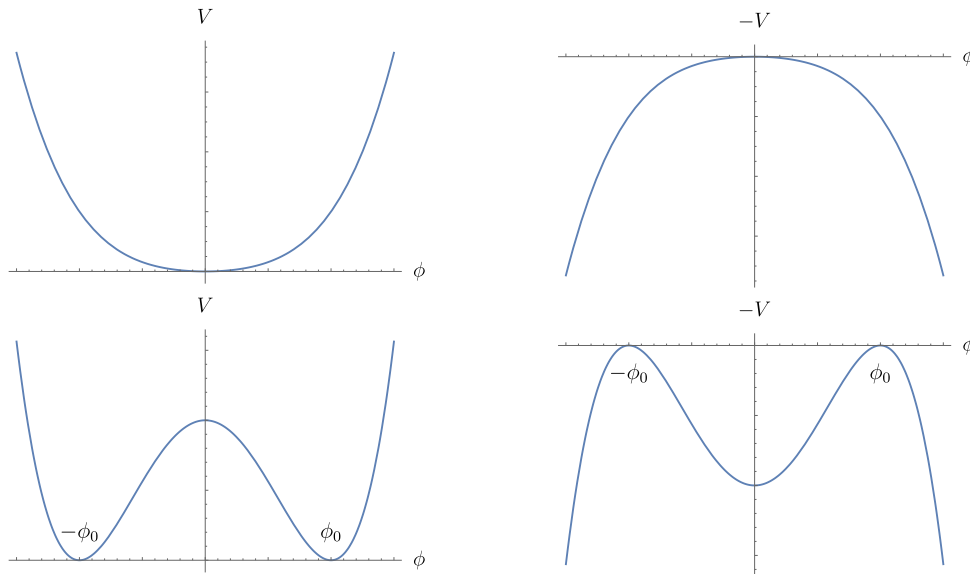


Figure 4.1: Bounded potential V and $-V$ with a unique global minimum (up) and with two degenerate minima (down).

is conserved and equals zero with our conventions for V . We then have

$$x = s \pm \int_{\phi_s}^{\bar{\phi}} d\phi (2V)^{-\frac{1}{2}}, \quad (4.3.5)$$

where $\bar{\phi}(s) = \phi_s$. We have a two-fold family of solutions parametrized by the real variable s , the integration constant in (4.3.5). They arise from the translation symmetry of the system: if $\bar{\phi}(x)$ is a viable configuration, so is $\bar{\phi}(x + s)$ for any s . We denote kink the finite energy configuration associated to $\bar{\phi}(x)$. The two-fold degeneracy coming from the \pm in (4.3.5) implies that for each kink we have an associated anti-kink configuration. The latter is the spatial reversal of the kink configuration.

The value of the Hamiltonian \bar{H} for a kink configuration $\bar{\phi}(x)$ equals

$$\bar{H} = \int_{-\infty}^{\infty} dx \left(\frac{1}{2} (\partial_x \bar{\phi})^2 + V(\bar{\phi}) \right) = \int_{-\infty}^{\infty} dx (\partial_x \bar{\phi})^2 = \int_{-\phi_0}^{\phi_0} d\phi \sqrt{2V(\phi)}, \quad (4.3.6)$$

where $\lim_{x \rightarrow \pm\infty} \bar{\phi}(x) = \pm\phi_0$. We now verify that $\bar{\phi}$ is stable under small perturbations $\delta\phi(x, t)$. The full equation of motion of the field ϕ reads

$$\square\phi + V'(\phi) = 0. \quad (4.3.7)$$

We have $\phi(x, t) = \bar{\phi}(x) + \delta\phi(x, t)$ and, to linear order in $\delta\phi$, (4.3.7) reads

$$\square\delta\phi + V''(\bar{\phi})\delta\phi = 0. \quad (4.3.8)$$

We decompose the fluctuations in modes:

$$\delta\phi(x, t) = \sum_n a_n e^{i\omega_n t} \psi_n(x) + c.c. \quad (4.3.9)$$

where a_n are complex coefficients and ψ_n satisfy the equations

$$-\partial_x^2 \psi_n + V''(\bar{\phi}) \psi_n = \omega_n^2 \psi_n. \quad (4.3.10)$$

The configuration $\bar{\phi}$ is stable if all the frequencies ω_n are real, i.e. the energy eigenvalues of the Schrödinger-like equation (4.3.10) has no negative-definite eigenvalues. We know that $\psi_1 = \partial_x \bar{\phi}$ is a valid perturbation, because it is associated to spatial translations. Since it costs no energy to go from one configuration to a shifted one, $\omega_1 = 0$.³ The configuration $\bar{\phi}$ is monotonic from one vacuum to another, which implies that ψ_1 has no zero. But then ψ_1 has to be the state of lowest energy, all other fluctuations having $E_n > 0$. We conclude that all frequencies are real and the kink is stable under small fluctuations. Modes with zero frequency are called *moduli*. In the case at hand the modulus is a constant x_0 , which represents the position of the kink.

As we mentioned, for large x the configuration stays close to either ϕ_0 or $-\phi_0$. We can expand (4.3.7) around $\phi = \pm\phi_0$ for very large positive or negative x . The corresponding approximate solution reads

$$\begin{aligned} \bar{\phi}(x) &\approx -\phi_0 + ce^{\mu x}, & x \ll 0, \\ \bar{\phi}(x) &\approx \phi_0 - ce^{-\mu x}, & x \gg 0, \end{aligned} \quad (4.3.11)$$

where c is a positive integration constant and

$$\mu^2 = V''(\pm\phi_0). \quad (4.3.12)$$

We see that the kink is a localized object in space, with a width of order $1/\mu$. If we replace $\phi_0 \leftrightarrow -\phi_0$ we get an anti-kink.

Consider as an example the ϕ^4 theory with a negative squared mass term, i.e. in a classically \mathbb{Z}_2 broken phase:

$$V(\phi) = \frac{\lambda}{2} \left(\phi^2 - \frac{m^2}{\lambda} \right)^2, \quad (4.3.13)$$

with $m^2 > 0$ and $\lambda > 0$. The kink configurations is obtained by inverting (4.3.5). We have

$$\bar{\phi}(x) = \pm\phi_0 \tanh \left(m(x - x_0) \right), \quad (4.3.14)$$

where

$$\phi_0 = \sqrt{\frac{m^2}{\lambda}}, \quad \mu = 2m, \quad (4.3.15)$$

and x_0 is a real parameter characterizing the position of the kink. The minus sign in (4.3.14)

³This is verified by applying ∂_x to (4.3.2) to get (4.3.10) with $\psi_1 = \partial_x \bar{\phi}$ and $\omega_1 = 0$.

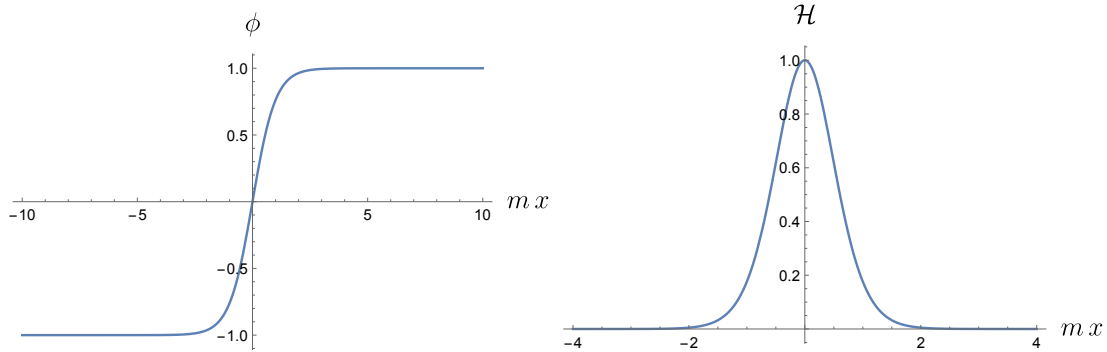


Figure 4.2: Kink profile (left) and energy density (right) as a function of x for the quartic scalar model. We have taken $\lambda = m^2$, and units of m for the energy density \mathcal{H} .

corresponds to the anti-kink configuration. We report in figure 4.2 the profile of a kink with $x_0 = 0$ (left) and its energy density

$$\mathcal{H} = \frac{m^2}{\lambda} \operatorname{sech}^4(mx), \quad (4.3.16)$$

as a function of mx (right). We see that most energy is concentrated in the region $\mu|x| \lesssim 1$, as expected. The total energy of the configuration equals

$$\bar{H} = \int_{-\infty}^{\infty} dx \mathcal{H} = \frac{4}{3} \frac{m^3}{\lambda}. \quad (4.3.17)$$

If we consider the kink as a sort a particle, \bar{H} should naturally be associated to its rest mass M_{kink} . By using the last identity in (4.3.6) we can reproduce (4.3.17) by performing an easier integral:

$$\bar{H} = M_{\text{kink}} = \int_{-\phi_0}^{\phi_0} \sqrt{2V} = \sqrt{\lambda} \phi_0^3 \int_{-1}^1 dt (1-t^2) = \frac{4}{3} \sqrt{\lambda} \phi_0^3 = \frac{4}{3} \frac{m^3}{\lambda}. \quad (4.3.18)$$

We see that at weak coupling $\lambda \ll m^2$, the kink mass is large and it blows up for $\lambda \rightarrow 0$, an indication that such excitation is not detectable by ordinary perturbation theory. We can also consider time-dependent field configurations (moving kinks). A general way to describe them, valid for slowly moving kinks, consists in giving a time-dependence to the moduli of the solution. In our case, $x_0 \rightarrow x_0(t)$ in (4.3.14). Then we plug the configuration into the action and integrate over x to obtain the effective theory for the light mode $x_0(t)$. We get

$$S = - \int dt M_{\text{kink}} + \int dt \int dx \frac{\dot{\phi}^2}{2} = - \int dt M_{\text{kink}} + M_{\text{kink}} \int dt \frac{\dot{x}_0(t)^2}{2}. \quad (4.3.19)$$

The equation of motion of x_0 is simply $\ddot{x}_0 = 0$, i.e. $x_0(t) = vt + y$. This is a configuration of a non-relativistic kink moving with velocity v and kinetic energy $M_{\text{kink}}v^2/2$.

In this simple case we can do better and get configurations of kinks moving at arbitrary speed u by applying a boost transformation to $\bar{\phi}(x)$ in (4.3.14):

$$\bar{\phi}_u(x, t) = \phi_0 \tanh\left(m \frac{x - x_0 - ut}{\sqrt{1 - u^2}}\right). \quad (4.3.20)$$

It is straightforward to verify that (4.3.20) satisfy the equation of motion (4.3.7). The energy associated to such configurations is

$$\bar{H}_u = \int_{-\infty}^{\infty} dx \left(\frac{1}{2} (\partial_x \bar{\phi}_u)^2 + \frac{1}{2} (\partial_t \bar{\phi}_u)^2 + V(\bar{\phi}) \right) = \frac{\gamma^2(1 + u^2) + 1}{2\gamma} \int_{-\infty}^{\infty} dx (\partial_x \bar{\phi})^2 = \gamma M_{\text{kink}}, \quad (4.3.21)$$

where $\gamma = 1/\sqrt{1 - u^2}$ is the usual Lorentz factor and we have used (4.3.6), a rescaling of x , and the fact that energy is conserved to set $t = 0$ and recast the computation in terms of the static configuration already computed. This is precisely the energy expected for a relativistic particle moving at the speed u . What about multi-kink states? Since kinks are well localized objects, we could construct approximate solutions of the equation of motion by superimposing kinks and anti-kinks. We say approximate because the equation of motion is not linear in ϕ and hence a superposition of solutions is in general not a solution. However, for well separated kinks and anti-kinks, the equation of motion will be satisfied with exponential accuracy. In contrast to ordinary multi-particle states, only combinations of kinks and anti-kinks alternating between each other are admissible configurations, compatibly with the boundary condition at infinity. Hence kinks and anti-kinks do not have proper multi-kink states. Even single kinks do not qualify as proper particles because after a scattering process they typically diffuse.

Kinks are topologically stable because they are charged under the topological current

$$J_T^\mu = c \epsilon^{\mu\nu} \partial_\nu \phi, \quad (4.3.22)$$

which is identically divergence free. The associated topological charge is

$$Q_T = \int_{-\infty}^{+\infty} dx J^0 = c \int_{-\infty}^{+\infty} dx \partial_x \phi = c [\phi(\infty) - \phi(-\infty)]. \quad (4.3.23)$$

We see that Q_T vanishes for trivial field configurations where the vacuum expectation value of ϕ is constant throughout space, but it is non-zero around the kink solution. We set

$$c = \frac{1}{2\phi_0}, \quad (4.3.24)$$

so that Q_T is integer-valued around kink or anti-kink solutions, taking values $Q_T = \pm 1$. Since kinks and anti-kinks have to alternate each other, we see that the topological charge Q_T can only take the values, $Q_T = 0, \pm 1$. Local fluctuations do not carry topological charge, so Q_T charge conservation is really a constraint on the dynamics of kinks and anti-kinks. For example, a configuration of a well separated kink and anti-kink in the far past has $Q_T = 0$ and hence can

decay in excitations around the trivial vacuum. In contrast, a configuration of separated kink, anti-kink and kink has $Q_T = 1$ and cannot lead to a trivial vacuum. A kink is then more than a particle, because small fluctuations around the kink lead to other excited states with the same Q_T . In fact kinks and anti-kinks give rise to different topological sectors.

We now show that kinks are stable because they are the field configurations with the lowest energy in the $Q_T = 1$ sector. In order to show this, we define a superpotential W such that

$$V = \frac{1}{2}(W')^2, \quad (4.3.25)$$

where V is the scalar potential of the $2d$ theory and $W' = \partial_\phi W$.⁴ We then have

$$\begin{aligned} H &= \int_{-\infty}^{\infty} dx \left(\frac{1}{2}(\partial_x \phi)^2 + V(\phi) \right) = \int_{-\infty}^{\infty} dx \frac{1}{2}(\partial_x \phi \pm W')^2 \mp \int_{-\infty}^{\infty} dx \partial_x \phi W' \\ &\geq \mp \int_{-\infty}^{\infty} dx \partial_x \phi W' = \mp \int_{-\phi_0}^{\phi_0} d\phi W' = |W(\phi_0) - W(-\phi_0)|. \end{aligned} \quad (4.3.26)$$

Kink configurations satisfies the linear equation

$$\partial_x \phi = \mp W', \quad (4.3.27)$$

which is nothing else but the square root of (4.3.4) and hence they saturate the bound. For example, for the quartic scalar potential (4.3.13) the superpotential reads

$$W = \sqrt{\lambda} \left(\frac{m^2}{\lambda} \phi - \frac{\phi^3}{3} \right). \quad (4.3.28)$$

With ϕ_0 as in (4.3.15) we immediately get in the $Q_T = 1$ sector

$$H \geq \frac{4m^3}{3\lambda} = \bar{H}, \quad (4.3.29)$$

where \bar{H} is the kink energy given in (4.3.17). The lower bound (4.3.26) is called Bogomolnyi bound and correspondingly (4.3.27) are denoted Bogomolnyi equations.

The analysis above can be repeated for theories admitting more than two degenerate vacua. A particular relevant example is provided by the Sine-Gordon theory, where we have an infinite number of degenerate vacua. Stable, finite energy configurations in the Sine-Gordon theory are denoted solitons. In contrast to kinks, they survive after collision. The Sine-Gordon theory is interesting for other reasons, but it will not be discussed here.

We finally comment on an important aspect of kinks, which applies for higher dimensional theories. The kink can be seen as a field configuration which splits space (a line in 1+1 dimensions) in two regions. Sufficiently far away from the kink, the field configuration is constant in

⁴The name superpotential arises from the similarities of (4.3.25) with the formulas relating the scalar and the superpotential in supersymmetric theories.

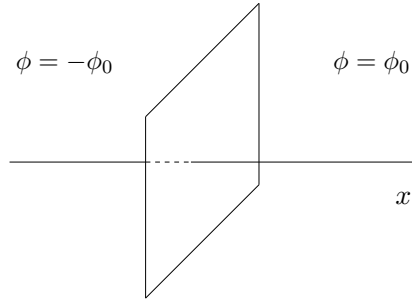


Figure 4.3: Domain wall interpolating between two different vacua. In the picture the thickness of the wall, given by the region where the kink energy density is non zero, has been neglected.

space and equals the trivial vacuum. We have equal and opposite vacuum expectation values in the two sides of the kink. The region of space where the kink energy density is not negligible defines a wall in space with a thickness of order $\Delta x \sim 1/m$. At distances $x \gg 1/m$ we can neglect the wall thickness and the kink looks like a codimension-1 *domain wall* in space. This interpretation holds in any number of space-time dimensions. As long as a \mathbf{Z}_2 symmetry is spontaneously broken, kink solutions interpolating between the two vacua exist and gives rise to domain walls, see fig. 4.3. For $d > 2$ kink configurations have necessarily infinite energy (recall section 4.2) but finite energy density per unit area, which corresponds to the domain wall tension. More in general, whenever a discrete symmetry is spontaneously broken domain walls between the different vacua are expected. If the symmetry is \mathbf{Z}_N , we have N vacua and in general different domain walls, depending on which vacua they separate. Domain walls can also cross to form codimension-2 junctions. See chapter 2 of [5] for further details on domain walls.

4.4 The 3d vortex

Vortices are topologically non-trivial field configurations, first found by Nielsen and Olesen [20], which can arise when a $U(1)$ symmetry is spontaneously broken. They are static, finite energy configurations of the abelian Higgs model in $2 + 1$ dimensions. The Hamiltonian density reads

$$\mathcal{H} = \frac{1}{4}F_{ij}^2 + \frac{1}{2}|D_i\phi|^2 + V(|\phi|), \quad i, j, = 1, 2, \quad (4.4.1)$$

where

$$D_i\phi = \partial_i\phi - ieA_i\phi, \quad V(|\phi|) = \lambda(|\phi|^2 - v^2)^2. \quad (4.4.2)$$

Finiteness of energy requires that $|\phi| \rightarrow v$ at spatial infinity S^1_∞ . Since $\pi_1(S^1) = \mathbb{Z}$, a topologically non-trivial solution is obtained when $\phi \rightarrow v \exp(i\theta)$, and θ wraps around the spatial circle. The associated charge is given by the topological current

$$J_T^\mu = c\epsilon^{\mu\nu\rho}\partial_\nu\phi^*\partial_\rho\phi, \quad \mu, \nu, \rho = 0, 1, 2, \quad (4.4.3)$$

with c an arbitrary constant. The current J_T^μ is locally a total derivative, so we have

$$Q_T = c \int d^2x \epsilon^{ij} \partial_i \phi^* \partial_j \phi = c \int_{S_\infty^1} d\theta (\phi^* \partial_\theta \phi - \partial_\theta \phi^* \phi), \quad (4.4.4)$$

where in the second equality we used radial coordinates with $0 \leq \theta \leq 2\pi$. Assuming that

$$\phi(x) \xrightarrow{|\vec{x}| \rightarrow \infty} v e^{in\theta}, \quad n \in \mathbb{Z}, \quad (4.4.5)$$

we get

$$Q_T = c 2inv^2 \int_0^{2\pi} d\theta = n, \quad c = \frac{1}{4i\pi v^2}. \quad (4.4.6)$$

The topological nature of the configuration is signalled by the charge n , which cannot be changed by small deformations. Under a $U(1)$ gauge transformation α , $\phi \rightarrow \exp(i\alpha)\phi$, $A \rightarrow A + d\alpha$. One would naively think that if at infinity $\alpha = -n\theta$, the topological charge could be removed and the asymptotic behaviour (4.4.5) would be trivialized. However, such gauge transformation is necessarily singular because smooth gauge transformations $\alpha(r, \theta)$ are necessarily single-valued under a 2π -rotation, i.e. $\alpha(r, 2\pi) = \alpha(r, 0)$.⁵ We conclude that regular gauge transformations cannot change the value of the topological charge Q_T . There is no need to consider asymptotic behaviours more general than (4.4.5), because they are all connected by regular gauge transformations. Indeed, consider two asymptotic behaviours $\phi \rightarrow \exp(if_{1,2}(\theta))\phi$ in the same topological sector, namely with $f_{1,2}(2\pi) - f_{1,2}(0) = n$, where $f_{1,2}$ are smooth arbitrary functions of θ . The difference function $f_{12} = f_1 - f_2$ is single-valued in θ and hence we can construct a smooth gauge transformation $\alpha(r, \theta)$ relating the two configurations with asymptotic behaviours f_1 and f_2 . Thanks to this property, in each winding sector n , we can choose the function $f(\theta) = n\theta$.

Having established that, modulo gauge transformations, (4.4.5) is the most general asymptotic behaviour to get non-trivial topological configurations, let us come back to check finiteness of energy. We know from the scaling argument of section 4.2 that finite energy solutions require a non vanishing gauge field profile, unless the potential V identically vanishes along the solution. But for the potential in (4.4.2), $V = 0$ identically only for the topologically trivial constant solution. It is however useful to identify the source of the divergence in the energy density. If we assume that $A_i = 0$, the only term to check is the scalar kinetic term. Passing to radial coordinates (r, θ) and recalling (4.4.5), we have

$$\int d^2x |D_i \phi|^2 = \int d^2x |\partial_i \phi|^2 = \int r dr d\theta \left[\frac{1}{r^2} (\partial_\theta \phi)^2 + (\partial_r \phi)^2 \right] \propto \int^\infty \frac{dr}{r} = \infty. \quad (4.4.7)$$

⁵For example, if we choose the gauge transformation $\alpha = -n\theta$ over the whole space, then we would have a constant, non-vanishing A_θ component, for any r . A regular connection should have a vanishing θ component when $r \rightarrow 0$ because $A_\theta = r(\cos\theta A_y - \sin\theta A_x)$, where $A_{x,y}$ are the Cartesian spatial directions.

In Cartesian coordinates, the asymptotic behaviour (4.4.5) for $n = 1$ can be written as

$$\partial_i \phi \xrightarrow{r \rightarrow \infty} -iv\epsilon_{ij} \frac{x_j}{r^2}. \quad (4.4.8)$$

We can cancel this asymptotic contribution, leading to a log divergent energy, by requiring that A_i approaches at infinity the value $-\epsilon_{ij}x_j/r^2$. In this way the covariant derivative $D_i\phi$ vanish at infinity sufficiently fast to give rise to finite energy configurations. Note that $-\epsilon_{ij}x_j/r^2$ is a pure gauge configuration leading to a vanishing field strength F_{ij} . This is a necessary condition in order to avoid a divergence from the integral of the F_{ij}^2 term in (4.4.1). We are finally led to the ansatz for the single vortex $n = 1$ configuration:

$$\begin{aligned} \phi &= ve^{i\theta} F(r), \\ A_i &= -\epsilon_{ij} \frac{x_j}{r^2} G(r), \end{aligned} \quad (4.4.9)$$

with

$$\lim_{r \rightarrow \infty} F(r) = 1, \quad \lim_{r \rightarrow \infty} G(r) = 1. \quad (4.4.10)$$

Smoothness of the solution requires also

$$\lim_{r \rightarrow 0} F(r) = 0, \quad \lim_{r \rightarrow 0} G(r) = 0. \quad (4.4.11)$$

Determining the explicit form of the functions F and G is non-trivial. It requires to solve the combined equations of motion for ϕ and A_i , which result in coupled second order differential equations. Such equations do not admit analytic solutions and can only be determined numerically. The equations depend on r and on two mass scales $m_W \sim ev$ and $m_H \sim \sqrt{\lambda}v$, the masses of the $U(1)$ gauge field and of the Higgs field in the broken phase. When $m_W \sim m_H$, the vortex has a mass of order m_W^2/e and a size of order $1/m_W$. Solutions with $n = -1$ corresponds to anti-vortices. Field configurations with $n > 1$ correspond to multiple vortices but they are in general not static solutions to the equations of motion, because vortices exert a force among them. Vortices attract or repel each other depending respectively on whether $m_H < m_W$ or $m_H > m_W$. We will not further discuss the interesting physics of vortices (see e.g. [6] for an extensive treatment). We simply comment that they play an important role in the physics of superconductivity. The abelian Higgs model is notably the EFT of superconductivity. An external magnetic field B cannot penetrate a superconductor up to some critical value B_c (Meissner effect). For $B > B_c$ superconductivity breaks down in two different ways, characterizing type I and type II superconductors. In type I, which have $e^2 > \lambda$, for $B > B_c$ superconductivity is lost and the magnetic field penetrates uniformly the material, which turns in an ordinary conducting phase. In type II, which have $e^2 < \lambda$, there exists instead a range $B_c \leq B \leq B'_c$, for some other critical value B'_c , where vortices form inside the superconductor. The material is still superconducting and the magnetic field is confined within the vortices. For $B > B'_c$ superconductivity is lost, vortices disappear and the material turns in an ordinary conductor.

The name vortex is due to the fact that in ordinary $3 + 1$ dimensions, such configurations, being independent of the third spatial direction, correspond to one-dimensional straight strings or straight thin vortices. For $d > 3$ vortex configurations have infinite energy but finite energy density per unit length, which corresponds to their string tension. More in general, whenever a $U(1)$ symmetry is spontaneously broken, vortices/strings can be generated.

4.5 Monopoles in $4d$

The spontaneous breakdown of discrete and $U(1)$ symmetries lead respectively to domain walls and strings in $4d$. In addition to such configurations, which have finite energy density but infinite total energy, we also have genuine finite energy point-like configurations, monopoles. The simplest instance of a monopole arises when a $SU(2)$ gauge theory is spontaneously broken to $U(1)$, first discussed by 't Hooft [21] and Polyakov [22]. Notably, the monopole carries a magnetic charge g_m with respect to the unbroken $U(1)$ symmetry. The electrically charged states in the theory are the W bosons, with charge $|e| = g$. Recall the Dirac quantization condition relating electrically and magnetically charged objects [23]:

$$2eg_m = n, \quad n \in \mathbb{Z}. \quad (4.5.11)$$

Magnetic monopoles and W bosons satisfy (4.5.11) with $|n| = 2$. Note that this is the minimal condition, because $U(1) \subset SU(2)$ and W bosons are in the adjoint representation of $SU(2)$. In general a field in the spin- j representation of $SU(2)$ give rise to states with $U(1)$ charges $e/g = -j, \dots, j - 1, j$. If we would add fields in the fundamental representation of $SU(2)$, then $e/g = -1/2, 1/2$ and (4.5.11) is satisfied with $|n| = 1$.

There also exist monopole configurations which are both magnetically and electrically charged, the so called *dyons*. They have been found in [24] by relaxing the constraint of having both static configurations and the gauge choice (4.1.18).⁶

Monopoles are stable finite energy configurations because they are charged under the topological current

$$J_T^\mu = \epsilon^{\mu\nu\rho\sigma} \epsilon_{abc} \partial_\nu \hat{\phi}^a \partial_\rho \hat{\phi}^b \partial_\sigma \hat{\phi}^c. \quad (4.5.12)$$

Their charge is associated to the non-triviality of the map at infinity $\hat{\phi} : S_\infty^2 \rightarrow S^2$, where $S^2 \cong SU(2)/U(1)$. All topologically stable configurations are given by $\pi_2(G/H)$. Using (4.1.2) and (4.1.7) we have $\pi_2(G/H) = \mathbb{Z}$. In addition to the monopole, which is in the homotopy class $n = 1$, we can have anti-monopoles with $n = -1$ and opposite magnetic charge. There are in general no static monopole solutions with $|n| > 1$. Intuitively this happens because monopoles exert a force among them. The leading interaction is due to their magnetic charge because the interaction induced by the Higgs scalar field and the W bosons decay exponentially with

⁶The two conditions are complementary, in the sense that we can either consider time-dependent field configurations keeping the gauge (4.1.18) or, as done in [24], choose another gauge different from (4.1.18). In the latter case $A_0^a \neq 0$, but conveniently all fields in the theory, including A_0^a themselves, remain time-independent.

Assignment n.2: 't Hooft-Polyakov monopole (4.5.1)

Consider an $SU(2)$ gauge theory coupled to a scalar field ϕ in the adjoint representation with a scalar potential $V(\phi)$. We are interested in finding finite energy, time-independent, solutions with $A_0^a = 0$ ($a = 1, 2, 3$). The Hamiltonian density reads

$$\mathcal{H} = \frac{1}{4}(F_{ij}^a)^2 + \frac{1}{2}(D_i\phi)^2 + V(\phi^2), \quad (4.5.2)$$

where

$$D_i\phi_a = \partial_i\phi_a + g\epsilon_{abc}A_i^b\phi_c, \quad V(\phi^2) = \lambda\left(\sum_{a=1}^3\phi_a\phi_a - v^2\right)^2, \quad (4.5.3)$$

with $\lambda, v > 0$. The theory is in a Higgs phase where $SU(2)$ is “spontaneously” broken to $U(1)$. Consider the following ansatz (monopole configuration)

$$\phi_a = v\hat{x}_a F(r), \quad A_i^a = \frac{1}{g}\epsilon_{aij}\frac{\hat{x}_j}{r}G(r), \quad \hat{x}_a = \frac{x_a}{r}, \quad r = |\vec{x}|, \quad (4.5.4)$$

where $F(r)$ and $G(r)$ are functions to be determined.

- (a) Plug the ansatz (4.5.4) in the Hamiltonian density (4.5.2). Determine the conditions to be imposed on the functions F and G and their first derivatives in order to have finite energy and smooth configurations.

- (b) Given that

$$Q = \frac{1}{8\pi} \int_{B_3} d^3x \epsilon_{ijk} \epsilon^{abc} \partial_i \hat{\phi}_a \partial_j \hat{\phi}_b \partial_k \hat{\phi}_c = 1, \quad (4.5.5)$$

where B_3 is the whole 3d space, show that the configuration (4.5.4) has magnetic charge

$$g_m = -\frac{1}{g} \quad (4.5.6)$$

with respect to the $U(1)$ field strength

$$\mathcal{F}_{\mu\nu} = F_{\mu\nu}^a \hat{\phi}_a - \frac{1}{g} \epsilon_{abc} \hat{\phi}_a D_\mu \hat{\phi}_b D_\nu \hat{\phi}_c. \quad (4.5.7)$$

- (c) Show that the monopole satisfies the Bogomolnyi bound

$$E \geq 4\pi v |g_m|, \quad (4.5.8)$$

where E is the energy and the equality holds asymptotically when $\lambda \rightarrow 0$ if

$$F_{ij}^a \mp \epsilon_{ijk} D_k \phi_a = 0. \quad (4.5.9)$$

Plug the ansatz (4.5.4) in (4.5.9) and find the two coupled linear order differential equations for F and G . Verify that

$$F = \coth \rho - \frac{1}{\rho}, \quad G = 1 - \frac{\rho}{\sinh \rho}, \quad \rho = grv, \quad (4.5.10)$$

is a solution (denoted BPS solution).

the distance. So monopoles repel each other, while a monopole and an anti-monopole attracts each other. As shown in point c) of the assignment (4.5.1), in the limit $\lambda \rightarrow 0$ the monopole saturates the Bogomolnyi bound (4.5.9) and admits the analytic solution (4.5.10), found by Prasad and Sommerfeld [25]. The Bogomolnyi-Prasad-Sommerfeld (BPS) limit is interesting because in the limit the scalar field becomes massless and its (attractive) force can compete with the magnetic interaction. In fact, in the limit the scalar force precisely cancels the repulsive magnetic interaction due to the $U(1)$ photon, so that two widely separated monopoles feel no force among them. In the BPS limit we can then have static multi-monopole solutions.⁷ See e.g. [6] for an account of how to construct multi-monopole solutions. The dynamics of monopoles is in general very complicated. We only mention here that slowly moving monopoles can be studied in the BPS limit by analyzing the motion on moduli space, assigning a time-dependence to their zero-mode fluctuations, as discussed below (4.3.18) in the kink case. See chapter 4 of [5] for an overview and chapter 8 of [6] for a detailed description.

Notably for the symmetry breaking $G = SU(2)_L \times U(1)_Y \rightarrow H = U(1)_{\text{em}}$, (4.1.7) does not apply (G is not simple) and monopoles cannot occur. The latter in general occur if we assume that the Standard Model group arises from an underlying simple group $G_{GUT} \supset G_{SM}$ which undergoes spontaneous symmetry breaking at the high scale M_{GUT} (grand-unified models). In the early universe, when the temperature $T \sim M_{GUT}$ and the breaking should have taken place, a plethora of monopoles and anti-monopoles should have been produced. In several models such monopole proliferation could give rise to cosmological problems, unless they annihilate with each other or an inflationary epoch dilutes their density.⁸ So far, no monopole has been detected yet.

Theoretically speaking, the t'Hooft-Polyakov like monopoles are very interesting because, in contrast to the original Dirac's monopole, they are smooth configurations. From an effective field theory point of view, magnetically charged states in a $U(1)$ theory do not necessarily require to introduce Dirac string singularities, but can be UV completed assuming that the $U(1)$ group arises from an underlying $SU(2)$, like in the $SU(2)$ Higgs model above. It is natural to conjecture that, whenever monopoles exist, they should be considered as (magnetically charged) particle states in the Hilbert space of the theory, very much like ordinary elementary particles. From this point of view, we could then assume that in a $U(1)$ gauge theory we can have all possible electrically and magnetically charged states, subject only to the constraint of the Dirac quantization condition (4.5.11).

Finding the explicit finite energy field configurations corresponding to 4d monopoles in more general set-ups (different gauge groups, matter fields, etc.) can be tedious. As in the $U(1)$ case, we can adopt a bottom-up approach which does not require an explicit construction of the UV monopole configuration. In this way we can generalize the study of $U(1)$ magnetic monopoles to a non-abelian group H and define non-abelian monopoles [26]. Given a theory with gauge

⁷Note that nowadays the acronym BPS is applied in a much wider context than the original $SU(2)$ 't Hooft-Polyakov monopole. In particular, it is used to denote generic supersymmetric configurations in supersymmetric field theories.

⁸A similar cosmological problem can occur with domain walls when a discrete symmetry is spontaneously broken.

group H , we can assume that we can always find a bigger group $G \supset H$, which we take simply connected, connected, and compact, and a set of Higgs fields in appropriate representations, such that G is broken to H . The group H is compact and taken to be connected. For simplicity, we also assume that H is semi-simple. The relation (4.1.7) applies and tells us that monopoles of H are classified by $\pi_1(H)$. The *global* structure of the gauge group matters. For example, take $SU(2)$ and $SO(3)$ gauge theories, which have the same gauge algebra. In the first case $\pi_1(SU(2)) = \emptyset$ and no topologically stable monopoles are allowed, while $\pi_1(SO(3)) = \mathbb{Z}_2$ and we have a non-trivial \mathbb{Z}_2 -valued magnetic charge. For this reason it is useful to write

$$H = \tilde{H}/k(\tilde{H}), \quad (4.5.13)$$

where \tilde{H} is the connected, simply connected, universal covering of H , and $k(\tilde{H}) \subseteq Z[\tilde{H}]$, where $Z[\tilde{H}]$ is the center symmetry of \tilde{H} . We have $\pi_1(\tilde{H}) = \emptyset$ and $\pi_1(H) \cong k(\tilde{H})$.

We want to determine the generalization of (4.5.11). To this purpose, recall that in a non-abelian theory the analogue of the charges are represented by the irreducible representations of the group. These are determined in terms of the weight lattice $\Lambda_w(H) \subseteq \Lambda_w(\tilde{H})$. More precisely, irreducible representations are in 1-1 correspondence to the coset $\Lambda_w(H)/W$, where W is the Weyl group of the Lie algebra \mathfrak{h} of H .⁹ It has been shown in [26] that the non-abelian generalization of (4.5.11) requires monopoles of H to sit in $\Lambda_w(H^*)/W$, where H^* is a *dual* group. The Lie algebra \mathfrak{h}^* of H^* is obtained by replacing simple roots α of \mathfrak{h} with the corresponding coroots α^\vee . Its global structure is

$$H^* = \tilde{H}^*/k(H^*), \quad k(H^*) = \Lambda_w(H)/\Lambda_r(H), \quad (4.5.14)$$

where \tilde{H}^* is the connected, simply connected, universal covering of H^* and Λ_r is the root lattice of H .

In order to clarify this rather abstract analysis, consider the case of simply laced A_n Lie algebras, where $\alpha^\vee = \alpha$, $\mathfrak{h}^* = \mathfrak{h} = \mathfrak{su}(\mathbf{N})$, and $\tilde{H} = \tilde{H}^* = SU(N)$. We take the global gauge group H as in (4.5.13) by choosing

$$k(\tilde{H}) = Z(\tilde{H}) = \mathbb{Z}_N. \quad (4.5.15)$$

The group $SU(N)/\mathbb{Z}_N$ is called $PSU(N)$ and corresponds to a gauge theory where the only allowed representations are those with N -ality zero. Since $\Lambda_w(H) = \Lambda_r(H)$, $k(H^*) = \emptyset$ and the dual group is $H^* = SU(N)$. In a $PSU(N)$ gauge theory monopoles can be in any representation of $SU(N)$. Since $\pi_1(H) = \mathbb{Z}_N$, not all such configurations are expected to be topologically stable. Yet, these are the most general configurations compatible with the generalized Dirac's condition. Consider now the opposite case where $H = SU(N)$ and $k(\tilde{H}) = \emptyset$. All representations in the H theory are allowed and hence $k(H^*) = \mathbb{Z}_N$. The dual group is now $H^* = PSU(N)$. The allowed monopoles should be in $SU(N)$ representations with N -ality zero. Since $\pi_1(H) = \emptyset$, all such

⁹Modding out by W is needed to ensure that we are in the Weyl chamber where all weights are positive definite.

configurations are topologically unstable. We see that $(H^*)^* = H$, which is true more generally.

The appearance of a dual magnetic group points towards a more democratic treatment between elementary particles and monopoles. The fact that monopoles appear as solitonic solutions could be an artefact of our Lagrangian description, and perhaps in some other description they appear as the fundamental particles (and possibly the latter play the role of the solitons). It turns out that such dualities do indeed exist, a notable example in 4d being the $\mathcal{N} = 4$ supersymmetric gauge theory. This duality will be analyzed in some detail in the SUSY II course.

We will further discuss monopole (and dyon) charges in chapters 5 and 6.

4.6 Charge fractionalization in presence of fermions

Dynamical fermions in presence of a soliton can give rise to the charge fractionalization effect, a phenomenon for which the soliton acquires a fractional charge. We discuss the effect for the $2d$ kink, where the analysis is simpler, but the phenomenon is more general. In particular it also occurs for vortices and monopoles, but we will not discuss these cases.

Consider a single Dirac fermion ψ in $2d$ coupled to a real scalar field ϕ through a Yukawa potential:

$$\mathcal{L} = \bar{\psi} i \not{\partial} \psi - g \phi \bar{\psi} \psi + \frac{1}{2} (\partial \phi)^2 - V(\phi), \quad (4.6.1)$$

where $V(\phi)$ is an even potential with two degenerate vacua at $\pm\phi_0$ leading to kink configurations and ψ a 2-component Dirac fermion. For concreteness, we choose as gamma matrices $\gamma^0 = \sigma_1$ and $\gamma^1 = i\sigma_2$, where $\sigma_{1,2,3}$ are the 2×2 Pauli matrices. Before discussing the solutions of the Dirac equation in the kink background $\bar{\phi}(x)$, let us quickly see the spectrum in the trivial vacuum where $\phi = \phi_0 > 0$. A non-trivial vacuum expectation value of ϕ gives a mass $m = g\phi_0$ to the fermions. The fermion field decomposes in waves (conventions as in [13])

$$\psi(x, t) = \int \frac{dp}{\sqrt{4\pi\omega}} \left(a(p) u_p e^{-i\omega t + ipx} + b^\dagger(p) v_p e^{i\omega t - ipx} \right), \quad (4.6.2)$$

In (4.6.2) $\omega^2 = p^2 + m^2$, $a, b, a^\dagger, b^\dagger$ are respectively annihilation and creation operators for particle and anti-particle, and u_p and v_p are spinors satisfying the equation $\not{p} u_p = m u_p$, $\not{p} v_p = -m v_p$. The Lagrangian (4.6.1) is invariant under $U(1)_V$ transformations

$$\psi \rightarrow e^{i\alpha} \psi, \quad \phi \rightarrow \phi, \quad (4.6.3)$$

and a \mathbb{Z}_2 axial transformation $\psi \rightarrow \sigma_3 \psi$, $\phi \rightarrow -\phi$. It is also invariant under parity and charge conjugation symmetry:¹⁰

$$\begin{aligned} P : \psi(x, t) &\rightarrow \psi^P(x, t) = \sigma_1 \psi(-x, t), & \phi(x, t) &\rightarrow \phi(-x, t), \\ C : \psi(x, t) &\rightarrow \psi^C(x, t) = \sigma_3 \psi^*(x, t), & \phi(x, t) &\rightarrow \phi^*(x, t). \end{aligned} \quad (4.6.4)$$

¹⁰It is also time reversal invariant, but we will not need to discuss this symmetry.

Let us now look for solutions of the Dirac equation in the kink background $\bar{\phi}(x)$. Since space translations are broken by the background, plane waves in the x -direction are no longer a convenient basis, but we can still use them along the time component. We then set

$$\psi_{1,2}(x, t) = e^{-i\omega t} \chi_{1,2}(x), \quad \psi = \begin{pmatrix} \psi_1 \\ \psi_2 \end{pmatrix}. \quad (4.6.5)$$

and write the Dirac equation for $\chi_{1,2}$ in components:

$$\begin{cases} \omega\chi_2 + i\chi_2' = g\bar{\phi}\chi_1, \\ \omega\chi_1 - i\chi_1' = g\bar{\phi}\chi_2. \end{cases} \quad (4.6.6)$$

Solutions of (4.6.6) with $\omega > 0$ correspond to multi-particle states in the Hilbert state, formed by the kink and the elementary fermion states. We are interested to possible solutions with $\omega = 0$, which are interpreted as a degeneracy of the kink spectrum. For $\omega = 0$, (4.6.6) can be rewritten as

$$\frac{d\chi_{\pm}}{\chi_{\pm}} = \pm g\bar{\phi}dx, \quad (4.6.7)$$

where $\chi_{\pm} = \chi_1 \pm i\chi_2$. Integrating, we get the zero mode solutions:

$$\chi_{\pm}(x) = c_{\pm} e^{\pm g \int_0^x \bar{\phi}(y) dy}, \quad (4.6.8)$$

where c_{\pm} are constants, fixed by normalization conditions. Since $\bar{\phi}$ approaches $\pm\phi_0$ as $x \rightarrow \pm\infty$, for large $|x|$

$$\int^x \bar{\phi}(y) dy \sim \phi_0 |x|. \quad (4.6.9)$$

The zero mode χ_+ is then non-normalizable and we have to set $c_+ = 0$. The solution χ_- is instead normalizable, and eventually we get a single zero mode which reads, up to a finite normalization constant,

$$\psi_0^k(x) = \begin{pmatrix} 1 \\ i \end{pmatrix} e^{-g \int_0^x \bar{\phi}(y) dy}, \quad (\text{kink}). \quad (4.6.10)$$

The zero mode around an anti-kink is obtained from ψ_0 by applying the parity transformation (4.6.4). Again, up to a normalization constant, we have

$$\psi_0^{\text{ak}}(x) = \begin{pmatrix} 1 \\ -i \end{pmatrix} e^{-g \int_0^x \bar{\phi}(y) dy}, \quad (\text{anti-kink}). \quad (4.6.11)$$

No zero modes appear in the trivial background ϕ_0 since the fermion spectrum is gapped by the mass m , i.e. $\omega \geq m$. More in general, we see that around any topologically trivial background, as $x \rightarrow \pm\infty$ $\bar{\phi}$ approaches either ϕ_0 or $-\phi_0$ in both limits. Therefore both χ_+ and χ_- will exponentially grow either for $x \rightarrow \infty$ or $x \rightarrow -\infty$, so both zero modes are non-normalizable. The zero modes (4.6.10) and (4.6.11) are both invariant under charge conjugation, $\psi_0^{\text{k,ak}} = \sigma_3(\psi_0^{\text{k,ak}})^*$

(they are Majorana spinors) so we have a single creation operator a^\dagger associated to it. Both kink and anti-kink are two-fold degenerate, we can have the kink state $|k\rangle$ with unoccupied zero energy level or the kink state $a^\dagger|k\rangle$ with occupied zero energy level (the same applies to the anti-kink).

If we normalize the charge Q under the $U(1)_V$ current of the vacuum to be vanishing, a direct computation leads to a fractional charge $Q = -1/2$ of the kink state. A similar result can be deduced by an indirect nice argument [4]. Suppose to start from the ground state in the topologically trivial sector and adiabatically change the background so that a kink and an anti-kink forms and move in opposite directions. Adopting a Dirac sea perspective, we have all negative energy levels occupied and all positive energy levels unoccupied in the trivial vacuum. As we slowly change the background, the fermion energy levels smoothly change. In particular we know that eventually two energy levels will approach zero, the two zero modes associated to kink and anti-kink. By charge conjugation symmetry, positive and negative energy levels move symmetrically, so one zero mode will arise from the positive energy spectrum and one from the negative energy spectrum. Eventually the system will be composed of either a kink and an anti-kink with one zero energy level occupied (either the one of the kink or of the anti-kink). Let us denote by $Q_e^{k,ak}$ the $U(1)_V$ charges of kink and anti-kink with empty zero energy level and by $Q_f^{k,ak}$ those with occupied zero energy level. The fermion state has unit charge so $Q_f^{k,ak} = Q_e^{k,ak} + 1$. The initial charge of the system vanishes, since we are in the trivial vacuum. So, assuming empty anti-kink sector (the choice does not matter) we have

$$Q_f^k + Q_e^{ak} = Q_e^k + Q_e^{ak} + 1 = 0. \quad (4.6.12)$$

By parity symmetry we must have $Q_e^k = Q_e^{ak}$, so necessarily

$$Q_e^k = Q_e^{ak} = -\frac{1}{2}. \quad (4.6.13)$$

This is the phenomenon of charge fractionalization. We start from a system with integer charges only (the fermions) and ended up with states (kink and anti-kink) with half-integer charge $\pm 1/2$ and a two-fold degeneracy. A link between charge fractionalization and 't Hooft anomalies will be discussed in section 6.4.2.

4.7 Chiral fermions from magnetic flux on S^2

In this section we show a relation between certain topological quantities and chiral fermions. We discuss a specific example of a famous theorem due to Atiyah and Singer, the index theorem [27], which applies more widely and relates the spectrum of differential operators to topological quantities defined on compact manifolds. Like in section 4.6 we focus on the Dirac equation of $2d$ fermions, but this time on the Euclidean S^2 sphere and coupled to a $U(1)$ gauge field. Since S^2 has curvature, we have to consider spinors in curved space-time. We start in section 4.7.1 by a brief recap on how to couple spinors in curved space-time for a general d -dimensional manifold

(this section can be read independently of the rest).

4.7.1 Spinors in curved space-times: vielbein formalism

Fermions are not in tensor product representations of the group $GL(d)$, namely they are not tensors. As a consequence we cannot introduce covariant derivatives made of Christoffel symbols to replace $\partial_\mu \rightarrow D_\mu$, because the $SO(d)$ spinor indices are “flat”. We have to rely on an alternative formalism in terms of vielbein fields. Given an Euclidean or Lorentzian d -dimensional manifold M_d , the key idea is to change the basis of vectors from the standard choice ∂_μ to the basis

$$E_a = E_a^\mu \partial_\mu, \quad E_a^\mu \in GL(d, \mathbb{R}), \quad (4.7.1)$$

such that the metric reads

$$g(E_a, E_b) = g_{\mu\nu} E_a^\mu E_b^\nu = \delta_{ab}, \quad (4.7.2)$$

where δ_{ab} is the flat metric (η_{ab} in a Lorentzian space). For concreteness we take in the following M_d to be an Euclidean manifold, the generalization to Lorentzian spaces being trivial. We also assume that there is no torsion. A vector field can be written as $V = V^\mu \partial_\mu = V^a E_a$, where

$$V^\mu = E_a^\mu V^a, \quad V^a = e_\mu^a V^\mu, \quad (4.7.3)$$

where e_μ^a is the inverse of E_b^μ : $e_\mu^a E_b^\mu = \delta_b^a$. We denote by e^a the one-forms dual to E_a :

$$e^a = e_\mu^a dx^\mu. \quad (4.7.4)$$

In components we have

$$g_{\mu\nu} = e_\mu^a e_\nu^b \delta_{ab}. \quad (4.7.5)$$

Since the metric in the E basis is flat, sometimes the indices a are denoted flat, to distinguish them from the ordinary basis with “curved” indices μ . The vielbeins e_μ^a are not uniquely defined, because any other choice $e_\mu^{a'}(x) = \Lambda_b^a(x) e_\mu^b(x)$, where Λ is an arbitrary x -dependent Lorentz transformation, leaves the metric (4.7.5) invariant. In this formalism we have essentially replaced diffeomorphism transformations with local Lorentz transformations. The advantage is clear since spinors are in representations of $SO(d)$. Moreover, the formalism is now identical with that used in non-abelian gauge theories. The covariant derivative is obtained by introducing a connection one-form ω such that $\partial \rightarrow D = \partial + \omega$. The connection is in the adjoint representation of $SO(d)$ so it transforms as

$$\omega \rightarrow \Lambda \omega \Lambda^{-1} - (d\Lambda) \Lambda^{-1}. \quad (4.7.6)$$

In components we have on vectors

$$D_\mu V^a = \partial_\mu V^a + \omega_\mu^a{}_b V^b. \quad (4.7.7)$$

Flat indices are lowered and raised with the flat metric: $\omega_{\mu}^a{}_b = \delta_{bc}\omega_{\mu}^{ac} = \omega_{\mu}^{ab}$. The $SO(d)$ adjoint representation is the antisymmetric tensor product of two fundamentals, so we have $\omega_{\mu}^{ab} = -\omega_{\mu}^{ba}$. A compatibility condition has to be imposed to ensure that the covariant derivative (4.7.7) is equivalent to that in terms of the Levi-Civita connection $\Gamma_{\nu\rho}^{\mu}$. We have

$$D_{\mu}V^a = \partial_{\mu}V^a + \omega_{\mu}^a{}_b V^b = e_{\nu}^a \nabla_{\mu}V^{\nu} = e_{\nu}^a (\partial_{\mu}V^{\nu} + \Gamma_{\mu\rho}^{\nu}V^{\rho}), \quad (4.7.8)$$

which is equivalent to impose $D_{\mu}e_{\nu}^a = 0$.¹¹ In contrast to connections A in gauge theories, the spin connection ω is not a fundamental field but is determined in terms of the vielbeins by means of (4.7.8). We can define a curvature two-form $R = d\omega + \omega \wedge \omega$. In mixed curved/flat components it reads

$$R_{\mu\nu}^{ab} = \partial_{\mu}\omega_{\nu}^{ab} - \partial_{\nu}\omega_{\mu}^{ab} + \omega_{\mu}^{ac}\omega_{\nu}^{cb} - \omega_{\nu}^{ac}\omega_{\mu}^{cb}. \quad (4.7.9)$$

For fermions the covariant derivative reads

$$D_{\mu}\psi_i = \partial_{\mu}\psi_i + \omega_{\mu}^{ab}(\Sigma_{ab})_{ij}\psi_j \quad (4.7.10)$$

where i is the spinor index ($i = 1 \dots, 2^{[d/2]}$ for a Dirac fermion) and Σ_{ab} are the Lorentz generators in the spinor representations. In terms of flat gamma matrices γ^a , they are given by

$$\Sigma_{ab} = \frac{1}{4}[\gamma_a, \gamma_b]. \quad (4.7.11)$$

Note that in curved space care should be paid between the usual constant gamma matrices γ^a , satisfying the Clifford algebra $\{\gamma^a, \gamma^b\} = 2\delta^{ab}$ and the curved x -dependent gamma matrices $\gamma^{\mu} = e_a^{\mu}\gamma^a$, which satisfy the anti-commutation relations $\{\gamma^{\mu}, \gamma^{\nu}\} = 2g^{\mu\nu}$.

4.7.2 Fermions on S^2

We are interested in determining the solutions of the massless Dirac equation

$$\gamma^a e_a^{\mu} D_{\mu}\psi = 0, \quad (4.7.12)$$

on the unit S^2 sphere. In (4.7.12) $\gamma_{1,2}$ are Euclidean gamma matrices chosen to be

$$\gamma^1 = \sigma_1, \quad \gamma^2 = \sigma_2. \quad (4.7.13)$$

The chirality matrix γ_3 is taken to be

$$\gamma_3 = -i\gamma^1\gamma^2 = \sigma_3. \quad (4.7.14)$$

¹¹The general relation is $de^a + \omega_b^a \wedge e^b = T^a$, where T^a is a torsion two-form.

Accordingly, the covariant derivative, including both gauge and spin connections, read

$$D = \partial + iA + \frac{i}{2}\omega\sigma_3. \quad (4.7.15)$$

We introduce spherical coordinates (θ_i, ϕ_i) ($i = N, S$), with $0 \leq \theta_i < \pi$, $0 \leq \phi_i < 2\pi$ on the two sets, so that $\theta_N = 0$ and $\theta_S = \pi$ represent the North and South poles of S^2 , respectively. Locally on each set $ds_i^2 = d\theta_i^2 + \sin^2\theta_i d\phi_i^2$. The two coordinate systems are related by the following transformations: $\theta_S = \pi - \theta_N$, $\phi_S = -\phi_N$. The spin connections on the two sets are

$$\omega_i = (1 - \cos\theta_i) d\phi_i, \quad (4.7.16)$$

and are related by a local $SO(2) \simeq U(1)$ Lorentz transformation: $\omega_S = \omega_N - 2d\phi_N$. By gluing northern and southern hemisphere one easily finds the Euler characteristic as an integral of a curvature two-form $R = d\omega$ ($\omega \wedge \omega = 0$ in $2d$):

$$\frac{1}{2\pi} \int_{S^2} R = \frac{1}{2\pi} \int_{\Sigma_N} d\omega_N + \frac{1}{2\pi} \int_{\Sigma_S} d\omega_S = \frac{1}{2\pi} \int_{S^1} (\omega_N - \omega_S) = \frac{1}{2\pi} \int_0^{2\pi} 2d\phi_N = 2, \quad (4.7.17)$$

where $S^2 = \Sigma_N \cup \Sigma_S$ and $S^1 = \Sigma_N \cap \Sigma_S$ is the equator $\theta_N = \theta_S = \pi/2$. A non-vanishing flux F is obtained by considering a gauge background proportional to the spin-connection:

$$A_i = \frac{\kappa}{2}\omega_i. \quad (4.7.18)$$

The constant κ is the magnetic flux on S^2 and must be an integer to have a well-defined $U(1)$ gauge field. We have

$$\frac{1}{2\pi} \int_{S^2} F = \kappa. \quad (4.7.19)$$

As we will show, κ turns out to be the number of left-moving minus the number of right-moving chiral fermions on S^2 in such a $U(1)$ background.

Fermion fields (of unit $U(1)$ charge) in the two sets are related by a local gauge and Lorentz transformation as

$$\psi^{(S)} = e^{i\phi_N(\kappa + \sigma_3)} \psi^{(N)}. \quad (4.7.20)$$

Given the form of the chirality matrix (4.7.14), the fermion ψ decomposes as follows in terms of left- and right-moving fields:

$$\psi^{(i)} = \begin{pmatrix} \psi_R^{(i)} \\ \psi_L^{(i)} \end{pmatrix}. \quad (4.7.21)$$

In both sets, the Dirac equation (4.7.12) reads

$$\gamma_1 \frac{\partial}{\partial\theta_i} + \frac{\gamma_2}{\sin\theta_i} \left[\frac{\partial}{\partial\phi_i} + \frac{i}{2}(1 - \cos\theta_i)(\kappa + \gamma_3) \right] \psi^{(i)} = 0. \quad (4.7.22)$$

A solution is found by setting

$$\psi_{L,R}^{(i)} = \rho_{L,R}^{(i)}(\theta) e^{iN_{L,R}^{(i)}\phi}, \quad (4.7.23)$$

in both sets, with $N_{L,R}^{(i)}$ integers. Modulo a normalization factor, one finds the following wave functions:

$$\begin{cases} \psi_L^{(i)} = (1 + \cos \theta_i)^{\frac{N_L^{(i)} + \kappa - 1}{2}} (1 - \cos \theta_i)^{-\frac{N_L^{(i)}}{2}} e^{iN_L^{(i)}\phi_i} \\ \psi_R^{(i)} = (1 + \cos \theta_i)^{-\frac{N_R^{(i)} + \kappa + 1}{2}} (1 - \cos \theta_i)^{\frac{N_R^{(i)}}{2}} e^{iN_R^{(i)}\phi_i} \end{cases}. \quad (4.7.24)$$

In order for the solutions to be normalizable on S^2 and well defined at $\theta_i = 0$, we must require that

$$N_R^{(i)} \geq 0, \quad N_L^{(i)} \leq 0, \quad i = N, S. \quad (4.7.25)$$

The local gauge+Lorentz transformation (4.7.20) implies

$$\begin{aligned} -N_L^{(S)} &= \kappa - 1 + N_L^{(N)}, \\ -N_R^{(S)} &= \kappa + 1 + N_R^{(N)}. \end{aligned} \quad (4.7.26)$$

The conditions (4.7.25) and (4.7.26) impose severe constraints on the allowed wave functions. For $\kappa < 0$, no left-handed fermions are allowed, whereas one has $|\kappa|$ right-handed fermions with $0 \leq N_R^{(N)} \leq -\kappa - 1$; on the contrary, for $\kappa > 0$ no right-handed fermions are allowed, whereas one has $|\kappa|$ left-handed fermions with $1 - \kappa \leq N_L^{(N)} \leq 0$. For $\kappa = 0$, no solution is allowed. We conclude that κ measures the total number of left-moving N_L minus right-moving N_R fermions, which is called the index of the Dirac operator:

$$\frac{1}{2\pi} \int_{S^2} F = \kappa = N_L - N_R. \quad (4.7.27)$$

The quantity κ is a topological invariant and cannot change under smooth deformations. As a consequence, while both N_L and N_R can vary under smooth deformations, their difference cannot. The relation (4.7.27) is a particular example of the Atiyah-Singer index theorem [27]. A similar result applies in higher dimensions and for more general compact manifolds with no boundaries. In any number of even dimensions, the index of the Dirac operator coupled to a gauge bundle G can be written in terms of the so called Chern character $\text{ch}(F)$, where $F = dA - iA^2$ is the field strength of the connection A of G , and of the so called roof genus $\hat{A}(R)$, where R is the curvature two-form. The Chern character and the roof genus are examples of characteristic classes, namely elements in cohomology classes of a manifold that measure the non-triviality of fiber bundles ($U(1)$ in the case of (4.7.27)). For a fermion in the representation r of G the Chern character is defined as

$$\text{ch}(F) = \text{tr}_r \exp\left(\frac{F}{2\pi}\right). \quad (4.7.28)$$

It is a generating functional for $2n$ -forms of the form $\text{tr}F^n$. Given a compact and closed manifold X_{2n} with dimension $d = 2n$, we are supposed to expand the exponential term and pick up the

top $2n$ -form. The expression

$$\int_{X_{2n}} \text{ch}(F) = \frac{1}{n!} \frac{1}{(2\pi)^n} \int_{X_{2n}} \text{tr}_r F^n \quad (4.7.29)$$

is a topological invariant and equals an integer. The expansion terms of the roof genus $\hat{A}(R) = 1 + \dots$ are $4j$ -forms, for $j = 0, 1, \dots$. We will not report here the definition of $\hat{A}(R)$ because it will not play a role in these lectures. Using these characteristic classes, we can write an index formula for the Dirac operator of a fermion in the representation r for a compact closed manifold X in any d :

$$\text{index } i\mathcal{D} = N_L - N_R = \int_X \text{ch}(F) \hat{A}(R), \quad (4.7.30)$$

where $N_{L,R}$ are the number of L, R massless chiral fermions on X . Evidently, (4.7.27) is an example of (4.7.30) for $X_2 = S^2$, $G = U(1)$. We will come back to (4.7.30) when we will discuss instantons in the next chapter 5.

The index theorem applies also to operators different from the Dirac one. See e.g. [18] for further details aimed at physicists.

Chapter 5

Instantons

Instantons are defined as solutions to the euclidean equations of motion with finite action. They play a crucial role in QFT as they are one of the few effects beyond perturbation theory which we are able to control to some extent.

From the point of view of the euclidean path integral, it is natural to consider their effect in correlation functions. From a mathematical point of view, ordinary perturbation theory corresponds to a saddle point approximation to the path integral, where we take the vacuum as leading saddle and the small fluctuations around it give rise to the loopwise expansion. However, other saddle points do in general contribute. Their contribution will be suppressed with respect to the trivial saddle by a factor of order $\exp(-S_0/\hbar)$, where S_0 is the action value at the saddle point (normalizing the action such that $S = 0$ for the leading saddle). This effect is manifestly invisible in perturbation theory and is exponentially suppressed at weak coupling. It can be important if, e.g., some selection rule forbids the perturbative contribution to the correlator, in which case this is the dominant effect, or to split some degeneracy present to all orders in perturbation theory.

From the point of view of the Lorentzian theory, instantons give rise to tunneling between degenerate vacua. The simplest occurrence of instantons is in quantum mechanics. We start in section 5.1 with this case and discuss in section 5.2 instantons in 4d gauge theories. In section 5.3 we discuss finite action configurations which describe tunnelling between non-degenerate vacua. These are called bounces and govern the decay amplitude of a meta-stable vacuum in QFT.

In presence of matter and gauge fields, instantons are possible for $d \leq 3$. Notable examples in $2d$ are instantons in the nonlinear $O(3)$ sigma model, the CP^N models, and the abelian Higgs model. Instantons in the latter model are related to the 3d vortices discussed in section 4.4. We will not consider these topics in the present lectures. Another notable example is given by so called monopole instantons in 3d QED, related to the $4d$ t'Hooft-Polyakov monopole analyzed in section 4.5.

5.1 Quantum mechanics

As we mentioned before, instantons are associated to tunneling events between degenerate vacua. According to the scaling arguments discussed in section 4.2, the simplest set-up where they can appear is in $d = 1$, quantum mechanics. It is pedagogically useful to introduce instantons in quantum mechanics first, because here their interpretation in terms of tunneling is manifest, the computations are technically much easier, and moreover we can understand tunneling by other means, such as the WKB approximation.¹ We consider a spin-0 particle with unit mass moving in a one-dimensional space with potential $V(x)$. The Hamiltonian reads

$$H = \frac{p^2}{2} + V(x). \quad (5.1.1)$$

In section 5.1.1 we practice with euclidean path integrals with the harmonic oscillator as an example of a potential with a unique global minimum. Instantons will be introduced in section 5.1.2, when we consider tunnelling between two vacua. Finally, in section 5.1.3 we consider instantons in periodic potentials.

5.1.1 Harmonic oscillator

Before discussing tunneling effects, it is useful to recall basics of path integral methods. We compute the transition amplitude

$$\langle q_0 | e^{-\frac{\beta H}{\hbar}} | q_0 \rangle = \mathcal{N} \int_{\substack{q(-\beta/2)=q_0 \\ q(\beta/2)=q_0}} \mathcal{D}q(t) e^{-\frac{S(q)}{\hbar}}, \quad (5.1.2)$$

where

$$S(q) = \int_{-\frac{\beta}{2}}^{\frac{\beta}{2}} dt \left(\frac{1}{2} \dot{q}^2 + V(q) \right) \quad (5.1.3)$$

is the euclidean action and \hbar is not set to one, given that we consider semi-classical expansions in \hbar in this section. We first consider the harmonic oscillator case where

$$V = \frac{1}{2} \omega^2 q^2. \quad (5.1.4)$$

There are several ways to compute (5.1.2). We adopt here a semiclassical computation, exact for the harmonic oscillator, which can more easily be generalized to interacting potentials. We look to the classical path \bar{q} satisfying the euclidean equation of motion $-\ddot{\bar{q}} + \omega^2 \bar{q} = 0$ with boundary conditions $\bar{q}(-\beta/2) = q(\beta/2) = q_0$. The unique classical solution is

$$\bar{q}(t) = q_0 \operatorname{sech} \left(\frac{\omega \beta}{2} \right) \cosh(\omega t). \quad (5.1.5)$$

¹The analysis in this section is inspired by chapter 7 of [3].

The action evaluated along this path equals

$$S(\bar{q}) = q_0^2 \omega \tanh\left(\frac{\omega\beta}{2}\right). \quad (5.1.6)$$

We split $q = \bar{q} + \sqrt{\hbar}\eta$, where η are the fluctuations around the classical trajectory, and we integrate over η :

$$\langle q_0 | e^{-\frac{\beta H}{\hbar}} | q_0 \rangle = \mathcal{N} e^{-\frac{S(\bar{q})}{\hbar}} \int_{\substack{\eta(\frac{-\beta}{2})=0 \\ \eta(\frac{\beta}{2})=0}} \mathcal{D}\eta(t) e^{-S(\eta)} = \mathcal{N} e^{-\frac{S(\bar{q})}{\hbar}} \det_0^{-\frac{1}{2}}(-\partial_t^2 + \omega^2), \quad (5.1.7)$$

where \mathcal{N} is a normalization constant to be determined, and the determinant is given by the product of all the eigenvalues of the eigenfunctions with the indicated boundary conditions, which we schematically denote by \det_0 . We determine \det_0 indirectly by computing the partition function of the harmonic oscillator:

$$Z(\beta) = \text{Tr}_{\mathcal{H}} e^{-\frac{\beta H}{\hbar}} = \int_{-\infty}^{\infty} dq_0 \langle q_0 | e^{-\frac{\beta H}{\hbar}} | q_0 \rangle = \mathcal{N} \int_P \mathcal{D}q(t) e^{-\frac{S(q)}{\hbar}} = \mathcal{N} \det_P^{-\frac{1}{2}}(-\partial_t^2 + \omega^2). \quad (5.1.8)$$

In contrast to (5.1.7), the determinant in (5.1.8) is given by eigenfunctions which are just periodic in β , with $q(-\beta/2) = q(\beta/2)$. We schematically denoted by \det_P the corresponding determinant. We proceed in this way because the evaluation of \det_P is easier than that of \det_0 .² We first match (5.1.8) with the known partition function of the harmonic oscillator to determine the path integral normalization \mathcal{N} and then use the result to determine \det_0 in (5.1.7). The periodic functions in β , eigenfunctions of $(-\partial_t^2 + \omega^2)$ are given by $\cos(2\pi nt/\beta)$, $\sin(2\pi nt/\beta)$, with $n \geq 1$, and the constant function, with eigenvalues $(4\pi^2 n^2/\beta^2 + \omega^2)$, $n \geq 0$. We have

$$\begin{aligned} \det_P^{-\frac{1}{2}}(-\partial_t^2 + \omega^2) &= \frac{1}{\omega} \prod_{n=1}^{\infty} \left(\frac{4\pi^2 n^2}{\beta^2} + \omega^2 \right)^{-1} = \frac{1}{\omega} \prod_{n=1}^{\infty} \frac{\beta^2}{4\pi^2} n^{-2} \left(1 + \frac{\omega^2 \beta^2}{4\pi^2 n^2} \right)^{-1} \\ &= \left(2 \sinh \frac{\beta\omega}{2} \right)^{-1} = \sum_n e^{-\beta\omega(n+1/2)} = Z(\beta), \end{aligned} \quad (5.1.12)$$

where we have used (5.1.11) and the identity

$$\prod_{n=1}^{\infty} \left(1 + \frac{x^2}{\pi^2 n^2} \right) = \frac{\sinh x}{x}. \quad (5.1.13)$$

We see that zeta-function regularization gives us the correct path integral normalization with $\mathcal{N} = 1$. It is now straightforward to determine \det_0 :

$$Z(\beta) = \int_{-\infty}^{\infty} dq_0 e^{-\frac{S(\bar{q})}{\hbar}} \det_0^{-\frac{1}{2}}(-\partial_t^2 + \omega^2) = \sqrt{\frac{\hbar\pi}{\omega}} \tanh^{-\frac{1}{2}}\left(\frac{\omega\beta}{2}\right) \det_0^{-\frac{1}{2}}(-\partial_t^2 + \omega^2), \quad (5.1.14)$$

²The direct evaluation of \det_0 is not actually difficult. We leave it as an exercise for the reader.

Zeta-function regularization A simple way to regulate infinities arising from the determinants in a path integral is provided by a zeta-function regularization. Recall the definition of the zeta function $\xi(s)$. For $\text{Re } s > 1$ we have

$$\xi(s) \equiv \sum_{n=1}^{\infty} n^{-s}. \quad (5.1.9)$$

By analytic continuation we can define the function everywhere in the complex plane, where it is holomorphic, with the exception of a simple pole at $s = 1$. In particular we have

$$\begin{aligned} \xi(0) &= -\frac{1}{2}, \\ \xi'(0) &= -\frac{1}{2} \log(2\pi). \end{aligned} \quad (5.1.10)$$

We can use these results to assign values to the otherwise divergent infinite products. We have

$$\begin{aligned} \prod_{n=1}^{\infty} c &= \exp\left(\log \prod_{n=1}^{\infty} c\right) = \exp\left(\sum_{n=1}^{\infty} \log c\right) = \exp\left(\log c \zeta(0)\right) = \frac{1}{\sqrt{c}}, \\ \prod_{n=-\infty}^{\infty} c &= c \left(\prod_{n=1}^{\infty} c\right)^2 = 1, \\ \prod_{n=1}^{\infty} n^a &= \exp\left(\log \prod_{n=1}^{\infty} n^a\right) = \exp\left(a \sum_{n=1}^{\infty} \log n\right) = \exp\left(-a \zeta'(0)\right) = (2\pi)^{\frac{a}{2}}. \end{aligned} \quad (5.1.11)$$

from which we get

$$\det_0^{-\frac{1}{2}}(-\partial_t^2 + \omega^2) = \sqrt{\frac{\omega}{\hbar\pi}} \frac{1}{\sqrt{2 \sinh(\omega\beta)}}. \quad (5.1.15)$$

For $\beta\omega \gg 1$,

$$\det_0^{-\frac{1}{2}}(-\partial_t^2 + \omega^2) \approx \sqrt{\frac{\omega}{\hbar\pi}} e^{-\frac{\omega\beta}{2}}. \quad (5.1.16)$$

We can check our computation taking the large β limit of (5.1.2):

$$\lim_{\beta \rightarrow \infty} \langle q_0 | e^{-\frac{\beta H}{\hbar}} | q_0 \rangle \approx e^{-\omega q_0^2} \sqrt{\frac{\omega}{\hbar\pi}} e^{-\frac{\omega\beta}{2}}. \quad (5.1.17)$$

On the other hand

$$\lim_{\beta \rightarrow \infty} \langle q_0 | e^{-\frac{\beta H}{\hbar}} | q_0 \rangle = \lim_{\beta \rightarrow \infty} \sum_n |\psi_n(q_0)|^2 e^{-\beta(n+1/2)} \approx |\psi_0(q_0)|^2 e^{-\frac{\omega\beta}{2}}, \quad (5.1.18)$$

where ψ_n are the wave functions of the harmonic oscillator at level n . We see that (5.1.17) matches (5.1.18) with the properly normalized ground state wave function.

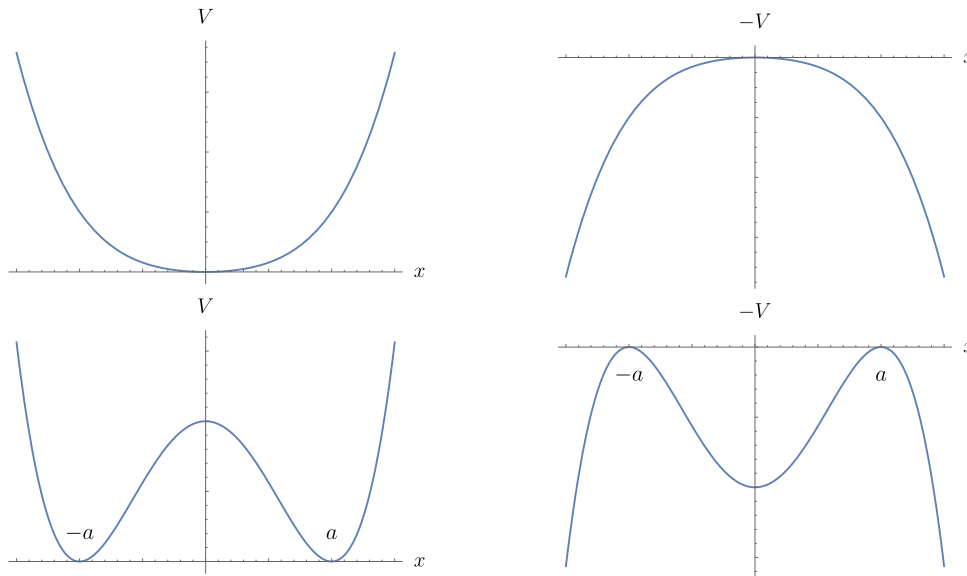


Figure 5.1: Bounded potential V and $-V$ with a unique global minimum (up) and with two degenerate minima (down).

Let us try to better understand the physical interpretation of the above results. In euclidean space we can use real time intuition provided we exchange the potential V with minus itself, see fig.5.1. The configuration (5.1.5) corresponds to motion along $-V$. The particle classically starts at the point x at $t = -\beta/2$, climbs the potential up to some point, and then turns back to reach again x at $t = \beta/2$. If we take $x = 0$, the only solution is $\bar{q} = 0$, and the particle stays there for ever. Quantum mechanically and for large β the amplitude $\langle x = 0 | e^{-\beta H} | x = 0 \rangle$ gives us the ground state energy and the probability to find the particle at the origin, as clear from (5.1.18).

More general bounded potentials with a unique global minimum (chosen to be at $x = 0$, where $V(0) = 0$) behave similarly. Although we cannot compute exactly the amplitude (5.1.2), the considerations made for the harmonic oscillator continue to apply up to $O(\hbar)$ corrections in a semiclassical expansion. There exists only one unique classical solution \bar{q} satisfying the boundary conditions, and again $\bar{q} = 0$ if $x = 0$. In a semi-classical expansion we get

$$\lim_{\beta \rightarrow \infty} \langle x = 0 | e^{-\frac{\beta H}{\hbar}} | x = 0 \rangle \approx \sqrt{\frac{\omega}{\hbar \pi}} e^{-\frac{\omega \beta}{2}} \left(1 + \mathcal{O}(\hbar) \right), \quad (5.1.19)$$

where

$$\omega^2 \equiv V''(0). \quad (5.1.20)$$

The classical solution (5.1.5) has finite action (also in the limit $\beta \rightarrow \infty$) and hence qualifies as an instanton. However, the euclidean configurations we are mostly interested in are transition amplitudes among classical vacua of the theory, and not generic transition amplitudes. For this reason in the next section we turn our attention to the more interesting cases with degenerate

vacua.

5.1.2 Symmetric double wells

We focus on even potentials, $V(x) = V(-x)$, and consider first the case of two minima at $x = \pm a$ where $V(\pm a) = 0$, as in the lower panels of figure 5.1. We are interested to compute the transition amplitudes

$$A_{\pm,+} \equiv \langle x = \pm a | e^{-\frac{\beta H}{\hbar}} | x = a \rangle. \quad (5.1.21)$$

By parity symmetry, we have $A_{-,-} = A_{+,+}$ and $A_{+,-} = A_{-,+}$, so we can drop the second subscript and simply write $A_{\pm} = A_{\pm,+}$. The leading contribution to A_{+} is given by $\bar{q} = a$ and the fluctuations around it. It can be read from (5.1.19), with $\omega^2 = V''(x = \pm a)$. There is no classical path contributing to A_{-} , but we know that quantum mechanically tunneling occurs. Even if we start with the particle at, say, $x = a$ at some real time t_0 , there is a non-vanishing probability to find it at $x = -a$ at some other real time $t = t_1$. At leading order in \hbar , the probability is given by the WKB formula

$$A_{-} \sim e^{-\frac{1}{\hbar} \int_{-a}^a dx \sqrt{2(V-E)}}, \quad (5.1.22)$$

where E is the classical energy of the configuration, vanishing in our case with the normalization chosen for V . In absence of tunnelling, we would have two degenerate ground states $|\pm\rangle$, each with a wave-function peaked around $x = \pm a$. Due to tunnelling, this degeneracy is broken and we get one ground state only.

From a euclidean perspective, the contribution (5.1.22) comes from the existence of other classical configurations contributing to the path integral (instantons). Their existence is clear from the lower right panel in fig.5.1. In addition to the obvious solutions $\bar{q} = -a$, a particle at $q = -a$ can move along the potential and reach $q = +a$ in finite time. For large β , the particle will stay half the time at $q = -a$ and then quickly move at $t \approx 0$ at $q = a$, where it will stay for the other half-time. In this case, in the normalizations chosen for V , we are dealing with a configuration with $E = 0$. Of course, we can consider the opposite situation of a particle starting at $q = a$ and move towards $q = -a$. We denote this configuration anti-instanton.

The reader might have recognized the close analogy between kink configurations in $1 + 1$ dimensions and instantons in 1 dimension (quantum mechanics). Mathematically speaking, we are facing the very same problem, as for large β the finite action solutions of (5.1.3) are identical to the finite energy configurations of (4.3.3), with the identifications $x \leftrightarrow t$ and $q(t) \leftrightarrow \phi(x)$. Although the physical implications are different, several technical results found for kinks in section 4.3 apply for instantons. We can determine the value of the action at the instanton configuration without knowing the explicit instanton solution by using the analogues of (4.3.4) and (4.3.6). We have

$$S(\bar{q}) = \int_{-\beta/2}^{\beta/2} dt \left(\frac{1}{2} \dot{\bar{q}}^2 + V(\bar{q}) \right) = \int_{-\beta/2}^{\beta/2} dt \dot{\bar{q}}^2 = \int_{-a}^a dx \sqrt{2V(x)}, \quad (5.1.23)$$

which is independent of \bar{q} . Note that $S(\bar{q})$ precisely coincides with the leading WKB factor appearing in (5.1.22). The analogue of (4.3.11) reads

$$\begin{aligned}\bar{q}(t) &\approx -a + ce^{\omega t}, & t \ll 0, \\ \bar{q}(t) &\approx a - ce^{-\omega t}, & t \gg 0,\end{aligned}\tag{5.1.24}$$

where c is a positive integration constant. Instantons are localized objects in time (which is at the origin of their name), with a width of order $1/\omega$.

Consider for example the symmetric double well with potential

$$V(q) = \frac{k^2}{2}(q^2 - a^2)^2,\tag{5.1.25}$$

where k is an arbitrary real constant. For $\beta \rightarrow \infty$, the solution with $\bar{q}(\infty) = a$, $\bar{q}(-\infty) = -a$ reads

$$\bar{q}(t) = a \tanh\left(\frac{\omega(t - t_0)}{2}\right), \quad \omega = 2ak,\tag{5.1.26}$$

where t_0 an arbitrary parameter defining the position of the instanton. Eq.(5.1.26) is nothing else but the static kink solution (4.3.13) with the appropriate identifications:

$$k^2 \rightarrow \lambda, \quad a \rightarrow \phi_0, \quad \omega \rightarrow \mu.\tag{5.1.27}$$

We can use (5.1.23) to get the instanton action:

$$S(\bar{q}) = \int_{-a}^a dx k(a^2 - x^2) = k(2 - 2/3)a^3 = \frac{4}{3}a^3k,\tag{5.1.28}$$

which again corresponds to the kink mass (4.3.17) with the identifications (5.1.27).

Like for kinks and anti-kinks, we expect to have other approximate semiclassical solutions when $\beta \rightarrow \infty$. For $\beta \rightarrow \infty$, instantons and anti-instantons can be centered around any arbitrary point in time, and if these are well separated, the corresponding configuration satisfies the equation of motion to exponential accuracy. A configuration of this kind describes a particle which starts at $q = -a$, moves at $q = a$, goes back at $q = -a$, and so on. Correspondingly we can have an infinite number of instantons and anti-instantons in series. We call the classical configuration where the particle moves n times from one vacuum to the other as n -instanton (and n -anti instanton the opposite series).

In a semi-classical expansion the transitions A_+ and A_- receive a contribution from a sum over all possible n -instantons, with n even and odd, respectively. For well separated instantons, the leading contribution of an n -instanton sector to the amplitude (A_+ or A_- , depending on n), denote it by $A^{(n)}$, equals the sum of the classical action of 1-instanton contributions, and is proportional to $\exp(-nS_0/\hbar)$, where $S_0 \equiv S(\bar{q})$ is the 1-instanton action. Since instantons are localized bumps in time, for most of the time the solution is either in the vacuum a or $-a$. The leading order contribution to the quantum fluctuations are then given by (5.1.19). In addition

to that, we have to consider the quadratic fluctuations around the instantons. In total we get

$$A_n \approx \sqrt{\frac{\omega}{\hbar\pi}} e^{-\frac{\omega\beta}{2}} e^{-\frac{nS_0}{\hbar}} \mathcal{K}^{(n)} \left(1 + \mathcal{O}(\hbar)\right). \quad (5.1.29)$$

where $\mathcal{K}^{(n)}$ denotes the remaining contribution coming from the quadratic fluctuations around the n -instantons. Let us first determine $\mathcal{K}^{(1)}$ by looking more closely to the quadratic fluctuations of the 1-instanton sector. The factor $\mathcal{K}^{(1)}$ is given by the determinant of the operator $(-\partial_t^2 + V''(\bar{q}))$, namely $\prod_n \lambda_n$, where λ_n are the eigenvalues of the orthonormal eigenfunctions q_n satisfying

$$-\ddot{q}_n + V(\bar{q})q_n = \lambda_n q_n. \quad (5.1.30)$$

However, care is needed to define the determinant. Because of time translation invariance in the limit $\beta \rightarrow \infty$, if $\bar{q}(t)$ is an instanton solution, so will be $\bar{q}(t - t_0)$, for any t_0 . Let us denote by q_1 the fluctuation associated to infinitesimal time shifts. This is given by $q_1 = \alpha \dot{\bar{q}}(t)$, with α a real parameter, which satisfies (5.1.30) with $\lambda_1 = 0$.³ A zero eigenvalue is problematic because it gives rise to a divergence in $\det^{-1/2}$. This zero arises because fluctuations in the direction q_1 are not “small”, but give rise to other instanton configurations centered at a shifted point. We should then integrate over all such configurations and consider the small fluctuations around them, removing the zero mode q_1 from the determinant. Integrating around small fluctuations mean integrating over the coefficients c_n entering in $q(t) = \bar{q}(t) + \sum_{n=1} c_n q_n(t)$. Before proceeding, let us fix the parameter α . We have

$$\bar{q}(t + dt) = \bar{q}(t) + \dot{\bar{q}}dt + \dots, \quad (5.1.31)$$

which implies that $\alpha dc_1 = dt$. On the other hand

$$1 = \int_{-\frac{\beta}{2}}^{\frac{\beta}{2}} dt q_1^2 = \alpha^2 \int_{-\frac{\beta}{2}}^{\frac{\beta}{2}} dt \dot{\bar{q}}^2 = \alpha^2 S_0 \longrightarrow \alpha = S_0^{-\frac{1}{2}}, \quad (5.1.32)$$

where in the last equality we used (5.1.23). The integral over dc_1 gives then a factor $\sqrt{S_0}\beta$. We have

$$A_1 \approx e^{-\frac{S_0}{\hbar}} \sqrt{S_0}\beta \left[\det'_0(-\partial_t^2 + V''(\bar{q})) \right]^{-\frac{1}{2}} \left(1 + \mathcal{O}(\hbar)\right), \quad (5.1.33)$$

where the ' in the determinant means that the zero mode has been removed from the product of eigenvalues. We can use (5.1.16) to rewrite (5.1.33) as

$$A_1 \approx \sqrt{\frac{\omega}{\hbar\pi}} e^{-\frac{\omega\beta}{2}} e^{-\frac{S_0}{\hbar}} \sqrt{S_0}\beta \sqrt{\left| \frac{\det_0(-\partial_t^2 + V''(a))}{\det'_0(-\partial_t^2 + V''(\bar{q}))} \right|} \left(1 + \mathcal{O}(\hbar)\right). \quad (5.1.34)$$

³This is the analogue of the mode ψ_1 defined below (4.3.10). Here however we are paying more attention to normalization factors which will be important in what follows.

Matching (5.1.34) with (5.1.29) with $n = 1$ gives

$$\mathcal{K}^{(1)} = \beta K, \quad K \equiv \sqrt{S_0} \sqrt{\left| \frac{\det_0(-\partial_t^2 + V''(a))}{\det'_0(-\partial_t^2 + V''(\bar{q}))} \right|} \left(1 + \mathcal{O}(\hbar)\right). \quad (5.1.35)$$

It is now straightforward to generalize the computation to get $\mathcal{K}^{(n)}$. The integral over the instanton centers gives a factor

$$\int_{-\frac{\beta}{2}}^{\frac{\beta}{2}} dt_1 \int_{-\frac{\beta}{2}}^{t_1} dt_2 \dots \int_{-\frac{\beta}{2}}^{t_{n-1}} dt_n = \frac{\beta^n}{n!}. \quad (5.1.36)$$

The $n!$ can also be understood by noting that instantons are indistinguishable from each other and hence we have to divide by their permutation to avoid overcounting. For well-separated instantons the contribution to small fluctuations around each instanton or anti-instanton factorizes and gives in total a factor of K^n . We then get

$$\mathcal{K}^{(n)} = \frac{\beta^n}{n!} K^n. \quad (5.1.37)$$

The amplitudes A_{\pm} are obtained by summing over all possible instanton contributions. In total we have

$$\begin{aligned} A_+ &\approx \sqrt{\frac{\omega}{\hbar\pi}} e^{-\frac{\omega\beta}{2}} \sum_{\text{even } n} \frac{(K\beta e^{-\frac{S_0}{\hbar}})^n}{n!} \left(1 + \mathcal{O}(\hbar)\right) = \sqrt{\frac{\omega}{\hbar\pi}} e^{-\frac{\omega\beta}{2}} \cosh(K\beta e^{-\frac{S_0}{\hbar}}) \left(1 + \mathcal{O}(\hbar)\right), \\ A_- &\approx \sqrt{\frac{\omega}{\hbar\pi}} e^{-\frac{\omega\beta}{2}} \sum_{\text{odd } n} \frac{(K\beta e^{-\frac{S_0}{\hbar}})^n}{n!} \left(1 + \mathcal{O}(\hbar)\right) = \sqrt{\frac{\omega}{\hbar\pi}} e^{-\frac{\omega\beta}{2}} \sinh(K\beta e^{-\frac{S_0}{\hbar}}) \left(1 + \mathcal{O}(\hbar)\right). \end{aligned} \quad (5.1.38)$$

We denote by $|1, 2\rangle$ the first two energy levels of the system. The ground state $|1\rangle$ is parity even, while the first excited state $|2\rangle$ is parity odd. For large β we have

$$\begin{aligned} A_+ &\approx |\psi_1(a)|^2 e^{-\beta E_1} + |\psi_2(a)|^2 e^{-\beta E_2} + \dots \\ A_- &\approx |\psi_1(a)|^2 e^{-\beta E_1} - |\psi_2(a)|^2 e^{-\beta E_2} + \dots \end{aligned} \quad (5.1.39)$$

We match (5.1.38) with (5.1.39) to get

$$\begin{aligned} E_1 &\approx \left(\frac{\hbar\omega}{2} - \hbar K e^{-\frac{S_0}{\hbar}}\right) \left(1 + \mathcal{O}(\hbar)\right), \\ E_2 &\approx \left(\frac{\hbar\omega}{2} + \hbar K e^{-\frac{S_0}{\hbar}}\right) \left(1 + \mathcal{O}(\hbar)\right), \\ |\psi_1(a)|^2 &= |\psi_2(a)|^2 \approx \frac{1}{2} \sqrt{\frac{\omega}{\hbar\pi}} \left(1 + \mathcal{O}(\hbar)\right). \end{aligned} \quad (5.1.40)$$

Crucially, the very same $\mathcal{O}(\hbar)$ perturbative corrections affect both E_1 and E_2 , so their splitting

is given by

$$E_2 - E_1 \approx 2\hbar K e^{-\frac{S_0}{\hbar}} \left(1 + \mathcal{O}(\hbar)\right). \quad (5.1.41)$$

5.1.3 Periodic potentials

We discuss in this section tunnelling effects in periodic potentials with

$$V(x) = V(x + 1). \quad (5.1.42)$$

This is interesting because it has some relation to instantons in 4d gauge theories. The minima are set at integer values of x and V is normalized such that $V(0) = 0$. Classically we have an infinite number of minima. Quantum mechanically, due to tunnelling, we expect a continuous band of energy eigenstates. Let us see how this arises from instanton considerations. We compute the amplitude

$$A_{pq} \equiv \langle x = p | e^{-\frac{\beta H}{\hbar}} | x = q \rangle, \quad (5.1.43)$$

with p and q two arbitrary integers (vacua). We sum again over all possible n instanton and \bar{n} anti-instantons connecting the vacua p and q . Since an instanton induces a transition from p to $p + 1$ and an anti-instanton from p to $p - 1$, in summing over n and \bar{n} we have the constraint that $n - \bar{n} = p - q$. We impose the constraint by introducing a Lagrange multiplier α :

$$\delta_{n-\bar{n}, p-q} = \frac{1}{2\pi} \int_0^{2\pi} d\alpha e^{i\alpha(n-\bar{n}+q-p)}. \quad (5.1.44)$$

Using the results of section 5.1.2 we have (omitting to write the $\mathcal{O}(\hbar)$ corrections)

$$\begin{aligned} \langle x = q | e^{-\frac{\beta H}{\hbar}} | x = p \rangle &= \int_{\substack{q(-\beta/2)=p \\ q(\beta/2)=q}} \mathcal{D}q(t) e^{-S(q)} \approx \sqrt{\frac{\omega}{\hbar\pi}} e^{-\frac{\omega\beta}{2}} \sum_{n, \bar{n}=0}^{\infty} \int_0^{2\pi} \frac{d\alpha}{2\pi} e^{i\alpha(n-\bar{n}+q-p)} \frac{(K e^{-\frac{S_0}{\hbar}} \beta)^{n+\bar{n}}}{n!\bar{n}!} \\ &= \sqrt{\frac{\omega}{\hbar\pi}} e^{-\frac{\omega\beta}{2}} \int_0^{2\pi} \frac{d\alpha}{2\pi} e^{2K e^{-\frac{S_0}{\hbar}} \beta \cos \alpha} e^{i\alpha(q-p)}, \end{aligned} \quad (5.1.45)$$

where $\omega^2 = V''(n)$, $n \in \mathbb{Z}$. The lowest energy states form a band $|\alpha\rangle$ parametrized by the angle α , with

$$E(\alpha) \approx \frac{\hbar\omega}{2} - 2\hbar K e^{-\frac{S_0}{\hbar}} \cos \alpha, \quad \psi_\alpha(x = q) \approx \left(\frac{\omega}{\hbar\pi}\right)^{\frac{1}{4}} \frac{e^{iq\alpha}}{\sqrt{2\pi}}, \quad q \in \mathbb{Z}. \quad (5.1.46)$$

If we denote by $|n\rangle$ the approximate eigenstates around the minimum at $x = n$ in the limit where tunnelling is neglected, we see that

$$|\alpha\rangle \approx \sum_n e^{in\alpha} |n\rangle. \quad (5.1.47)$$

Which saddles? In a path integral approach, observables such as correlation functions of local operators, are given by integrating over all possible trajectories with given boundary conditions. Perturbation theory in \hbar (loopwise expansion) corresponds to a saddle-point approximation, where the path integral is evaluated keeping only the leading saddle point and studying fluctuations around it. In euclidean QFT instantons correspond to additional saddle points with higher action. So far we have tacitly assumed that including them in the evaluation is supposed to give a better approximation to the final result. In fact, this is generally the correct thing to do, but there are subtleties. Mathematically speaking, saddle-point approximation is based on the method of steepest-descent and requires an analytic continuation over complex field configurations to be properly defined. As such, we should in general look also for *complex* finite action solutions to the equations of motion (complex instantons) and not only to real ones. Moreover, it is not true that all saddle points contribute in saddle-point approximation. Which saddles are we then supposed to include and which ones should be neglected? For finite dimensional integrals we have a criterion based on Picard-Lefschetz theory (see e.g. section 3 of [28] for an elementary introduction aimed at physicists) to determine which saddles are supposed to contribute. In quantum mechanics, where we can get the results by other means, ordinary (real) instantons and multi instantons seem to always contribute. It can be shown that for bounded potentials, whenever the euclidean action has only a single global minimum and hence no real instantons, no complex instanton should be considered. The perturbative saddle in this case captures all the observables (namely the associated divergent series is Borel resumable). For path integrals in QFT the situation is less clear and we do not have a complete understanding at the moment. Note that complex instantons, even when they should not be included in the evaluation of an observable, are useful to determine the large order behaviour of the perturbative series expansion.

In quantum mechanics tunnelling events are generally responsible for a restoration of an otherwise spontaneously broken symmetry. A common lore states that no symmetry (continuous or discrete) can be spontaneously broken in quantum mechanics. This lore is actually wrong. There are situations where tunnelling is suppressed (exactly) and degenerate vacua persist quantum mechanically. The underlying reason for this is the presence of an anomaly that forbids to have a single gapped vacuum. We will discuss a specific example of this phenomenon in section 6.4.2.

5.2 Instantons in $4d$ non-abelian gauge theories

We are now ready to discuss instantons in QFT. From the analysis in section 4.2 we know that instantons in pure gauge theories can only appear in $d = 4$. We consider in this section in some detail instantons in pure $4d$ $SU(2)$ non-abelian gauge theories. They were first found in [29, 30] and were earlier dubbed “pseudo-particles”, but afterwards the name instanton took over. We can determine the topological properties of instantons before constructing the explicit form of

its solution $\bar{A}(x)$. Consider a pure non-abelian gauge theory with Euclidean action

$$S = \frac{1}{2g^2} \int d^4x \operatorname{tr} F_{\mu\nu} F^{\mu\nu}, \quad (5.2.1)$$

where $\mu, \nu = 1, 2, 3, 4$, with 4 being the euclidean time direction. We will make use of an index-free differential form notation. Recall that in a Riemannian four-dimensional space the Hodge dual operation $*$ is such that $*^2 = 1$ on two-forms, and

$$\frac{1}{2} F_{\mu\nu} F^{\mu\nu} d^4x = F \wedge *F. \quad (5.2.2)$$

We can then write the following Bogomolnyi-like inequalities starting from the action (5.2.1):

$$S = \frac{1}{g^2} \int \operatorname{tr} F \wedge *F = \frac{1}{2g^2} \int \operatorname{tr} (F \pm *F) \wedge *(F \pm *F) \mp \frac{1}{g^2} \int \operatorname{tr} F \wedge F \geq \mp \frac{1}{g^2} \int \operatorname{tr} F \wedge F, \quad (5.2.3)$$

where we used that $*F \wedge *F = F \wedge F$. The equality in the second line of (5.2.3) holds if and only if

$$F = \mp *F, \quad (5.2.4)$$

namely for field configurations that are either self-dual (+) or anti self-dual (-). Instantons (anti-instantons) are field configurations saturating the bound which are self-dual (anti self-dual). The integral of $\operatorname{tr} F \wedge F$ appearing in (5.2.3) is a topological invariant, and hence instantons are the field configurations with the minimum action in a given topological sector. We now show that

$$\operatorname{tr} F \wedge F = d\Omega_3(A), \quad \Omega_3(A) = \operatorname{tr} \left(AdA - \frac{2}{3}iA^3 \right). \quad (5.2.5)$$

Acting with the exterior derivative on Ω_3 gives

$$\begin{aligned} d\Omega_3 &= \operatorname{tr} \left[(dA)^2 - \frac{2i}{3}(dAA^2 - AdAA + A^2dA) \right] \\ &= \operatorname{tr} \left[(F + iA^2)^2 - \frac{2i}{3}(F + iA^2)A^2 - A(F + iA^2)A + A^2(F + iA^2) \right] \\ &= \operatorname{tr} \left[F^2 + 2iFA^2 - \frac{2i}{3}3FA^2 \right] = \operatorname{tr} F^2, \end{aligned} \quad (5.2.6)$$

where we used that

$$\operatorname{tr} A^4 = 0, \quad (5.2.7)$$

and the cyclicity of the trace (paying attention in signs coming from the differential forms). We leave to the reader to prove (5.2.7). In order to have a finite action configuration, we require that $F \rightarrow 0$ at infinity, namely that the connection A approaches a pure gauge:

$$A \rightarrow igdg^{-1}, \quad (5.2.8)$$

with $g \in SU(2)$. We consider space-time in a $4d$ ball B_4 with radius approaching infinity. We then have, by Stokes theorem,

$$\int_{B_4} \text{tr} F \wedge F = \int_{\partial B_4} \Omega_3(A) = - \int_{S_\infty^3} \text{tr} \left(A(F + iA^2) - \frac{2}{3} iA^3 \right) = -\frac{i}{3} \int_{S_\infty^3} \text{tr} A^3, \quad (5.2.9)$$

where we have set $F = 0$ on S_∞^3 . Note that in (5.2.9) we have taken the orientation of S^3 such that $\partial B_4 = -S^3$, because this corresponds to an instanton in our conventions, as we will verify by an explicit computation below. Plugging (5.2.8) in (5.2.9) gives

$$\int_{B_4} \text{tr} F \wedge F = -\frac{1}{3} \int_{S_\infty^3} \text{tr} (gdg^{-1})^3, \quad (5.2.10)$$

which is of the form (4.1.10), with Ω the $SU(2)$ volume form. The arguments in section 4.1 ensure that (5.2.10) is invariant under small deformations and is in fact a topological invariant. Moreover, from (4.1.5) we have that $\pi_3(SU(2)) = \mathbb{Z}$ and hence the existence of topologically non-trivial configurations is guaranteed. The topologically trivial configuration corresponds to the map $g = I$, which gives a vanishing result for (5.2.10). A non-trivial map with winding number 1 from S^3 to $SU(2)$ is given by

$$g^{-1} = \sigma_\mu \hat{x}_\mu, \quad \hat{x}_\mu = \frac{x_\mu}{|x|}, \quad \sigma_\mu = (-i\sigma_k, I_2), \quad k = 1, 2, 3, \quad (5.2.11)$$

with σ_k the 2×2 Pauli matrices. We also have $g = \sigma_\mu^\dagger \hat{x}_\mu$, with $\sigma_\mu^\dagger = (i\sigma_k, I_2)$. The map (5.2.11) is uniform on S^3 , which means that we can compute it for any fixed value on S^3 . We choose the North pole $\hat{x}_4 = 1$, $\hat{x}_i = 0$, so that $gdg^{-1} = -i\sigma_k d\hat{x}_k$ and

$$\text{tr} (gdg^{-1})^3 = 6i \text{Tr} (\sigma_1 \sigma_2 \sigma_3) d\hat{x}_1 \wedge d\hat{x}_2 \wedge d\hat{x}_3 = -12 d\hat{x}_1 \wedge d\hat{x}_2 \wedge d\hat{x}_3. \quad (5.2.12)$$

Recalling that the volume of the unit 3-sphere equals $2\pi^2$, we get

$$\int_{B_4} \text{tr} F \wedge F = -\frac{1}{3} \times 2\pi^2 \times (-12) = 8\pi^2. \quad (5.2.13)$$

Given the map (5.2.11) we could alternatively compute the winding number by performing explicitly the integral over S^3 in (5.2.10). Check by an explicit computation that the map $g_2 = g^2$ has winding number 2. In general, the map $g_n = g^n$ has winding number n , with n any positive integer. Replacing $g \leftrightarrow g^{-1}$ gives the maps with winding number $-n$. The integer n is called instanton number. There are no other non-trivial configurations.

From a more mathematical point of view it is often convenient to consider closed compact spaces. We can do that by adding a point at infinity to turn \mathbb{R}^4 to S^4 . This is a non-trivial change, because S^4 is a non-trivial manifold. On S^4 (5.2.5) can only hold *locally*, otherwise by Stokes theorem we would always have a vanishing instanton number as $\partial S^4 = \emptyset$. The computation above would then be interpreted as follows. We split S^4 in two charts, corresponding to, say, the

northern and the southern “emispheres” B_N and B_S , topologically equivalent to $4d$ balls. We then have

$$\int_{S^4} \text{tr} F \wedge F = \int_{B_N} \text{tr} F \wedge F + \int_{B_S} \text{tr} F \wedge F = - \int_{S^3} \Omega_3(A_N) + \int_{S^3} \Omega_3(A_S), \quad (5.2.14)$$

the relative minus sign coming from the different orientations as $B_N \cup B_S = S^4$ has no boundary. We take $A_N = igdg^{-1}$, as in (5.2.8), while $A_S = 0$. In this way we reproduce the results above and see that instantons are associated to non-trivial fiber bundles, with fiber $SU(2)$ and base S^4 . Instantons can appear on more general base manifolds. It turns out that for an arbitrary closed and compact four-dimensional manifold X , we have

$$\frac{1}{8\pi^2} \int_X \text{tr} F \wedge F = n \in \mathbb{Z}. \quad (5.2.15)$$

The computation we performed is a special case of (5.2.15) with $X = S^4$ and $n = 1$. We also learn from (5.2.3) that the value of the action at the 1-instanton sector is

$$S_0 = \frac{8\pi^2}{g^2}. \quad (5.2.16)$$

Having an understanding of the asymptotic form of the instanton solution and its topological properties we can now look for the full solution. To this purpose it is convenient to introduce the 't Hooft symbols mixing spatial and $SU(2)$ indices:

$$\eta_{\mu\nu}^a = \begin{cases} \epsilon_{aij}, & \mu, \nu = i, j = 1, 2, 3 \\ \delta_{\mu a}, & \nu = 4 \\ -\delta_{\nu a}, & \mu = 4 \\ 0, & \mu = \nu = 4 \end{cases} \quad (5.2.17)$$

where ϵ_{ijk} is the totally antisymmetric 3-index with $\epsilon_{123} = 1$. The $\eta_{\mu\nu}^a$ satisfy the self-duality condition

$$\frac{1}{2} \epsilon_{\mu\nu\rho\sigma} \eta_{\rho\sigma}^a = \eta_{\mu\nu}^a, \quad (5.2.18)$$

where $\epsilon_{\mu\nu\rho\sigma}$ is the completely antisymmetric tensor in Euclidean space, with $\epsilon_{1234} = 1$. We also have $\eta_{\mu\nu}^a = -\eta_{\nu\mu}^a$. We leave to the reader to check the validity of (5.2.18). In order to find a suitable ansatz for the connection A , we rewrite the asymptotic form of the connection in Cartesian coordinates. We denote it A_∞ to distinguish it from the full-fledged connection A valid over all space-time. We have

$$A_\infty = i\sigma_\mu^\dagger \hat{x}_\mu \sigma_\nu d\hat{x}_\nu. \quad (5.2.19)$$

Using

$$\partial_\mu \hat{x}_\nu = \frac{\delta_{\mu\nu} - \hat{x}_\mu \hat{x}_\nu}{r}, \quad r^2 = x_\mu^2, \quad (5.2.20)$$

the connection in components reads

$$A_{\infty,\nu} = i\sigma_{\mu}^{\dagger}\sigma_{\rho}\hat{x}_{\mu}\frac{\delta_{\nu\rho} - \hat{x}_{\nu}\hat{x}_{\rho}}{r}. \quad (5.2.21)$$

We now use the relation (check left to the reader)

$$\sigma_{\mu}^{\dagger}\sigma_{\rho} = \delta_{\mu\rho} + i\eta_{\mu\rho a}\sigma_a \quad (5.2.22)$$

to rewrite (5.2.21) as

$$A_{\infty} = -\eta_{\mu\nu a}\sigma_a\hat{x}_{\mu}\frac{1}{r}. \quad (5.2.23)$$

The natural ansatz for a solution is then

$$\bar{A}_{\nu} = -\eta_{\mu\nu a}\sigma_a\hat{x}_{\mu}\frac{f(r)}{r}, \quad (5.2.24)$$

where $f(r)$ is an unknown function of the radial coordinate, subject to the boundary condition $\lim_{r \rightarrow \infty} f(r) = 1$. Given (5.2.24) we can determine with a bit of algebra the field strength $F = dA - iA^2$. To this purpose it is useful to use the identity

$$\eta_{\mu\rho b}\eta_{\nu\sigma c}\epsilon_{abc} = \delta_{\mu\nu}\eta_{\rho\sigma a} - \delta_{\mu\sigma}\eta_{\rho\nu a} - \delta_{\rho\nu}\eta_{\mu\sigma a} + \delta_{\rho\sigma}\eta_{\mu\nu a}. \quad (5.2.25)$$

Skipping elementary tedious steps, we have in components

$$\bar{F}_{\mu\nu} = 2\eta_{\mu\nu a}\sigma_a\frac{f(f-1)}{r^2} + (\eta_{\rho\nu a}\hat{x}_{\mu}\hat{x}_{\rho} - \eta_{\rho\mu a}\hat{x}_{\nu}\hat{x}_{\rho})\sigma_{\rho}\left(\frac{2f(1-f)}{r^2} - \frac{f'}{r}\right). \quad (5.2.26)$$

Instead of solving the equations of motion, we now impose the self-duality condition (5.2.4). Since self-dual configurations saturate the Bogomolnyi bound (5.2.2), we are guaranteed that the equations of motion will be automatically satisfied for (anti) self-dual configurations.⁴ The first term in (5.2.26) is manifestly self-dual thanks to the property (5.2.18), while the other terms are not. In order to have a self-dual configuration, we have then to set to zero the second term in (5.2.26). In this way we get the equation for f :

$$f' = \frac{2f(1-f)}{r}, \quad (5.2.27)$$

which admits the solutions

$$f(r) = \frac{r^2}{r^2 + \rho^2}, \quad (5.2.28)$$

for any $\rho^2 > 0$. The connection (5.2.24) together with (5.2.28) represent the $n = 1$ instanton solutions we were looking for. The total action and action density associated to the configuration

⁴In fact, for (anti) self-dual configurations the Bianchi identity turn into the equations of motion.

reads

$$S_0 = \frac{1}{2g^2} \int d^4x \operatorname{tr} \bar{F}_{\mu\nu} \bar{F}^{\mu\nu} = \frac{48}{g^2} \operatorname{Vol}(S^3) \int_0^\infty dr r^3 \frac{\rho^4}{(r^2 + \rho^2)^4} = \frac{8\pi^2}{g^2}, \quad (5.2.29)$$

where we used that $\operatorname{Vol}(S^3) = 2\pi^2$ and

$$\int_0^\infty dx \frac{x^3}{(1+x^2)^4} = \frac{1}{12}. \quad (5.2.30)$$

The parameter ρ sets the scale of the instanton, i.e. the scale where we have a non-trivial action density. Since pure Yang-Mills theories in $4d$ are classically scale invariant, we can have instantons of any size. We will briefly comment on the effect of the quantum breaking induced by the running coupling later on. The result (5.2.29) is nicely in agreement with (5.2.16), obtained using topological arguments.

There is no need to check the stability of the instanton solution, since it saturates the Bogomolnyi bound and hence cannot have fluctuations lowering its action. We can however have zero modes, whose number determine the dimensionality of the family of instanton solutions (dimension of the moduli space) and are important to determine the correct instanton measure (recall the quantum mechanical examples discussed in section 5.1). It turns out that $|n| = 1$ instantons have 8 independent zero modes, associated to i) 4 translations in space-time (the position of the instanton in space-time), ii) 1 associated to dilatation (the size of the instanton), iii) 3 associated to global $SU(2)$ rotations. The $SU(2)$ instanton solution we found can be embedded in higher rank gauge groups to give rise to instantons for more general gauge theories. Instanton solutions with $|n| > 1$ have also been constructed. The moduli space of n instantons in a $SU(m)$ gauge theory turns out to be $4nm$ -dimensional. A detailed study of multi-instantons and instanton moduli space go beyond these lectures. See e.g. [5, 6] for more details.

Instantons are supposed to describe tunneling effects between degenerate vacua. Which are these vacua? In quantum mechanics the initial and final vacua were the starting point of the analysis, and instantons connecting them were required to satisfy the appropriate boundary conditions at $x_4 = \tau = \pm\infty$. In Yang-Mills theory, we have more abstractly determined the instanton first and we can read off which vacua are connected by looking at the asymptotic behaviour of the instanton solution for $x_4 \rightarrow \pm\infty$. The analysis requires some care because we have to pay attention to gauge-fixing, which so far did not play any role. We will not elaborate on this, but only mention the final output of the procedure. A gauge-fixing which can be used to this purpose is the temporal gauge $A_0^a = 0$. In this gauge we expect

$$\lim_{\tau \rightarrow \pm\infty} A_i(\vec{x}, \tau) = g_\pm(\vec{x}) \partial_i g_\pm^{-1}(\vec{x}). \quad (5.2.31)$$

By exploiting the residual space-dependent gauge freedom, we can impose that both g_\pm approach a constant as $|\vec{x}| \rightarrow \infty$. This implies that spatial infinity is compactified to a 3-sphere. Let m_\pm be the homotopy classes of $g_\pm(\vec{x})$ associated to the group $\pi_3(SU(2)) = \mathbb{Z}$, where now the S^3 is the 3-sphere associated to ordinary space. An n -instanton configuration is associated to the

tunneling between the initial and final vacua with winding number m_- and m_+ :

$$m_+ - m_- = n. \quad (5.2.32)$$

The semi-classical leading order contribution to the tunneling is $\exp(-8\pi^2 n/g^2)$, non-perturbative in the coupling constant.

5.2.1 Theta vacua

In QFT we are interested in computing correlation functions of local operators. In a path integral approach in Euclidean space-time X this is written as

$$\langle \Psi \rangle = \frac{\int_X \mathcal{D}\phi e^{-S(\phi)} \Psi}{\int_X \mathcal{D}\phi e^{-S(\phi)}}, \quad (5.2.33)$$

where ϕ and Ψ denote very schematically all the fields in the theory (gauge fields included) and arbitrary products of local operators, respectively. We omitted to write gauge-fixing, ghosts, etc. since these issues are irrelevant for what follows. We have seen at the end of the last section that non-abelian gauge theories have degenerate ground states with different winding numbers $|m\rangle$. Transitions among such states are possible and are determined by instantons. However, since instantons are finite action configurations with a non-trivial topological number, one might think that we could forbid such transitions by simply demanding that in the path integral (5.2.33) we only consider the topologically trivial sector. We will soon see that this is not possible. More in general, let us sum over the topological sectors with instanton number n with a weight $f(n)$, where f is so far an arbitrary function. We replace (5.2.33) with

$$\langle \Psi \rangle = \frac{\sum_n f(n) \int_{X,n} \mathcal{D}\phi e^{-S(\phi)} \Psi}{\sum_n f(n) \int_{X,n} \mathcal{D}\phi e^{-S(\phi)}}, \quad (5.2.34)$$

where \int_n means performing the path integral restricted to the instanton sector n . Let us now split the space-time X in two regions X_1 and X_2 , and let us assume that the local operators in Ψ are all in region X_1 . We denote by $\phi_{1,2}$ the local operators in regions $X_{1,2}$. The sum over n splits then in $n = n_1 + n_2$, where $n_{1,2}$ are the topological sectors with instanton numbers $n_{1,2}$ in $X_{1,2}$:

$$\langle \Psi_1 \rangle = \frac{\sum_{n_1, n_2} f(n_1 + n_2) \int_{X_1, n_1} \mathcal{D}\phi_1 e^{-S_1(\phi_1)} \Psi_1 \int_{X_2, n_2} \mathcal{D}\phi_2 e^{-S_2(\phi_2)}}{\sum_{n_1, n_2} f(n_1 + n_2) \int_{X_1, n_1} \mathcal{D}\phi_1 e^{-S_1(\phi_1)} \int_{X_2, n_2} \mathcal{D}\phi_2 e^{-S_2(\phi_2)}}, \quad (5.2.35)$$

where by locality $S = \int_X \mathcal{L}(\phi) = \int_{X_1} \mathcal{L}(\phi_1) + \int_{X_2} \mathcal{L}(\phi_2) = S_1 + S_2$. By cluster decomposition we expect that $\langle \Psi_1 \rangle$ should not depend on what happens in region X_2 . Given (5.2.35), this requires that

$$f(n_1 + n_2) = f(n_1)f(n_2), \quad (5.2.36)$$

which in turn fixes the function f to be

$$f(n) = e^{i\theta n}, \quad (5.2.37)$$

where θ is an arbitrary parameter. Since n is an integer, without loss of generality we can restrict $0 \leq \theta \leq 2\pi$, so this is an angular variable. Cluster decomposition not only requires that we cannot arbitrarily restrict the sum over topological sectors in any form, but it also dictates us the precise form in which we should sum over them. Recalling (5.2.15), we see that the weight factor $f(n)$ can be rewritten as a new term in the action:

$$\langle \Psi \rangle = \frac{\int_X \mathcal{D}\phi e^{-S(\phi)+S_\theta} \Psi}{\int_X \mathcal{D}\phi e^{-S(\phi)+S_\theta}}, \quad (5.2.38)$$

where

$$S_\theta = i \frac{\theta}{8\pi^2} \int_X \text{tr} F \wedge F, \quad (5.2.39)$$

and we integrate over all possible topological sectors in the path integral. The term (5.2.39) is a gauge and Lorentz-invariant dimension-4 term that we could have introduced purely from dimensional arguments. At the perturbative level it does not alter the dynamics since, as we have seen, it is locally a total derivative. Non-perturbatively, observables do depend on θ , which is a genuine coupling in the theory. It dictates the way we weight the sum over topological sectors or, alternatively, the linear combination of ground state we take in the theory:

$$|\theta\rangle = \sum_{m=-\infty}^{\infty} e^{im\theta} |m\rangle, \quad (5.2.40)$$

where $|m\rangle$ are the ground states with winding number m introduced at the end of section 5.2.

In Euclidean space the θ term is purely imaginary and it reduces to the phase (5.2.37) in the n instanton sector. The θ -term has several physical consequences. Notably, it breaks charge conjugation C and CP , the product of C with the space parity symmetry P . By the CPT theorem, this implies that it also breaks time reversal symmetry T . In the context of QCD its presence gives rise to the strong CP problem. We will not enter in details, since these are discussed in the QFT I course, see section 9.8 of [13].⁵

In the early days there was hope that instantons, being non-perturbative phenomena, could shed light, if not solve, the problem of confinement in non-abelian gauge theories. Unfortunately the dream did not come true. The essence of the problem is in the impossibility to perform reliable quantum computations. Let us then look to quantum fluctuations and try to understand the effect of integrating over small fluctuations around instanton backgrounds. Like in the quantum mechanical models discussed in section 5.1, it is important to separate the zero modes from the

⁵At this stage you should appreciate the power of the chiral QCD effective field theory which allowed us to determine several (non-perturbative in the QCD coupling) properties of axion physics from elementary considerations based on symmetry principles with no reference to instanton physics.

massive fluctuations. Let us focus on the 1-instanton measure $d\mu_1$. We already mentioned that $|n| = 1$ instantons have in total 8 zero modes, related to translations, $SU(2)$ global rotations, and scaling. Dimensional analysis and the fact that $S_0 \propto g^{-2}$ allows us to fix the zero mode contribution to the instanton measure up to an overall constant:

$$d\mu_1^{(0)} = \frac{d^4x_0 d\rho}{\rho^5} e^{-\frac{8\pi^2}{g^2}} (\sqrt{S_0})^8 \propto \frac{d^4x_0 d\rho}{\rho^5} \frac{e^{-\frac{8\pi^2}{g^2}}}{g^8}, \quad (5.2.41)$$

where x_0 denotes the position of the instanton and ρ its size. The massive fluctuations are difficult to be determined, but we can use indirect arguments to fix their form F . At the quantum level we know that g^2 is a running coupling and (5.2.41) is not a well-defined quantity, since we should specify the scale where g^2 is evaluated or better express everything in terms of the dynamically generated RG invariant scale $\Lambda \sim \mu \exp(-1/(g(\mu)|\beta_0|))$, where $\beta_0 < 0$ is the one-loop coefficient of the β function of the theory and μ is the RG scale. The only RG-invariant combination that we can make to reproduce the exponential factor in (5.2.41) is

$$e^{-\frac{8\pi^2}{g^2(\mu)}} F(\rho\mu) \propto (\Lambda\rho)^{8\pi^2\beta_0}, \quad (5.2.42)$$

so the full instanton measure, including massive fluctuations, should scale as

$$d\mu_1 \propto \frac{d^4x_0 d\rho}{\rho^5} (\Lambda\rho)^{8\pi^2\beta_0}, \quad (5.2.43)$$

where we neglected sub-leading logarithmic corrections coming from the g^8 term in (5.2.41). Since $\beta_0 \sim \mathcal{O}(1)$, we get a divergence from the measure when integrating over large instantons. The instanton dilute gas approximation breaks down as large instantons dominate and overlap with each other. Most importantly we loose perturbative control because perturbation theory around the instanton background becomes strongly coupled, as it happens to the $n = 0$ perturbative sector.

Aside from this technical problem, large N considerations makes us believe that the mechanism of confinement is not directly related to instanton physics. Indeed, the good predictions of large N considerations in QCD suggest that gauge theories confine at $N = \infty$, as we assumed in section 3.1. However, at large N instantons are suppressed as the instanton action $S_0 \propto N$.

5.2.2 Fermions in instanton background and a non-perturbative anomaly

There are several interesting effects which occur in presence of fermions in an instanton background. An important one was already pointed out in QFT I [13]. In presence of massless fermions, the θ term becomes unphysical, as it can always be rotated away by a (anomalous) $U(1)_A$ axial rotation involving the massless fermion. The irrelevance of θ is explained microscopically as a suppression of the tunnelling between ground states with different winding number m . The suppression is due to the presence of fermionic zero modes in the path integral measure

which cannot be paired and makes the amplitude vanish. The presence of zero modes is predicted from the Atiyah-Singer index theorem (4.7.30) which for $X = S^4$ and a single Dirac fermion in a representation r of the gauge group reads⁶

$$\text{index } i\cancel{D}_r = N_L - N_R = \frac{1}{8\pi^2} \int_{S^4} \text{tr}_r F \wedge F = 2x_r n, \quad (5.2.44)$$

where n is the instanton number and x_r is the Dynkin index of the representation. This is normalized so that $x_f = 1/2$ in the fundamental representation of $SU(n)$. In an instanton background with $n \neq 0$, Dirac fermions have necessarily zero modes. This is the $4d$ equivalent of the chiral zero modes discussed in $2d$ in section 4.7.2.

Fermions suffer from a $U(1)_A$ axial anomaly which reveals itself in an instanton background. The divergence of the axial current J^A is in fact given by the topological term $F \wedge F$. In the non-canonical basis (5.2.1) it reads

$$d * J^A = \frac{1}{8\pi^2} \text{tr}_r F \wedge F. \quad (5.2.45)$$

Under a finite $U(1)_A$ chiral transformation with parameter α we have⁷

$$\psi \rightarrow e^{i\alpha\gamma_5}\psi, \quad \bar{\psi} \rightarrow e^{i\alpha\gamma_5}\bar{\psi}, \quad (5.2.46)$$

and the path integral measure picks up a phase given by

$$\exp\left(2i\alpha \times \frac{1}{8\pi^2} \int \text{tr}_r F \wedge F\right) = e^{4ix_r\alpha n}. \quad (5.2.47)$$

While the axial anomaly is detectable from perturbative one-loop diagrams, we see that it is only in non-trivial instanton sectors that it is explicitly broken. In other words, instantons carry effectively a $U(1)_A$ charge. Tunneling has then to vanish in presence of fermions, unless fermion fields are included in the path integral which soak up the zero modes present in the fermion measure.

We also see from (5.2.47) that $U(1)_A$ is not totally broken by instantons but it reduces to a discrete subgroup. The largest breaking is induced in the $n = 1$ instanton sector. We have

$$U(1)_A \rightarrow \mathbb{Z}_{4x_r}. \quad (5.2.48)$$

More in general, for n_i Dirac fermions in representations r_i , we have

$$U(1)_A \rightarrow \mathbb{Z}_{4n_i \sum_i x_i}. \quad (5.2.49)$$

Note that the \mathbb{Z}_2 axial symmetry under which both ψ and $\bar{\psi}$ change sign (equivalent to fermion

⁶On S^4 the roof genus does not give any contribution.

⁷Recall that in Euclidean space ψ and $\bar{\psi}$ are independent Grassmann fields.

parity) is always unbroken.

For Weyl fermions the anomalous phase is reduced by half and $U(1)_A \rightarrow \mathbb{Z}_{2n_i \sum_i x_i}$. This phase allows us to detect a non-perturbative gauge anomaly which occurs for $SU(2)$ gauge theories [31]. All $SU(2)$ representations are equivalent to their complex conjugates, which implies the vanishing of the associated anomaly coefficient $D_{abc} = 0$ for any choice of fermion spectrum. This guarantees absence of anomalies for gauge transformations which can be obtained starting from infinitesimal ones, namely the one connected to the identity element. Gauge transformations can be seen as maps from S^4 to $SU(2)$, and

$$\pi_4(SU(2)) = \mathbb{Z}_2, \quad (5.2.50)$$

which means that all gauge transformations split in two equivalence classes. In [31] it has been shown that there can be a \mathbb{Z}_2 anomaly for gauge transformations belonging to the nontrivial homotopy class (5.2.50). The original analysis made use of index theorems and will not be discussed here. This anomaly appears in a simpler way when we consider fermions in an instanton background, as above. Consider the 1-instanton sector and n Weyl fermions in the spin j representation of $SU(2)$, $j = 1/2$ being the fundamental. Under the fermion parity transformation

$$\psi \rightarrow -\psi, \quad \bar{\psi} \rightarrow -\bar{\psi}, \quad (5.2.51)$$

the fermion measure transforms as

$$\mathcal{D}\psi \mathcal{D}\bar{\psi} \rightarrow e^{2i\pi x_j n} \mathcal{D}\psi \mathcal{D}\bar{\psi}, \quad (5.2.52)$$

where

$$x_j = \frac{j(j+1)(2j+1)}{3}. \quad (5.2.53)$$

The transformation (5.2.51) can also be seen as an $SU(2)$ gauge transformation, the central element of $SU(2)$ with $g = -1$. When n is odd and x_j is a half-integer, the fermion measure changes sign and is not gauge invariant. We conclude that the theory is inconsistent in this case. It is simple to see that this occurs for

$$j = \frac{1}{2} + 2k, \quad \text{with integer } k. \quad (5.2.54)$$

For all other values of j , x_j is an integer, and no anomaly occurs. In particular, an even number of Weyl fermions in the fundamental representation is required in order to have a consistent $SU(2)$ gauge theory.

5.2.3 Witten effect and dyons

We have seen that the magnetic charge g_m of a monopole is subject to the Dirac quantization condition (4.5.11). As pointed out in [32,33], Dirac's quantization condition should be generalized

because it is not invariant under a symmetry of Maxwell theory in presence of electric and magnetic charges. In the following we rescale the normalization of magnetic charges $g_m \rightarrow g/(4\pi)$ so that (4.5.11) reads

$$eg = 2\pi n. \quad (5.2.55)$$

The argument is very simple. In presence of electric and magnetic sources J_e, J_m , the equations of motion and Bianchi identity read

$$\begin{aligned} d * F &= J_e, \\ dF &= J_m. \end{aligned} \quad (5.2.56)$$

The equations (5.2.56) are manifestly invariant under $SO(2)$ rotations O under which

$$\mathcal{F} \rightarrow O\mathcal{F}, \quad \mathcal{J} \rightarrow O\mathcal{J}, \quad \mathcal{F} = \begin{pmatrix} *F \\ F \end{pmatrix}, \quad \mathcal{J} = \begin{pmatrix} J_e \\ J_m \end{pmatrix}. \quad (5.2.57)$$

Let us denote by (e, g) the electric and magnetic charges of a particle (a dyon if both e and g are different from zero). Under the $SO(2)$ rotation (5.2.57), we have $(e, 0) \rightarrow (\cos \alpha, -\sin \alpha)e$, $(0, g) \rightarrow (\cos \alpha, \sin \alpha)g$ and hence for an electric particle $(e_1, 0)$ and a magnetic monopole $(0, g_2)$, we would have

$$e_1 g_2 \xrightarrow{?} (\cos \alpha)^2 e_1 g_2, \quad (5.2.58)$$

which is not invariant. The $SO(2)$ invariant Schwinger-Zwanziger quantization condition, which reduces to (5.2.55) for purely electric and magnetic charges, is

$$e_1 g_2 - e_2 g_1 = 2\pi n. \quad (5.2.59)$$

When $g_1 = 0$, (5.2.59) does not put any constraint on the allowed values of e_2 for a magnetic monopole with charge g_2 . However, it gives us a constraint for the relative charges of two monopoles with unit magnetic charge $g = 2\pi/e$:

$$e_1 - e_2 = en. \quad (5.2.60)$$

The individual values of e_1 and e_2 are however unconstrained. If the theory is CP invariant, since $e \rightarrow -e$, $g \rightarrow g$ under CP, the CP transformed monopole with charge $(e_1, 2\pi/e)$ has charges $(-e_1, 2\pi/e)$. Demanding (5.2.59) between the monopole and its CP transformed state gives

$$e_1 \frac{4\pi}{e} = 2\pi n, \quad (5.2.61)$$

which is satisfied only for

$$e_1 = ne \quad \text{or} \quad e_1 = \left(n + \frac{1}{2}\right)e. \quad (5.2.62)$$

Assignment n.3: Quantum mechanics with a θ -angle (5.2.64)

Consider a one-dimensional quantum mechanical model with Lagrangian

$$L = \frac{\dot{q}^2}{2} - V(q) + \theta \dot{q}, \quad V(q) = 1 - \cos(2\pi nq), \quad n \in \mathbb{N}, \quad (5.2.65)$$

where $q(t)$ is a dimensionless variable describing the motion of the particle on a circle, so $q \sim q + 1$, and $0 \leq \theta \leq 2\pi$ is a theta angle. For $n = 1$ the Lagrangian (5.2.65) corresponds to a pendulum subject to a gravitational potential V . The additional coupling to a connection results in the θ angle interaction.

- (a) For $n = 1$ compute the ground state energy as a function of θ by resumming instanton and anti-instanton configurations.
- (b) Consider now (5.2.65) with $n = 2$. The system has two inequivalent vacua at $q = 0$ and at $q = 1/2$. Compute the transition amplitude

$$A_{\frac{1}{2},0} \equiv \langle q = \frac{1}{2} | e^{-\beta H} | q = 0 \rangle \quad (5.2.66)$$

as a function of θ . Show that at $\theta = \pi$ the amplitude (5.2.66) exactly vanishes and argue that $\mathcal{O}(\hbar)$ quantum fluctuations around the instanton action do not change the result.

Due to (5.2.60) the two solutions are mutually exclusive. If CP is broken, however, the argument does not hold and magnetic monopoles are allowed to have an unconstrained electric charge. A particular source of CP violation is the θ -term in (5.2.39). It has been shown in [34] that the θ term in fact turns magnetic monopoles into dyons with a calculable electric charge e_m given by

$$|e_m| = \frac{e\theta}{2\pi}. \quad (5.2.63)$$

We will not derive (5.2.63). At $\theta = \pi m$, for any integer m , CP is restored and (5.2.63) reduce to (5.2.62), as it should be. Notably, (5.2.63) is an exact expression.

5.2.4 Topologically non-trivial configurations in the Higgs phase

According to the scaling arguments presented in section 4.2, no instanton solution can exist in $d = 4$ in presence of gauge and matter fields. Hence no instantons can arise in the Higgs phase of a gauge theory. However, this does not imply that there is no tunneling between the topologically different ground states of the theory. Instantons are a saddle point approximation of the path integral. Quantum mechanically we are supposed to integrate over all possible field configurations and not only the saddle points. It turns out that in the Higgs phase we can have finite action, topologically non-trivial, configurations. These are not exact extrema of the action, but nevertheless can contribute to tunnelling. For some aspects these configurations are more amenable to a semi-classical treatment, because they do not have the problem of large-size instantons (now suppressed). Anyhow, tunnelling effects in weakly coupled Higgs phases, like in

the SM, are totally negligible, because their suppression factor is at least of order $\exp(-8\pi^2/g^2)$, which is tiny.

In the Higgs phase it is possible to determine the height of the potential barrier separating the vacua with different winding numbers. At the top of this potential we should have a finite energy configuration, solution of the equations of motion, which is perturbatively unstable. Such configurations are denoted sphalerons.⁸ The height of the barrier is simply given by the energy of the sphaleron E_{sp} . While tunnelling is highly suppressed, at a sufficiently high temperature $T_c \sim E_{\text{sp}}$ thermal fluctuations start to be large enough that we can overcome the barrier instead of tunnelling through it. In this way we can activate explicit breaking of $U(1)$ global symmetries which have anomalies, in particular lepton and baryon symmetries. Violation of baryon number induced by sphalerons at finite temperature is a notable and much studied mechanism to explain the baryon asymmetry of the universe.

5.3 Bounces and vacuum decay

Finite action solutions describing tunnelling between non-degenerate vacua are called bounces. The theory of vacuum decay has been developed by Coleman and collaborators in [35–37]. We will follow in this section the evergreen analysis in [3] with the trivial generalization to arbitrary space-time dimensions $d > 2$.

Consider a scalar field in d space-time dimensions with a potential like the one in figure 5.2. The vacuum expectation value $\langle\phi\rangle = \phi_f$ corresponds to a meta-stable minimum of the theory (false vacuum). Since the potential is locally convex, to all orders in perturbation theory no instabilities occur. On the other hand, tunnelling effects at some point will induce a decay into the true minimum of the theory at $\langle\phi\rangle = \phi_t$. As we will see, in real space-time the tunnelling will occur through the creation of spherical bubbles of true vacua within the space in the false vacuum. Small bubbles have a surface tension which is bigger than the energy gain we get from having the true vacuum inside. At some point, a sufficiently large bubble will form which is energetically favored. As soon as this bubble forms, it will start to expand at a speed which quickly approach the speed of light making the transition to the global minimum. The theory of vacuum decay consists in describing this process and estimate the decay width per unit (space) volume Γ/V_{d-1} .

Like for instantons, the tunnelling process can be described looking for finite Euclidean action configurations. The analysis is greatly simplified by looking for solutions with $O(d)$ symmetry for which $\phi(x) = \phi(r)$, where $r^2 = x_d^2 + \vec{x}^2$. The system becomes effectively one-dimensional and we can use real time intuition by thinking about the motion of a particle in the potential $-V$. The potential V is normalized so that $V(\phi_f) = 0$. We look for solutions of the equation of motion such that in the far past and future $x_d \rightarrow \pm\infty$ we are in the false vacuum. Both

⁸The analogue of this configuration in the symmetric double well discussed in section 5.1.2 would be the configuration $\bar{q} = 0$.

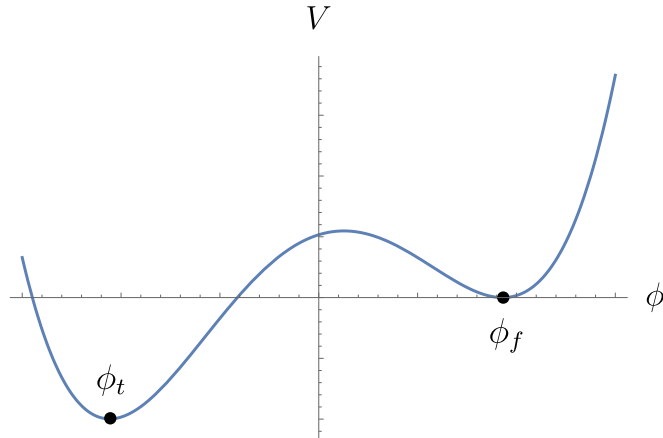


Figure 5.2: Scalar potential with two non-degenerate minima.

conditions can be expressed as

$$\lim_{r \rightarrow \infty} \bar{\phi}(r) = \phi_f. \quad (5.3.1)$$

The no-go theorem of section 4.2 forbidding finite action solutions for scalar configurations for $d > 3$ is avoided because the potential is not positive definite. From (4.2.5) we get

$$\int d^d x \frac{1}{2} (\partial_i \bar{\phi})^2 = \frac{d}{2-d} \int d^d x V(\bar{\phi}) > 0. \quad (5.3.2)$$

Also, (4.2.6) gives

$$\left. \frac{d^2 \bar{S}_\lambda}{d\lambda^2} \right|_{\lambda=1} < 0. \quad (5.3.3)$$

Bounces are unstable configurations. This is a nice feature because the small fluctuations around the bounce, the analogue of the factor K in (5.1.35), is expected to be complex in order to give rise to a decay width (imaginary component of the energy). Of course, we should check how many negative eigenvalues we have before claiming victory, but as a matter of fact this is the only one (we will not prove this statement). The equation of motion of ϕ in radial coordinates with radius r is given by

$$\frac{d^2 \bar{\phi}}{dr^2} + \frac{d-1}{r} \frac{d\bar{\phi}}{dr} = \frac{dV}{d\phi}, \quad (5.3.4)$$

which is equivalent to a particle moving in r -time subject to a potential $-V$ and to a friction given by the $1/r$ term. In addition to (5.3.1), we demand

$$\left. \frac{d\bar{\phi}}{dr} \right|_{r=0} = 0, \quad (5.3.5)$$

so that the solution of (5.3.4) is regular at the origin. It is easy to heuristically understand why a bounce solution should exist by looking at figure 5.3. The boundary conditions (5.3.1) and (5.3.5) are equivalent to find a particle trajectory which starts at $\phi_0 = \bar{\phi}(r=0)$ and asymptotically

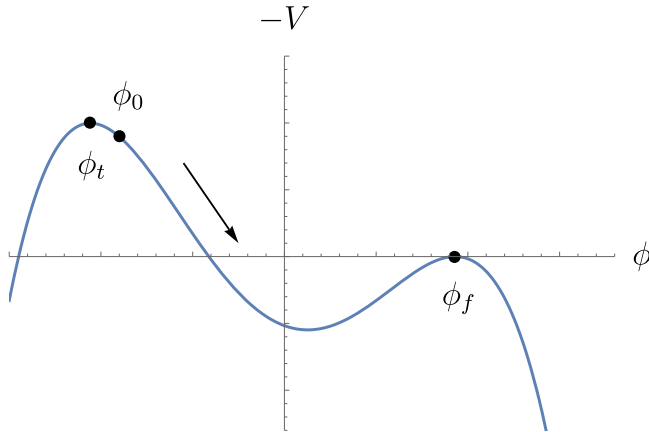


Figure 5.3: Inverted scalar potential with two non-degenerate minima. We show the location of the point $\phi_0 = \bar{\phi}(r=0)$ for which a bounce solution exists.

reaches ϕ_f as $r \rightarrow \infty$. It is clear that if ϕ_0 is not chosen at a sufficiently high point in V , due to the friction term it will not be able to reach the point ϕ_f . On the other hand, if we start the motion very close to ϕ_t , the particle will not move much for a long time, because the friction term is large for small r . When $r \gg 1$ the friction term can be neglected and we are still very close to ϕ_t , so the particle will overshoot ϕ_f . So there will exist a point ϕ_0 such that the particle will precisely reach ϕ_f . The solution of (5.3.4) with the condition $\phi_0 = \bar{\phi}(r=0)$ is guaranteed to be of finite action. Given the relation between r and Euclidean time, the bounce is given by the solution which stays most of the time at ϕ_f , moves up to ϕ_0 and then comes back to ϕ_f for the remaining time. Let $S_0 = S(\phi = \bar{\phi})$ be the value of the action at the bounce. The origin of the euclidean coordinates $r=0$ is of course arbitrary, as the bubble can appear anywhere and at anytime in space-time. Correspondingly, the fluctuations around the bounce include d zero modes for translations which give a factor $V_{d-1}T$, V_{d-1} being the volume of space and T the total time. We also get one unstable direction which gives rise to an imaginary factor. Summing over a gas of dilute bounces, similarly to what we did in section 5.1.2 for instantons, gives our final estimate for the vacuum decay width per unit three-volume:

$$\frac{\Gamma}{V_{d-1}} \propto e^{-S_0}. \quad (5.3.6)$$

Determining the proportionality factor requires a more complicated one-loop computation, see [36]. It can be shown that bounce solutions which break the $O(d)$ symmetry lead to higher actions.

In general there are no analytic solutions for the differential equation (5.3.4) subject to the boundary conditions (5.3.1) and (5.3.5). Progress can be made assuming that $V(\phi_f) - V(\phi_t)$ is infinitesimal. So let us consider a potential of the form

$$V = V_0 + \epsilon V_1, \quad (5.3.7)$$

where $V_0(-\phi) = V_0(\phi)$ has two degenerate minima at $\langle\phi\rangle = \pm v$ and V_1 breaks the \mathbb{Z}_2 parity $\phi \rightarrow -\phi$. We take $V_0(\pm v) = 0$, $V_1(-v) = -1$ and $V_1(v) = 0$. We have $V(\phi_f) - V(\phi_t) = \epsilon$ and at leading order in ϵ $\phi_f \approx v$, $\phi_t \approx -v$. Since the gap between the two vacua is small, we have to choose the point ϕ_0 in figure 5.3 very close to ϕ_t . In this case the solution stays close to ϕ_t until a large value of $r = R$, quickly moves towards ϕ_f , and asymptotically reaches ϕ_f as $r \rightarrow \infty$. In Minkowski space-time this configuration corresponds to a large bubble of radius R with a thin wall separating the two vacua.⁹ For this reason this approximation goes under the name of “thin wall approximation”. We can determine the value of R as follows. The bounce action in radial coordinates reads

$$S_0 = \Omega_d \int_0^\infty dr r^{d-1} \left(\frac{1}{2} (\partial_r \bar{\phi})^2 + V(\bar{\phi}) \right), \quad (5.3.8)$$

where

$$\Omega_d = \frac{2\pi^{d/2}}{\Gamma(d/2)} \quad (5.3.9)$$

is the solid angle in d -dimensions. We can perform the integral in (5.3.8) by splitting it in three regions:

$$S_0 = S_0^{\text{I}} + S_0^{\text{II}} + S_0^{\text{III}}, \quad (5.3.10)$$

where I corresponds to the interior of the bubble $r < R$, II to the shell of the bubble $r \sim R$, III to the exterior of the bubble $r > R$. The contribution to S_0^{I} and S_0^{III} are easy to estimate, since the field is approximately constant there, and respectively equal to $\bar{\phi} \sim \phi_t$ and $\bar{\phi} \sim \phi_f$. We get

$$S_0^{\text{I}} \approx -\frac{\Omega_d}{d} \epsilon R^d, \quad S_0^{\text{III}} = 0. \quad (5.3.11)$$

Since R is large, in estimating S_0^{II} we can neglect the friction term in (5.3.4). In this way, S_0^{II} is to a good approximation given by the instanton contribution discussed in section 5.1.2 for a particle in a symmetric double well, see (5.1.23)

$$S_0^{\text{II}} \approx \Omega_d R^{d-1} S_1, \quad S_1 = \int_{-v}^v \sqrt{2V_0} d\phi. \quad (5.3.12)$$

The size of the bubble is determined by extremizing S_0 with respect to R . We have

$$R_0 = \frac{(d-1)S_1}{\epsilon}, \quad (5.3.13)$$

and an analytic estimate for the bounce action:

$$S_0(R_0) \approx \frac{(d-1)^{d-1} \Omega_d}{d} \frac{S_1^d}{\epsilon^{d-1}}. \quad (5.3.14)$$

We have been a bit cavalier in saying that ϵ has to be small, as the ϵ defined above is an energy

⁹The requirement of a large bubble can also be seen from energetic considerations in real space: since the energy gain between the two vacua is small, we need a large bubble to overcome its surface tension.

density, not a dimensionless parameter. We can now amend this by specifying more appropriately the regime of validity of the thin wall approximation. The thickness of the wall is of order $1/m$, where $m^2 = V_0''(\pm v)$ controls the size where the instanton density (5.3.12) is non-negligible. Hence the thin wall approximation is reliable when $R_0 \gg 1/m$, i.e. when $S_1 m \gg \epsilon$. The value of S_1 can vary. For example, for a quartic scalar field theory in $4d$, we have $S_1 \sim m$, see (5.1.28). The life-time of the false vacuum is parametrically large for small ϵ .

The bounce action allows us to also have a clue of how the vacuum decays by analytically continuing the solution in Minkowski space-time. As we mentioned a few times, tunnelling in real space occurs through the appearance of a bubble of true vacuum within the universe in the false vacuum. After its appearance, the time evolution of the bubble is given by its equation of motion, which is $\square\phi = V'(\phi)$. This is the analytic continuation $x_4 \rightarrow it$ of (5.3.4), so the bubble evolution is given by

$$\phi(\vec{x}, t) = \bar{\phi}(r = \sqrt{\vec{x}^2 - t^2}), \quad (5.3.15)$$

subject to the boundary condition $\partial_t \phi(\vec{x}, t)|_{t=0} = 0$, where $t = 0$ is the instant where the true vacuum appears in a region around $\vec{x} = 0$. The $O(d)$ invariance of the bounce turns into a $O(d-1, 1)$ Lorentz invariant evolution of the bubble. In the thin-wall approximation, the condition $r = R$ turns into

$$\vec{x}^2 - t^2 = R^2. \quad (5.3.16)$$

As time evolves, the bubble expands with velocity

$$v = \frac{d|\vec{x}|}{dt} = \sqrt{1 - \frac{R^2}{|\vec{x}|^2}}, \quad (5.3.17)$$

and very rapidly approaches the speed of light. The wall of the expanding bubble carries a lot of energy, which has to compensate for the energy gained in passing from the false to the true vacuum. Considering that S_1 is the bubble tension per unit area, we have

$$E_{\text{wall}} = \Omega_{d-2} |\vec{x}|^{d-2} \gamma S_1, \quad (5.3.18)$$

where γ is the Lorentz factor $\gamma = (1 - v^2)^{-1/2}$. Plugging in (5.3.18) the relations (5.3.13) and (5.3.17) gives

$$E_{\text{wall}} = \frac{\Omega_{d-2}}{d-1} |\vec{x}|^{d-1} \epsilon = \text{Vol}(B_{d-1}) \epsilon, \quad (5.3.19)$$

which is exactly the energy gain in passing from the false to the true vacuum in the $(d-1)$ dimensional ball B_{d-1} . All the energy is converted into kinetic energy of the bubble and no energy is released in form of radiation.

5.3.1 Metastability of the Standard Model

The potential of the Standard Model (SM) Higgs is notoriously quartic in the field with a negative quadratic term. In this way, at the minimum of the potential we have (with obvious

notation) the electroweak spontaneous symmetry breaking pattern $SU(2)_L \times U(1)_Y \rightarrow U(1)_{\text{EM}}$. One can wonder if the minimum of the Higgs potential is non-perturbatively stable or not. In other words, if the quartic Higgs coupling λ remains positive definite all the way up to the Planck scale, the maximum scale above which gravity should be included and our considerations would break down. It's clear that if λ turns negative at some energy scale M , there is the possibility of having bounce solutions which induce a tunneling and the decay of the SM vacuum. Let us see which kind of bounce solutions are induced, assuming that $M \gg 10^2$ GeV, the electroweak scale. In this approximation, the Euclidean action of the real scalar Higgs field h at the scale M , setting to zero vector and fermion fields, is

$$S[h] = \int d^4x \left(\frac{1}{2} (\partial h)^2 + V(h) \right), \quad V(h) = -\frac{|\lambda|}{4} h^4, \quad (5.3.20)$$

where we have neglected the Higgs mass term, and taken a negative quartic coupling. The equation for the bounce can be read from (5.3.4):

$$\frac{d^2 \bar{h}}{dr^2} + \frac{3}{r} \frac{d\bar{h}}{dr} + |\lambda| \bar{h}^3 = 0, \quad (5.3.21)$$

and can be solved exactly. Demanding the two conditions

$$\lim_{r \rightarrow \infty} \bar{h}(r) = 0, \quad \left. \frac{d\bar{h}}{dr} \right|_{r=0} = 0, \quad (5.3.22)$$

we get

$$\bar{h}(r) = \sqrt{\frac{2}{|\lambda|} \frac{2R}{x^2 + R^2}}. \quad (5.3.23)$$

The parameter R corresponds to the size of the bounce. Its value is undetermined at this order, due to the classical scale invariance of the action (5.3.20). The action at the bounce equals

$$S[\bar{h}] = \frac{8\pi^2}{3|\lambda|}. \quad (5.3.24)$$

Note that we have determined the existence of a bounce (actually a whole family parametrized by R) and the value of the action (5.3.24) without knowing the location (if any) of the true global minimum. The instability occurs as long as λ turns negative. Is this situation compatible with our own existence? Yes, provided the life-time of the metastable electroweak minimum is greater than the current age of the Universe $T_U \sim 10^{10}$ years. The value of R which maximizes the decay width is found by considering radiative corrections which break scale invariance. It is also important to compute the quadratic fluctuations around the bounce. Including such corrections, the life-time τ_U of our Universe is roughly given by

$$\frac{T_U}{\tau_U} \approx \max_R \frac{T_U^4}{R^4} e^{-\frac{8\pi^2}{3|\lambda|(1/R)}}. \quad (5.3.25)$$

In writing (5.3.25) we used the fact that the spatial volume of our Universe is roughly given by T_U^3 . We have three scenarios:

$$\frac{T_U}{\tau_U} = \begin{cases} 0, & \text{absolute stability} \\ \ll 1, & \text{meta-stability} \\ \gtrsim \mathcal{O}(1), & \text{instability} \end{cases} \quad (5.3.26)$$

The first scenario occurs for $\lambda > 0$, in which case no bounce can appear.¹⁰

The key parameter is the value of the Higgs quartic coupling at the scale $1/R$, so let us now turn to see how this coupling runs in the SM. The schematic form of the one-loop beta-functions of the SM couplings is¹¹

$$\begin{cases} \beta_\lambda \sim \lambda^2 - \alpha_{1,2}\lambda + \alpha_{1,2}^2 + \alpha_t\lambda - \alpha_t^2, \\ \beta_{\alpha_t} \sim \alpha_t^2 - \alpha_i^2, \\ \beta_{\alpha_i} \sim \alpha_i^2, \quad i = 1, 2, 3. \end{cases} \quad (5.3.27)$$

In (5.3.27) α_i are the SM gauge couplings, 1,2,3 referring to $U(1)_Y$, $SU(2)_L$ and $SU(3)_c$, respectively and α_t is the square of the top Yukawa coupling. Yukawa couplings for all other fermions give a negligible effect and can be neglected. While we do not report the precise numerical coefficients multiplying the various terms in the beta-functions above, we paid attention to their signs. We see from (5.3.20) that β_λ is a sum of positive and negative terms. An important role is played by the top Yukawa coupling, which gives a relevant contribution, due to its large value. At fixed electroweak scale, the mass of the Higgs field varies with λ , as the mass of the top varies with α_t . Since both Higgs and top masses have been measured, the values of λ and α_t are known at the electroweak scale. Interestingly enough, plugging the actual experimental values of the couplings at the electroweak scale and evolving them using the precise form of (5.3.27), we get that the quartic Higgs coupling $\lambda(1/R)$ decreases at high energies and becomes negative at some large energy scale. The values of the couplings are such that we are right close to the edge of the stability region. If the top mass would have been a few GeV lighter, or the Higgs mass a few GeV heavier, we would have safely sit at a stable region. The critical location of the SM vacuum motivated more accurate analysis. Beyond one-loop level, the QCD coupling α_3 , because of its non-negligible size, enters into consideration. Note from (5.3.27) that α_3 governs already at one-loop level the RG behaviour of α_t .

The state of the art is provided by [39], where the SM potential has been computed at NNLO order.¹² See in particular fig.5 of [39]. The SM vacuum is meta-stable and, luckily enough, very long-lived: $\tau_U \gg T_U$. The quartic Higgs coupling turns negative at around 10^{11} GeV, while the maximum in (5.3.25) is obtained for very small bounces, with $1/R \sim 10^{17}$ GeV. The Higgs mass

¹⁰The third is hopefully ruled out by experiment!

¹¹See e.g. appendix A of [38] for the precise formulas.

¹²Recall that NⁿLO means using the RG improved n -loop effective potential, where the $n+1$ -loop beta-functions are used for the running of the couplings.

term is completely negligible at such high scales, justifying our initial assumption.

An important comment is in order. The stability analysis above applies in the assumption that the RG behaviour of the couplings is governed by SM fields up to very high energy scales, at least 10^{11} GeV or, in other words, that the SM is a viable effective theory up to those scales. Being the SM perturbatively renormalizable, with a trans-Planckian Landau pole associated to hypercharge, this essentially boils down to assume no new electroweak particles beyond the SM.

Chapter 6

Phases of gauge theories

Gauge theories present different phases which can be separated by cross-over, first or second-order phase transitions. Understanding the full phase diagram of gauge theories, in particular $4d$ non-abelian gauge theories, as a function of particle densities, temperature T , etc. is of fundamental importance. For example, the knowledge of the phases of QCD at finite temperature and density would be of immense value in astrophysics in the study of ultradense objects such as neutron stars. Unfortunately, this is to a large extent still unknown territory, because of limited availability of analytical tools and technical problems with numerical methods. As first, yet non-trivial, step we can focus on gauge theories at zero temperature and in the vacuum. We characterize which phases can appear, and how they depend on the number and kind of charged matter fields. This is also a formidable task in $4d$ non-abelian gauge theories, where confinement has yet to be analytically proved.

Aim of this chapter is to present the basic tools used in classifying phases of $4d$ gauge theories at $T = 0$ and in the vacuum, and give a brief description of them. We will reformulate this classification using a recent approach in terms of so called higher-form symmetries, which allow for a sharper definition of such phases in terms of spontaneously broken global symmetries. We start in section 6.1 by introducing a notable class of non-local operators, the Wilson (and t'Hooft) line operators. In section 6.2 we reconsider Ward identities for ordinary global symmetries in QFT in a new perspective where symmetries are associated to the existence of topological operators in the theory. From this perspective higher-form symmetries, discussed in 6.2.1, naturally follow. After the first two preparatory sections, phases of gauge theories are discussed in section 6.3. In section 6.4 we reconsider the t'Hooft anomaly matching conditions and upgrade them for discrete (higher-form) symmetries. We first discuss an example of use of generalized 't Hooft anomaly matching conditions for one-form continuous symmetries in section 6.4.1 and discrete zero-form symmetries in quantum mechanics in section 6.4.2. We quickly discuss a relation between 't Hooft anomalies and charge fractionalization in section 6.4.3. An example of use of generalized anomaly matching conditions in the context of pure Yang-Mills theory is finally reported in section 6.4.4.

Several important results in the classification of gauge theory phases have been obtained on

the lattice. Due to lack of time we will not discuss lattice gauge theories in these lectures.

6.1 Wilson and 't Hooft Lines

In weakly coupled QFTs with a reliable Lagrangian description, the vacuum is easily determined by looking at the classical potential for scalar fields. Once the vacuum is known, we can consider perturbations around it, how particles scatter with each other, etc. In strongly coupled QFTs, in contrast, determining the property of the vacuum is generally a hard problem. We can determine the nature of the vacuum by looking at the kind of force external non-dynamical particles are subject to.

Consider as an elementary example a free abelian gauge theory coupled to an external current J^μ . The partition function reads

$$Z[J] = \int \mathcal{D}A_\mu e^{iS + i \int d^4x J^\mu A_\mu}, \quad (6.1.1)$$

where S is the Maxwell action term, including a gauge-fixing term. Since the theory is free, we can integrate out A_μ exactly to get

$$Z[J] = \exp\left(-\frac{1}{2} \int d^4x d^4y J^\mu(x) G_{\mu\nu}(x-y) J^\nu(y)\right). \quad (6.1.2)$$

We take as external sources two particles with electric charges q_1 and q_2 , at positions \vec{x}_1 and \vec{x}_2 . The corresponding electric current is $J^\mu(x) = \delta_0^\mu (q_1 \delta^{(3)}(\vec{x} - \vec{x}_1) + q_2 \delta^{(3)}(\vec{x} - \vec{x}_2))$. The particles are at rest and are taken infinitely heavy, so that we are allowed to neglect their fluctuations. In Feynman gauge we have

$$\begin{aligned} -\frac{1}{2} \int d^4x d^4y J^\mu(x) G_{\mu\nu}(x-y) J^\nu(y) &= -e^2 q_1 q_2 \int dx_0 dy_0 \int \frac{d^4p}{(2\pi)^4} \frac{-ie^{ip_0(x_0-y_0) - i\vec{p}\cdot\vec{x}_{12}}}{p_0^2 - \vec{p}^2} + \dots \\ &= -ie^2 q_1 q_2 T \int \frac{d^3\vec{p}}{(2\pi)^3} \frac{e^{-i\vec{p}\cdot\vec{x}_{12}}}{\vec{p}^2} + \dots = -iT \left(\frac{\alpha q_1 q_2}{|\vec{x}_{12}|} + \dots \right). \end{aligned} \quad (6.1.3)$$

In (6.1.3) $\alpha = e^2/(4\pi)$, $\vec{x}_{12} = \vec{x}_1 - \vec{x}_2$, T is the (regulated) total time and \dots represent UV divergent terms coming from propagator self-contractions. We recognize in (6.1.3) the Coulomb force between two objects of charges q_1 and q_2 . Plugging the explicit expression of the current in (6.1.1), we see that what we computed is

$$Z[\vec{x}_1, \vec{x}_2] = \int \mathcal{D}A_\mu e^{iS} e^{i \int_{-T/2}^{T/2} dt (q_1 A_0(\vec{x}_1) + q_2 A_0(\vec{x}_2))}, \quad (6.1.4)$$

which can be reinterpreted as the one-point function of the non-local line operator $e^{i \int_{-T/2}^{T/2} \dots}$, the world-line spanned by the two sources.

Instead of adding explicit sources, a more elegant, covariant, and general way to probe

the system consists in considering directly their “remnant” line operators. In this way we can consider an arbitrary path γ between two points x_1 and x_2 in space-time, and define the Wilson line operator

$$W_\gamma \equiv \exp \left(i \int_0^1 \frac{dx^\mu(s)}{ds} A_\mu(x(s)) ds \right), \quad (6.1.5)$$

where $x^\mu(s)$ is the curve γ parametrized by $0 \leq s \leq 1$, with $x(0) = x_1$, $x(1) = x_2$. Under a finite gauge transformation $A \rightarrow A + d\alpha$, the Wilson line W_γ transforms as

$$W_\gamma \rightarrow W_\gamma \exp \left(i \int_0^1 \frac{dx^\mu(s)}{ds} \partial_\mu \alpha(x(s)) ds \right) = W_\gamma \exp \left(i \int_0^1 \frac{d\alpha}{ds} ds \right) = g(x_2) W_\gamma g^{-1}(x_1), \quad (6.1.6)$$

where

$$g(x) = e^{i\alpha(x)}. \quad (6.1.7)$$

In order to have a gauge-invariant quantity it is convenient to take $x_1 = x_2$ and consider closed paths γ . Schematically

$$W_\gamma^{(q)} = e^{iq \oint_\gamma A}, \quad (6.1.8)$$

where q is a parameter labelling the line. By consistency q has to be an integer. Let indeed be Σ_+ and Σ_- two different surfaces such that $\partial\Sigma_+ = -\partial\Sigma_- = \gamma$. By Stokes theorem we have

$$e^{iq \oint_\gamma A} = e^{iq \int_{\Sigma_+} F} = e^{-iq \int_{\Sigma_-} F} \implies e^{iq \int_\Sigma F} = 1, \quad \Sigma = \Sigma_1 \cup \Sigma_2, \quad (6.1.9)$$

with Σ a closed surface. The integral of the flux along a closed surface is quantized,

$$\frac{1}{2\pi} \int_\Sigma F = p, \quad p \in \mathbb{Z}, \quad (6.1.10)$$

from which it follows that $q \in \mathbb{Z}$. The operators (6.1.8) are called Wilson loops. They physically correspond to the world-lines of two particles, with *opposite* charges q and $-q$, which are somehow created at some space-time point, propagate for a while, and then they annihilate at some later stage.¹

An abelian gauge theory can also be probed by external magnetic sources. Recall from (5.2.57) that electric and magnetic sources are dual to each other. In particular, the transformation $F \rightarrow *F$ turns electric sources into magnetic ones. Since the free abelian action is invariant under this transformation, proceeding as before we would obtain the same Coulomb term in (6.1.3), with e replaced by g , the minimal magnetic charge. The line operator associated to magnetic charge, however, is not naively the Wilson line (6.1.8) with $e \rightarrow g$. Indeed, while (locally) $F = dA$, $*F = d\tilde{A} \neq dA$, where \tilde{A} is a connection, *non-locally* related to A . Magnetic

¹Such interpretation is however not mandatory, as we can consider Wilson loops for arbitrary contours, including those that cannot be spanned by physical heavy particles in a causal way.

charges are represented by 't Hooft line operators

$$T_\gamma^{(n)} \equiv e^{in \oint_\gamma \tilde{A}}. \quad (6.1.11)$$

As in the Wilson line case it can be shown that $n \in \mathbb{Z}$. In absence of other charged particles we can rotate the field strength F to the basis we want. However, if both electric and magnetic particles are present at the same time, we have to be more careful. Keeping the electric frame, the formal definition (6.1.11) becomes of little use practically. A more proper, though a bit abstract, definition of t' Hooft operator is as follows. Recall that for a magnetic charge the integral (6.1.10) is non-vanishing when Σ is a closed surface surrounding the magnetic particle. In a (Euclidean) path integral representation of a correlation function, a t' Hooft operator is inserted by declaring that, given a line γ , we have a flux of F given by (6.1.10) for any small S^2 within the three-dimensional space normal to the line. Note that while Wilson line operators are lines in any dimension (A is a one-form), a t' Hooft line/loop has in general dimension $d - 3$ (\tilde{A} is a $d - 3$ form) and is thus a line in $d = 4$ only. The formal definition above still applies because the normal space remains three-dimensional for any d . In principle we can also combine Wilson and 't Hooft lines and define more general dyonic lines, which would correspond to the world-lines of external dyon particles. We will not further discuss such kind of lines.

We can also define Wilson lines/loops in non-abelian gauge theories. Given a line γ and an irreducible representation r of the gauge group G , a Wilson line is defined as

$$W_\gamma^{(r)} = \text{tr}_r P e^{i \int_\gamma A} = \text{tr} P \exp \left(i \int_0^1 \frac{dx^\mu(s)}{ds} A_\mu^\alpha(x(s)) t_\alpha^{(r)} ds \right), \quad (6.1.12)$$

where $t_a^{(r)}$ are the group generators in the representation r and P stands for path ordering. More explicitly

$$P e^{i \int_\gamma A} = \sum_{n=0}^{\infty} \frac{i^n}{n!} \int_0^1 ds_n \int_0^{s_n} ds_{n-1} \dots \int_0^{s_2} ds_1 A(s_n) \dots A(s_1), \quad (6.1.13)$$

where

$$A(s_i) = \frac{dx^\mu}{ds_i} A_\mu^\alpha(x(s_i)) t_\alpha^{(r)}. \quad (6.1.14)$$

The path ordering is necessary in order to have a well-defined transformation of $W_\gamma^{(r)}$ under gauge transformations. They read as (6.1.6), where $g(x)$ is the non-abelian version of (6.1.7). In particular, Wilson loops are gauge invariant. Non-abelian Wilson loops can be seen as a pair of external quarks, transforming in representations r and r^* , where r^* is the representation conjugate of r , which pop-out from the vacuum, propagate for a while, and then annihilate at some later stage.

We have seen in section 4.5 that non-abelian gauge theories can have monopole states, compatibly with Dirac's quantization condition. The allowed states depend on the global structure of the gauge group. The lines associated to such magnetic monopoles, when considered external

non-dynamical sources, are the non-abelian 't Hooft monopoles. A precise definition of non-abelian 't Hooft line/loop operator is a bit involved and won't be needed for our purposes. We denote in what follows by $T_\gamma^{(r)}$ a 't Hooft line/loop operator on a curve γ in the representation r of the gauge group. A 't Hooft loop $T_\gamma^{(r)}$ can be seen as the world-lines of a pair of external monopoles transforming in representations r and r^* . Note that such monopoles don't need to be topologically stable.

Phases of gauge theories are classified by looking at the behaviour of one-point function of large Wilson loops. For a rectangular Wilson loop W with sizes L and T , we have

$$\langle W \rangle \propto e^{-TV(L)}, \quad (6.1.15)$$

where $V(L)$ is the potential felt by the two external sources. We will see that useful information arises by also looking at one-point function of large 't Hooft loops.

It is important to distinguish dynamical and external charged fields. Given an abelian or non-abelian gauge theory, we distinguish two different charged states:

- Dynamical matter, namely matter fields which can fluctuate and whose dynamics we want to consider quantum mechanically. These fields enter directly in the Lagrangian and we have to path integrate over them. In an effective field theory approach such states are either massless or very light.
- External sources, namely matter fields which do not fluctuate. These fields do not enter directly, but their effect is captured by Wilson and 't Hooft lines. We usually assume such fields to be very heavy.

The distinction is important because we can consider situations where the two sets are quite different. A notable example is in the study of pure Yang-Mills theory, where no dynamical quarks are present, yet we can probe the theory with heavy sources represented by Wilson and 't Hooft lines.

6.2 Symmetries as topological operators

In this section we reconsider symmetries in QFT in terms of topological operators and introduce new kind of symmetries denoted higher-form symmetries. Global symmetries in QFT implement selection rules in correlation functions by means of Ward identities. For example, given a theory invariant under a $U(1)$ global symmetry with a conserved Noether current J_μ , we have

$$i\partial_\mu^x \langle J^\mu(x) O_1(x_1) \dots O_n(x_n) \rangle = \sum_{k=1}^n \delta^{(d)}(x - x_k) \langle O_1(x_1) \dots \delta O_k(x_k) \dots O_n(x_n) \rangle, \quad (6.2.1)$$

where O_i are local operators of the theory with charge q_i under $U(1)$, and $\delta O_k = iq_k O_k$. The conserved charge operator reads

$$Q = \int d^{d-1}\vec{x} J^0(\vec{x}, t). \quad (6.2.2)$$

Q is the integral over the full space of a local operator and as such is a non-local operator, but crucially it is conserved in time. If we integrate (6.2.1) over the whole space-time we get

$$0 = i \int d^d x \partial_\mu^x \langle J^\mu(x) O_1(x_1) \dots O_n(x_n) \rangle = i \sum_{k=1}^n q_k \langle O_1(x_1) \dots O_n(x_n) \rangle, \quad (6.2.3)$$

which implies that

$$\langle O_1(x_1) \dots O_n(x_n) \rangle \neq 0 \quad \text{only if} \quad \sum_{k=1}^n q_k = 0, \quad (6.2.4)$$

namely charge conservation of the $U(1)$ symmetry. However, we are not forced to integrate over the whole space. If we integrate over a finite region M_d in space-time, which includes the point x , we have

$$\begin{aligned} \int_{M_d} \partial_\mu^x \langle J^\mu(x) O_1(x_1) \dots O_n(x_n) \rangle &= \int_{M_{d-1}} n_\mu \langle J^\mu(x) O_1(x_1) \dots O_n(x_n) \rangle \\ &= \sum_{k=1}^n q_k \int_{M_d} \delta^{(d)}(x - x_k) \langle O_1(x_1) \dots O_n(x_n) \rangle, \end{aligned} \quad (6.2.5)$$

where $\partial M_d = M_{d-1}$ and n_μ is the direction normal to the surface M_{d-1} . Define now the operator

$$Q(M_{d-1}) \equiv \int_{M_{d-1}} n_\mu J^\mu(x) = \int_{M_{d-1}} *J_1, \quad (6.2.6)$$

where in the last equality we introduced a more compact and convenient expression in terms of differential forms where the current J_1 is a one-form. If M_d does not contain any of the points x_k , we have

$$\langle Q(M_{d-1}) O_1(x_1) \dots O_n(x_n) \rangle = 0, \quad (6.2.7)$$

while if M_d contains, e.g., the points x_1, x_2 , up to x_p for some p , we get

$$\langle Q(M_{d-1}) O_1(x_1) \dots O_n(x_n) \rangle = \sum_{k=1}^p q_k \langle O_1(x_1) \dots O_n(x_n) \rangle. \quad (6.2.8)$$

We can vary M_{d-1} at will, but as long as we do not cross local operators, the correlator (6.2.7) does not change. The operator $Q(M_{d-1})$ is a generalization of the “full space” charge operator Q (6.2.2) and, like Q , it is topological because it is invariant under small deformations (change of time for Q).

The topological nature of Q allows to multiply such operators among themselves without worrying about the usual UV divergences that would occur for general local operators at coincident points. The current J^μ is in fact conserved and does not renormalize, namely it is finite when expressed in terms of renormalized fields, and cannot acquire an anomalous dimension.

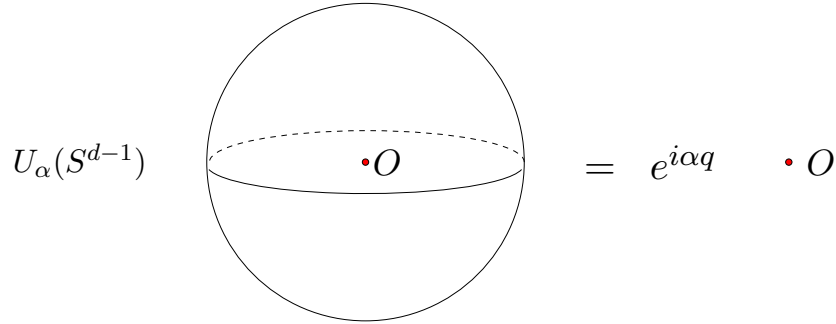


Figure 6.1: A topological operator U_α supported on a sphere S^{d-1} surrounding a local operator O (red dot) with charge q implements a global $U(1)$ transformation.

We can then exponentiate the operator $Q(M_{d-1})$ to get another topological operator

$$U_\alpha(M_{d-1}) = \exp\left(i\alpha \int_{M_{d-1}} *J_1\right). \quad (6.2.9)$$

If M_{d-1} surrounds a point x , where a local operator O of charge q is inserted, we have

$$U_\alpha(M_{d-1})O(x) = e^{i\alpha q}O(x). \quad (6.2.10)$$

Note that (6.2.10) is the analogue of the transformation of a local operator in the Hilbert space which is ordinarily written as

$$U_\alpha O(x) U_\alpha^\dagger = e^{i\alpha q} O(x), \quad (6.2.11)$$

where U_α is the exponential of the equal-time charge operator (6.2.2). In order to see that, we take $t + \epsilon$ in U_α and $t - \epsilon$ in U_α^\dagger , with $\epsilon \ll 1$, where t is the time insertion of the operator $O(x)$. As $\epsilon \rightarrow 0$, the only non-vanishing contribution to the left-hand side arises from an infinitesimal surface M_{d-1} surrounding the operator, reproducing (6.2.10).

In order to gain a better intuition on topological operators, it is useful to consider Euclidean spaces, where the finite region M_d can be taken to be e.g. a d -dimensional ball B_d , with boundary $\partial M_d = M_{d-1} = S^{d-1}$. See figure 6.1 for a visualisation of (6.2.10). The operators U_α implement a global $U(1)$ transformation with phase α and realize the group action

$$U_\alpha U_\beta = U_{\alpha+\beta}, \quad U_\alpha U_{-\alpha} = U_{-\alpha} U_\alpha = I, \quad (6.2.12)$$

where we omitted to write the common support M_{d-1} of the operators. The generalization for non-abelian symmetries is straightforward. We can now derive the selection rules (6.2.4) using the operators U_α bypassing the Ward identities and the Noether current.

Consider a generic correlator of n local operators O_i at points x_i , $i = 1, \dots, n$. Let S^{d-1} be a large sphere surrounding all operators. If the vacuum is invariant under the symmetry,

$U_\alpha(S^{d-1})|0\rangle = |0\rangle$, and we have

$$\begin{aligned} \langle O_1(x_1) \dots O_n(x_n) \rangle &= \langle U_\alpha(S^{d-1})O_1(x_1) \dots O_n(x_n) \rangle = e^{i\alpha \sum_{k=1}^n q_k} \langle O_1(x_1) \dots O_n(x_n) U_\alpha(S^{d-1}) \rangle \\ &= e^{i\alpha \sum_{k=1}^n q_k} \langle O_1(x_1) \dots O_n(x_n) \rangle \neq 0, \quad \text{only if } \sum_{k=1}^n q_k = 0. \end{aligned} \quad (6.2.13)$$

Discrete symmetries do not have an associated conserved current, yet there should exist topological operators $U_\alpha(M_{d-1})$ implementing the symmetry transformation on local operators. Hence (6.2.13) applies also in this case. Note that the selection rule (6.2.13) does not apply if the symmetry is spontaneously broken, since in that case $U_\alpha(S^{d-1})|0\rangle \neq |0\rangle$.

The meaning of the Euclidean topological operators $U_\alpha(M_{d-1})$ when we Wick rotate back to ordinary Minkowski space-time crucially depends on the causal structure of the space M_{d-1} . In real time QFT we define an Hilbert space at some fixed time and then we evolve the states according to the Hamiltonian. Topological operators U_α where M_{d-1} in Minkowski space corresponds to space-like separated points give rise to proper conserved operators acting on the Hilbert space, like the ordinary charge operator (6.2.2). In contrast, the topological operators U_α where M_{d-1} in Minkowski space corresponds to time-like separated points cannot be interpreted as an operator acting on the Hilbert space. It is rather interpreted as a defect, a sort of “topological” domain wall in space in which local operators acquire a phase (twist) when crossing them. This twist effectively defines a new Hilbert space. In most of the considerations that follows we will remain in Euclidean signature and this distinction will be immaterial, but it is important to keep it into account.

6.2.1 Higher-form symmetries

Higher-form global symmetries are symmetries which act on extended objects like lines, surfaces, etc. A p -form symmetry is defined to be a symmetry where the charged objects are p -dimensional (in space). We denote it by $G^{(p)}$, where G denotes the group action. In this language, we refer to the ordinary symmetries acting on local (point-like) operators discussed in section 6.2 as 0-form symmetries.

In order to understand higher-form symmetries, it is useful to consider their gauged version. A gauged- p form symmetry is a $U(1)$ gauge theory where we replace the connection one form A_1 with a $p+1$ -form A_{p+1} . Under a $U(1)$ gauge transformation

$$A_{p+1} \rightarrow A_{p+1} + d\xi_p, \quad (6.2.14)$$

where ξ_p is a p -form representing the gauge transformation. The objects charged under $U(1)^{(p)}$ are understood by looking at the minimal coupling, which reads in components

$$A_{\mu_1 \dots \mu_{p+1}} J^{\mu_1 \dots \mu_{p+1}}, \quad (6.2.15)$$

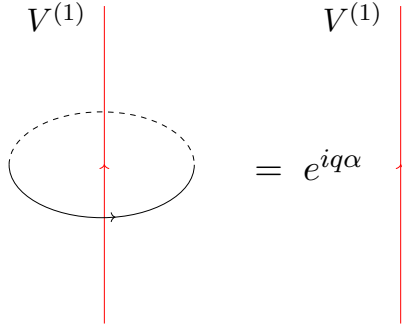


Figure 6.2: A topological operator for a 1-form symmetry U_α supported on a sphere S^{d-2} (black circle) and surrounding a line operator $V^{(1)}$ (red straight line) with charge q under $U(1)^{(1)}$.

and is the natural generalization for $p > 0$ of the ordinary minimal coupling for 1-form connections. A source whose current is a $p + 1$ -form is a surface of space dimension p . This is easily understood by looking at external sources. For 0-form symmetries the minimal coupling reads as the world-line considered in section 6.1:

$$\int A_\mu \frac{dx^\mu(s)}{ds} ds, \quad (6.2.16)$$

where s is the world-line parameter. We can always choose as variable s the proper time t of the particle, so that $x^0 = t$ and $x^i = x^i(t)$ ($i = 1, \dots, d - 1$). In particular, a particle at rest couples to A^0 . For 1-form symmetries the currents has to be a two-form and hence the $1d$ world-line is replaced by a $2d$ world-sheet

$$\int A_{\mu\nu} \epsilon^{\alpha\beta} \partial_\alpha x^\mu(\sigma) \partial_\beta x^\nu(\sigma) d^2\sigma, \quad (6.2.17)$$

where $\alpha, \beta = 0, 1$, $\epsilon_{\alpha\beta}$ is the completely antisymmetric (Lorentzian) 2-tensor and σ_α are world-sheet coordinates. We choose as one of the variables σ_α the proper time t of the string, so that $x^0 = \sigma^0$. The coupling of the string to $A_{\mu\nu}$ depends on its orientation. For example, a static straight string along direction x^k at the origin in the other directions ($x^k = \sigma^1$, $x^i = 0$, $i \neq 0, k$) couples to A_{0k} . Similarly for $p > 1$. For 0-form symmetries global $U(1)$ transformations are those which are constant and do not depend on x . In terms of (6.2.14) they are the ones where $d\xi_0 = 0$. The $U(1)$ global p -form symmetries are similarly the transformations for which the connection A_{p+1} is invariant, namely

$$d\xi_p = 0. \quad (6.2.18)$$

In contrast to 0-form symmetries, global $U(1)^{(p)}$ transformations do not require constant parameters of the transformations. The topological charge operators are obtained by integrating the charges over the space transverse to the source. Since the source is now p -dimensional, the topological operators for p -form symmetries are $d - p - 1$ dimensional. For any p , we can write

them as (in differential form notation)

$$U_\alpha(M_{d-p-1}) = \exp\left(i\alpha \int_{M_{d-p-1}} *J_{p+1}\right). \quad (6.2.19)$$

The operators in the Hilbert space creating or annihilating the sources are given by p -dimensional line/surface operators $V^{(p)}(C)$, where C is the p -dimensional support of the operator. If M_{d-p-1} links with $V^{(p)}(C)$,² then we have

$$U_\alpha(M_{d-p-1})V^{(p)}(C) = e^{i\alpha q}V^{(p)}(C), \quad (6.2.20)$$

which is the generalization of (6.2.10) for p -form symmetries, see e.g. figure 6.2.

In contrast to 0-form symmetries p -form symmetries with $p > 0$ are necessarily abelian. This is a consequence of the fact that the associated topological operators are lower dimensional (codimension $p + 1$ in space-time) and hence we can freely move them around:

$$U_\alpha(M_{d-p-1})U_\beta(M_{d-p-1}) = U_\beta(M_{d-p-1})U_\alpha(M_{d-p-1}), \quad p > 0. \quad (6.2.21)$$

For example, in figure 6.2 the action of $U_\alpha U_\beta$ on $V^{(1)}$ is given by two circles surrounding the line. The order cannot matter since we are free to move them at will and past each other. In contrast, in figure 6.1 the action of $U_\alpha U_\beta$ on O can be different from that of $U_\beta U_\alpha$ because there is no way to smoothly connect one configuration to the other.

In these lectures we will mostly be interested in one-form global symmetries associated to ordinary connections and field strengths in $4d$ gauge theories. From now on we then set $d = 4$. For a $U(1)$ gauge field A a global one-form symmetry transformation with parameter α is given by

$$A \rightarrow A + \frac{\alpha}{2\pi}\xi, \quad (6.2.22)$$

where $0 \leq \alpha \leq 2\pi$ and ξ is a closed one-form. Note that this is different from an ordinary zero-form gauge symmetry because i) ξ is closed but not exact, and ii) local operators are invariant under the transformation (6.2.22). The connection associated to the gauged version of the transformation (6.2.22) is $F = dA$, which is invariant when ξ is closed. Since A is a $U(1)$ gauge field, for any 1-cycle γ in space we should have

$$\int_\gamma \xi = \frac{2\pi p_\gamma}{e}, \quad p_\gamma \in \mathbb{Z}, \quad (6.2.23)$$

in order to have the correct flux quantization (6.1.10). The line operators charged under (6.2.22) are the Wilson lines. From (6.1.8) we immediately get

$$W_\gamma^{(q)} \rightarrow e^{iq\alpha p_\gamma} W_\gamma^{(q)}. \quad (6.2.24)$$

²An heuristic explanation of the notion of linking is given below (6.2.24) for one-form symmetries. The generalization to p -form symmetries is straightforward.

The transformation can be seen as due to the action of topological operators $U_\alpha(M_{d-2})$. In this case p_γ corresponds to the linking number between M_{d-2} and the line. Roughly speaking, the linking is given by the number of points (counted plus or minus depending on the orientation) in which γ crosses the space M_{d-1} with boundary M_{d-2} . For example, in figure 6.2 $M_{d-2} = S^{d-2}$ is represented by a circle surrounding the line and $M_{d-1} = B_{d-1}$ is the disk inside the circle. As the line crosses the disk once, we have $p_\gamma = 1$. The black arrow on the circle distinguishes U_α from U_α^\dagger , while the red arrow on the charged line distinguishes a charge q from a charge $-q$ line. If we reverse any of these arrows $p_\gamma = -1$. If we reverse both $p_\gamma = 1$. We see from (6.2.24) that α is in fact an angular variable with period 2π . In this case the topological operators implementing the symmetry are easily found because the current two-form coincides (up to a normalization) with the field strength F . For a free Maxwell field

$$J_{\mu\nu}^{(e)} = 2F_{\mu\nu} \quad (6.2.25)$$

is conserved as $\partial_\mu F^{\mu\nu} = 0$ are the equations of motion in absence of charged matter. The topological surface operators read

$$U_\alpha^{(e)}(M_2) = \exp\left(i\alpha \int_{M_2} *J_2^{(e)}\right). \quad (6.2.26)$$

Note that the factor of 2 in (6.2.25) matters to normalize the current in such a way that $U_{2\pi}$ acts as the identity on Wilson lines. We added a superscript (e) (for electric) in (6.2.25) and (6.2.26) because a free $U(1)$ gauge theory has in fact an additional ‘‘magnetic’’ $U(1)_m^{(1)}$ one-form symmetry. This is the symmetry under which ’t Hooft lines are charged and is given by

$$J_2^{(m)} = \frac{*F}{2\pi}, \quad (6.2.27)$$

automatically conserved due to the Bianchi identity, valid in absence of magnetic sources. The topological surface operators read

$$U_\alpha^{(m)}(M_2) = \exp\left(i\alpha \int_{M_2} *J_2^{(m)}\right). \quad (6.2.28)$$

Under $U(1)_m^{(1)}$ with parameter α , the ’t Hooft lines (6.1.11) transform as

$$T_\gamma^{(n)} \rightarrow e^{in\alpha} T_\gamma^{(n)}. \quad (6.2.29)$$

Dynamical charged states explicitly break $U_e^{(1)}$. This is clear since $\partial_\mu F^{\mu\nu} \neq 0$ in presence of sources. In terms of the geometric description in figure 6.2, the breaking is due to the fact Wilson lines can now end. In presence of charged states, we can indeed define a gauge invariant open Wilson line by simply attaching a local operator at its end, which compensates for the

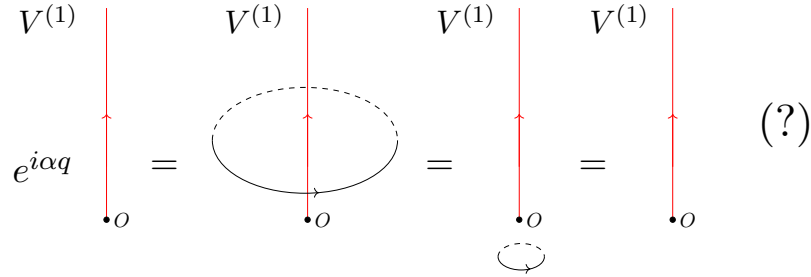


Figure 6.3: In presence of a charged local operator O , a 1-form symmetry is explicitly broken as the effect of the associated topological operator on a line $V^{(1)}$ (red straight line) depends on its position (black circle). The set of equalities in the figure cannot hold for $q \neq 0$.

transformation (6.1.6). For example, if $O(x)$ is a local operator with charge 1, the combination

$$e^{ie \int_x^\infty A} O(x) \quad (6.2.30)$$

is gauge-invariant. If the Wilson line can end, an inconsistency between having a topological operator U_α and a well-defined charge arises. Suppose that the line has a non-trivial charge $q \neq 0$ under U_α . If U_α is topological, we are free to move it at will in space. In particular, we can disentangle it from the Wilson line and shrink it to zero, which would lead to a contradiction. We conclude that the symmetry is broken and U_α is no longer topological (its position does matter). See figure 6.3 for an illustration. More precisely, $U(1)_e^{(1)}$ is generally broken to a discrete subgroup depending on the charges of dynamical matter. For example, if we add a charged particle with charge $|Q|$, Wilson lines with charges $|q| < |Q|$ cannot be broken. The operator $U_{2\pi/Q}^{(e)}$ remains topological and generates a discrete unbroken \mathbb{Z}_Q subgroup. Similarly, dynamical magnetic monopoles generally break $U_m^{(1)}$ to a discrete subgroup (or to nothing), depending on their magnetic charges.

Non-abelian gauge theories do not have continuous one-form symmetries, because they have charged dynamical fields, the gluons. We can detect the presence of a discrete one-form symmetry by looking at the Wilson lines which cannot be broken by gluons, similarly to what we did above to argue that $U(1)_e^{(1)} \rightarrow \mathbb{Z}_Q^{(1)}$ in presence of a charge $Q > 1$ state in an abelian gauge theory. Let us consider for definiteness $SU(N)$ gauge theories. Gluons are in the adjoint representation, which has N -ality $n = 0$. Since N -ality is conserved in decomposing products of irreducible representations, gluon operators can only attach and break Wilson lines based on representations r with $n_r = 0$. Wilson lines with $n_r = 1, \dots, N-1 \neq 0$ are instead unbreakable. We conclude that there is a one-form symmetry which is associated to the center symmetry $Z[SU(N)] = \mathbb{Z}_N$. Under the generator of $\mathbb{Z}_N^{(1)}$, a Wilson loop $W_\gamma^{(r)} \rightarrow e^{2i\pi n_r/N} W_\gamma^{(r)}$. The addition of dynamical quarks in a representation with N -ality n_q explicitly breaks $\mathbb{Z}_N^{(1)}$ to $\mathbb{Z}_Q^{(1)}$ where $Q = \gcd(n_q, N)$. In particular, fundamental matter completely breaks the one-form symmetry. $SU(N)$ gauge theories do not have a magnetic one-form symmetry, since $\pi_1[SU(N)] = \emptyset$. As discussed in section 4.5, the allowed monopoles in $SU(N)$ span the lattice $\Lambda_w(PSU(N))/W$ which has only

representations with $n_r = 0$. Hence all 't Hooft loops can be screened. The global form of the gauge group matters. For example, for a $PSU(N)$ gauge theory, Wilson loops must have $n_r = 0$ and no electric one-form symmetry survives. In contrast, all 't Hooft loops are allowed and hence we get now a $\mathbb{Z}_N^{(1)}$ magnetic one-form symmetry.

Note the key difference between dynamical matter and external sources in terms of the one-form symmetries. The former explicitly breaks one-form symmetries, while the latter provide the states charged under them in terms of Wilson and 't Hooft lines. Correlation functions involving Wilson and 't Hooft lines are subject to selection rules according to (6.2.24) and (6.2.29). In particular, a non-zero one-point function of a large Wilson loop ('t Hooft loop) implies that $U(1)_e^{(1)}$ ($U(1)_m^{(1)}$) is spontaneously broken. Since gauge theories phases are classified according to the behaviour of Wilson and 't Hooft loops, one-form symmetries allow us for a sharp characterization of such phases in terms of global (one-form) symmetries and their breaking.

6.3 Phases of abelian and non-abelian gauge theories

We are now ready to characterize the different possible phases of $4d$ gauge theories. According to the Landau criterion briefly discussed in section 2.1, different phases are classified using global symmetries. In gauge theories such global symmetries are the electric and magnetic one-form symmetries. There is yet no universally accepted precise definition of which order parameter to use, though the idea is clear. We can take as order parameter the one-point function of a rectangular Wilson loop $W(L, T)$ with sizes L and T , and consider, at finite T ,

$$\mathcal{K}_e \equiv \lim_{L \rightarrow \infty} \langle W(L, T) \rangle. \quad (6.3.1)$$

Different phases are characterized by having $\mathcal{K}_e = 0$ or $\mathcal{K}_e \neq 0$, corresponding respectively to unbroken or spontaneously broken electric one-form symmetry. We can define a similar order parameter for the magnetic one-form symmetry using the 't Hooft loops:

$$\mathcal{K}_m \equiv \lim_{L \rightarrow \infty} \langle T(L, T) \rangle. \quad (6.3.2)$$

We first give an overview of the various phases we can have, valid for general $4d$ gauge theories, and afterwards discuss in more detail different cases, abelian $U(1)$, pure Yang-Mills, Yang-Mills in presence of matter.

A gauge theory is in a confined phase if $\mathcal{K}_e = 0$. Confinement means that an infinite energy is required to separate two external sources, which feel a constant force between them. This corresponds to a potential $V(L) \propto L$ in (6.1.15). Historically, a confined phase was defined as the phase where $\langle W(L, T) \rangle \sim \exp(-LT)$ for large L and T . Since the exponent scales with the area of the loop, this was denoted “area law”. *A confined phase is characterized by having unbroken electric one-form symmetry.*

A gauge theory is in a deconfined phase if $\mathcal{K}_e \neq 0$. This corresponds to either having long-

range Coulomb interactions among sources ($V(L) \propto 1/L$) or to a Higgs phase where $V(L)$ is exponentially damped at large distances. The Coulomb phase is a particular instance of a conformal phase, where the CFT at large distances is free (a free photon). Historically, a deconfined phase was defined as the phase where $\langle W(L, T) \rangle \sim \exp(-T)$ for large L and T .³ Since the exponent scales with the perimeter of the loop, this was denoted “perimeter law”. A *deconfined phase is characterized by having spontaneously broken electric one-form symmetry*. We can distinguish the Coulomb/conformal and the Higgs phases by looking at ’t Hooft loops, as we will discuss below.

After this brief overview, we can turn to a somewhat more detailed discussion. For concreteness, we consider below a few notable cases: abelian theories, pure $SU(N)$ and $PSU(N)$ gauge theories, $SU(N)$ with fundamental matter, $SU(N)$ and $PSU(N)$ with adjoint matter.

6.3.1 Abelian gauge theories

Continuum $4d$ abelian gauge theories do not have a confinement phase.⁴ In absence of dynamical matter, we just have a free photon theory, which is a free CFT, with $U(1)_e^{(1)} \times U(1)_m^{(1)}$ one-form symmetries. As we have seen in (6.1.3), both Wilson and ’t Hooft loops satisfy a perimeter law and hence $U(1)_e^{(1)} \times U(1)_m^{(1)}$ are both spontaneously broken. We will not elaborate on that, but note that the appearance of a massless photon in the Coulomb phase can be interpreted as the Goldstone boson associated to the spontaneous breaking of the one-form symmetry (a vector and not a scalar, because we are dealing with a one-form, and not a zero-form global symmetry).

In presence of dynamical matter, the IR value of the charge in the Coulomb phase is set by the mass m of the lightest charged particle. We have

$$V(r) \sim \frac{\alpha(m)}{r}. \quad (6.3.3)$$

If charged massless particles are present, the $U(1)$ theory is formally IR free and we get a modified Coulomb phase

$$V(r) \sim \frac{\alpha(r)}{r} \sim \frac{1}{r \log r}. \quad (6.3.4)$$

Abelian gauge theories present another phase which can be accessed perturbatively, the Higgs phase. In the Higgs phase the photon gets a mass and the force between charged sources is completely screened, as the propagator is exponentially damped. The Wilson lines W_γ obey a perimeter law, like in the Coulomb phase, but they no longer characterize phases, because the electric one-form symmetry $U(1)_e^{(1)}$ is explicitly broken by the charged matter. $U(1)_m^{(1)}$ remains however unbroken and, interestingly enough, ’t Hooft lines behave differently. In nature the Higgs phase of a $U(1)$ gauge theory is realized in superconductors. Due to the Meissner effect, a

³In a general renormalization scheme the regularization of the contact terms like the ... in (6.1.3) leaves a finite constant term. Hence $V(L)$ generically goes to a constant in both the Coulomb and Higgs phases.

⁴The word continuum is necessary, because $U(1)$ gauge theories at strong coupling on the lattice do indeed confine. Such confinement does not persist in the continuum limit.

sufficiently weak magnetic field cannot penetrate a superconductor. The flux lines focus instead inside vortices, as briefly discussed in section 4.4. We can interpret a large 't Hooft loop as the world-lines of a pair of opposite magnetically charged sources which are placed inside the superconductor far away from each other. Magnetic lines from one source to another are then aligned in a thin one-dimensional vortex. Since the propagator of a massless particle in one dimension grows linearly with the distance, we have $V(L) \propto L$ and hence we get an area law behaviour for the 't Hooft loop in the Higgs phase:

$$\langle T_\gamma \rangle \propto e^{-A(\gamma)}, \quad A \sim LT. \quad (6.3.5)$$

6.3.2 Yang-Mills theory

Independently of the global structure of the gauge group, pure non-abelian Yang-Mills theory (no dynamical matter) are expected to be in a confined phase. In the IR the strength of the interactions among gluons is strong and the particle spectrum consists of color singlet bound states of gluons called glueballs. Similarly to the magnetic flux in superconductors, the chromo-electric flux between a pair of external massive quarks focuses in a one-dimensional string and results in a linear potential between the two quarks which cannot be separated and remain confined in a color singlet bound state. Evidence of confinement in pure non-abelian Yang-Mills theory and other theories which are not real world QCD arise from numerical lattice simulations. Unfortunately the detailed mechanism of how confinement occurs is still unknown.

Let us focus on gauge theories based on $su(N)$ Lie algebra and consider for simplicity the two cases of $SU(N)$ and $PSU(N)$ global groups. $SU(N)$ gauge theories have an unbroken $\mathbb{Z}_N^{(1)}$ electric one-form symmetry under which Wilson loops are charged according to the N -ality n of their representation. Wilson loops with $n \neq 0$ satisfy an area law. We expect that the tension T_n of the string between Wilson loops, responsible for the linear potential term between the external quarks, depends on n . Charge conjugation symmetry requires $T_n = T_{N-n}$, so we expect in general $[N/2]$ string tensions. In $PSU(N)$ gauge theory there is no electric one-form symmetry, the allowed Wilson loops have $n = 0$, but we have a magnetic $\mathbb{Z}_N^{(1)}$ one-form symmetry under which 't Hooft loops with $n \neq 0$ are charged. The confinement in this case is signalled by the fact that the magnetic $\mathbb{Z}_N^{(1)}$ symmetry is spontaneously broken, namely 't Hooft loops satisfy a perimeter law. Note the analogy with the Higgs phase in superconductors, with the replacement of electric and magnetic sources. In the $U(1)$ case the condensation of charged particles leads to the confinement of the magnetic flux. If we replace the role of electric and magnetic forces, we expect that condensation of magnetic particles leads to the confinement of the electric flux. This simple observation led 't Hooft long ago to propose that perhaps confinement is given by condensation of monopoles in non-abelian gauge theories. If the condensing states are dyons rather than monopoles, we have what is called *oblique* confinement. A concrete realization of both monopole and dyon condensation is famously provided in the Seiberg-Witten solution of certain supersymmetric theories [40], see the lectures by M. Bertolini for a pedagogical introduction to this beautiful subject.

6.3.3 Yang-Mills theory with fundamental matter

Fundamental dynamical matter ($n = 1$) is only possible for $SU(N)$ gauge theories. The electric one-form symmetry in this case is completely broken and all Wilson loops satisfy a perimeter law. The Yang-Mills strings are now breakable. If we try to separate two external sources, the energy of the configuration increases due to the linear force between them.⁵ At some point the energy accumulated in the string will be large enough that it will be energetically favourable to break the string and create out of the vacuum a particle-anti particle pair that attaches to the end-points of the two strings. Eventually confinement still takes place, as no colored particle in isolation is allowed in the Hilbert space, only color-neutral configurations. This is of course the notable case occurring in real world QCD, where the color neutral states are mesons and baryons. Confinement in presence of fundamental matter (QCD included) is sometimes denoted “quark confinement” or “charge screening”, to distinguish it from the “true” confinement where strings cannot break, sometimes denoted “strict confinement”, the one occurring in pure non-abelian Yang-Mills theories.

In $SU(N)$ gauge theories the magnetic one-form symmetry is also absent, so we do not have an intrinsic characterization in terms of one-form symmetries. However, we can characterize the theory by the possible zero-form symmetries arising from the matter sector. Consider for example N_f Dirac fermions in a $SU(N)$ gauge theory with equal mass m and let us keep track of the $SU(N_f)_A$ global chiral symmetry and what dynamics we can have starting from large N_f .⁶ For $N_f \geq 11N/2$ the theory is not UV free and we expect to be in a somewhat exotic non-abelian IR free phase. Depending on m , the Coulomb potential will read as (6.3.3) or (6.3.4). The chiral symmetry is unbroken. For $N_f < 11N/2$ the theory is UV free, but its IR fate depends on N_f . For $N_f^* < N_f < 11N/2$, where N_f^* is an unknown constant, the theory is expected to flow to a non-trivial CFT where again the chiral symmetry is unbroken. The existence of such phase (called conformal window) can be analytically established by taking the limit $N \rightarrow \infty$, $N_f \rightarrow \infty$ with $x = N_f/N$ fixed. As far as phase characterization is concerned, the above two phases are identical and lead to a gapless CFT. For $N_f \leq N_f^{**}$, where $N_f^{**} \leq N_f^*$ is also unknown, an actual phase transition occurs and chiral symmetry spontaneously breaks. For which values of N_f quark confinement takes place is still unclear. A conservative scenario is to assume that chiral symmetry breaking and quark confinement occurs at the same time, i.e. $N_f^{**} = N_f^*$, and as soon as we exit the conformal window the theory confines. However, we might also have another phase where chiral symmetry is unbroken and the theory is confining, if $N_f^{**} \neq N_f^*$. We do not further discuss the notable real world case of chiral symmetry breaking and quark confinement since it has been extensively discussed in the QFT I course. When $N_f = 0, 1$ we have no chiral symmetry and strict or quark confinement is expected.

In presence of scalar fundamental matter we can also have a Higgs phase. If the gauge group

⁵We are of course assuming that we do not have enough dynamical matter to change the IR properties of the theory, see below.

⁶We do not consider the $U(N_f)_V$ global symmetry since it has been shown that such symmetry cannot be broken in vector-like theories at $\theta = 0$ [41].

is completely Higgsed, the theory is gapped, like in a confining phase. If no global symmetry is broken in the matter sector, we cannot distinguish, in terms of order parameters, a confining (in the sense of charge screening) and a Higgs phase. It is in fact believed that confining and Higgs phases are smoothly connected with a cross-over, roughly like the liquid to vapor phases at high temperatures in figure 2.2.

6.3.4 Yang-Mills theory with adjoint matter

Adjoint matter ($n = 0$) is allowed for both $SU(N)$ and $PSU(N)$ theories. We distinguish the two cases by the set of allowed Wilson and 't Hooft loops, as discussed several times. For $SU(N)$, the electric $\mathbb{Z}_N^{(1)}$ is a good order parameter. Consider N_f Dirac fermions with equal mass m . As N_f varies the qualitative picture is similar to that described in section 6.3.3 for fermion matter, with the difference that we can use both $SU(N_f)_A$ and $\mathbb{Z}_N^{(1)}$ to classify the various phases. In the gapless CFT phases $SU(N_f)_A$ is unbroken and $\mathbb{Z}_N^{(1)}$ is spontaneously broken (perimeter law for Wilson loops), while in the confining phase (assuming $N_f^{**} = N_f^*$) $SU(N_f)_A$ is spontaneously broken and $\mathbb{Z}_N^{(1)}$ is unbroken (area law for Wilson loops).

As before, in presence of scalar adjoint matter we can have a Higgs or Coulomb phase, depending on whether the gauge group is completely Higgsed or abelian factors are left (note that with a single adjoint field generically $SU(N) \rightarrow U(1)^{N-1}$). Again, $\mathbb{Z}_N^{(1)}$ is spontaneously broken (perimeter law for Wilson loops). In contrast to the case of fundamental matter, the confining and the Higgs phase are distinguished by $\mathbb{Z}_N^{(1)}$ being unbroken or not. In the Coulomb case, in addition, we have the appearance of emergent spontaneously broken electric and magnetic one-form symmetries $U(1)_e^{(1)} \times U(1)_m^{(1)}$, a pair for each $U(1)$ factor.

Consider N_f Dirac fermions with equal mass m in a $PSU(N)$ gauge theory. In the gapless CFT phase both $SU(N_f)_A$ and the magnetic $\mathbb{Z}_N^{(1)}$ are unbroken (area law for 't Hooft loops), while in the confining phase (assuming $N_f^{**} = N_f^*$) both $SU(N_f)_A$ and $\mathbb{Z}_N^{(1)}$ are spontaneously broken (perimeter law for 't Hooft loops).

In presence of scalar adjoint matter we can have in addition a Coulomb or Higgs phase. In the Coulomb case the IR theory is gapless and emergent spontaneously broken $U(1)_e^{(1)} \times U(1)_m^{(1)}$ symmetries appear. In the Higgs case the theory is gapped, but it is distinguished by the confining phase by the magnetic $\mathbb{Z}_N^{(1)}$ symmetry.

6.4 Generalized 't Hooft anomaly matching conditions

The 't Hooft anomaly matching conditions are one of the few first-principle methods we have to constrain the possible IR phases of a strongly coupled theory. In its original implementation, the anomalies entering the matching conditions are associated to continuous global symmetries. In addition, the anomalies in the UV theory are uniquely induced by chiral transformations on fermions. This set-up is too restrictive and can be extended in various ways, leading to generalized 't Hooft anomaly matching conditions.

- (1) Anomalies are not necessarily associated to fermions and chiral transformations.
- (2) Higher-form global symmetries can also have t' Hooft anomalies. We can also have mixed anomalies involving p -form symmetries with different p 's.
- (3) Anomalies can also affect discrete global symmetries (both ordinary and higher-form symmetries).

Notably, 't Hooft anomalies are invariant under RG flow (they are topologically protected). So the more 't Hooft anomalies we find, the more we can constraint the IR behaviour of strongly coupled QFTs. A way to detect them, which can also be taken as the definition of having a 't Hooft anomaly, is to check what happens if we couple the global symmetry to an external field, or we gauge the symmetry, affected by the anomaly. If the theory cannot be made gauge-invariant, or some other global symmetry gets broken in the process, we say that a 't Hooft anomaly is present. For continuous symmetries, coupling a p -form global symmetry $G^{(p)}$ to an external field amounts to add a connection A_{p+1} with coupling $A_{p+1} \wedge *J_{p+1}$, where J_{p+1} is the Noether current associated to $G^{(p)}$. Gauging means to make A_{p+1} dynamical, add a kinetic term for it, and path integrate over this field as well. Note that both cases require to consider “local” space-dependent transformations.

How do we couple a discrete symmetry to an external field, or how do we gauge the symmetry? A proper discussion of these topics is beyond the aim of these lectures. For our purposes it is enough to heuristically explain what a gauging of a discrete abelian symmetry does. A global discrete symmetry G in a QFT allows us to split the Hilbert space of states into classes with a definite charge under G . Coupling the symmetry to an external source amounts in this case to add some phases among the different sectors. Gauging the symmetry mean sum over all possible phases (the equivalent of path integrating over all fluctuations of A_{p+1} in the continuous case). Such phases can be interpreted to arise from the insertion of proper topological operators U (M_{d-1} with space-like separated points). This sum effectively projects out all the states with $q \neq 0$. This is what we expect from a gauging procedure: physical states of the gauged theory are only the ones with $q = 0$ of the original theory. In addition, however, other states which were not physical in the original theory become physical in the gauge theory. These are called twisted sectors, and are the ones which are generated when topological operators U associated to the symmetry G are supported in (Minkowski) spaces M_{d-1} with time-like separated points, recall the discussion at the end of section 6.2. It can be shown that whenever we gauge a discrete $\mathbb{Z}^{(p)}$ global symmetry in a d -dimensional QFT, the resulting gauged theory acquires a new global symmetry which is $\mathbb{Z}_N^{(d-p-2)}$ (sometimes called dual or quantum symmetry). 't Hooft anomalies for discrete symmetries are not visible from Feynman diagram computations and can be hard to detect.

t' Hooft anomaly matching of discrete symmetries is not as powerful as its continuous counterpart. The latter allows us to predict that the IR phase of a given UV theory must be gapless (a CFT). The non-trivial IR dynamics can arise because some global symmetry gets spontaneously

broken and massless Goldstone bosons appear, or the symmetry is unbroken and massless states occur. Anomalies in discrete symmetries are instead compatible with having a gapped spectrum. However, in presence of such anomalies, the ground state of the gapped theory cannot be unique (trivially gapped), because a single state cannot carry a non-trivial anomaly. Anomaly arguments alone do not allow us to predict what precisely happens but it allows us to restrict the possible IR scenarios. Together with some other physical input or assumption leads to reasonable hypothesis on the fate of the theory at low energies. For example, a natural and minimal hypothesis consistent with the presence of a \mathbb{Z}_N -valued anomaly is to assume that the discrete symmetry is spontaneously broken and N degenerate vacua appear.

A general classification of global anomalies in QFT is beyond these lectures. In what follows, we focus on the case of zero and one-form symmetries only and present three examples. In section 6.4.1 we show an anomaly for continuous one-form symmetries in Maxwell theory. In section 6.4.2 we show an example of a \mathbb{Z}_2 anomaly for discrete global symmetries in quantum mechanics, and point out a relation between charge fractionalization and anomalies in section 6.4.3. The third example in section 6.4.4 is more interesting and complicated. It is about a mixed anomaly between a one-form and a zero-form symmetry which arises in pure $SU(N)$ Yang-Mills theories at $\theta = \pi$.

6.4.1 A mixed $U(1)^{(1)} \times U(1)^{(1)}$ 't Hooft anomaly in Maxwell theory

In the free Maxwell theory a mixed 't Hooft anomaly arises between the $U(1)_e^{(1)}$ and $U(1)_m^{(1)}$ symmetries. We detect the anomaly by checking the impossibility of consistently coupling to external sources both global symmetries. The currents associated to the $U(1)_e^{(1)} \times U(1)_m^{(1)}$ global symmetries are given in (6.2.25) and (6.2.27). We couple $U(1)_e^{(1)}$ to a two-form gauge connection B_e by relaxing the requirement that ξ in (6.2.22) is a closed one-form. Since the field strength $F = dA$ transforms, we require

$$B_e \rightarrow B_e + \frac{\alpha}{2\pi} d\xi \quad (6.4.1)$$

under $U(1)_e^{(1)}$ so that the action

$$S_0 = \int \left[-\frac{1}{4e^2} (F - B_e) \wedge *(F - B_e) \right] \quad (6.4.2)$$

is $U(1)_e^{(1)}$ gauge-invariant. We now add an external two-form B_m which minimally couples to the magnetic current by means of the coupling $B_m \wedge F/(2\pi)$. If we insist in having unbroken $U(1)_e^{(1)}$ gauge symmetry, we add a counterterm so that B_m couples to the gauge invariant combination $F - B_e$. The total action reads then

$$S = S_0 + \frac{1}{2\pi} \int B_m \wedge (F - B_e). \quad (6.4.3)$$

Consider now a $U(1)_m^{(1)}$ gauge transformation under which $B_m \rightarrow B_m + d\lambda_m$, with λ_m a one-form. We have

$$\delta_m S = \frac{1}{2\pi} \int \lambda_m \wedge dB_e \neq 0. \quad (6.4.4)$$

The action S is $U(1)_e^{(1)}$ gauge-invariant, but not $U(1)_m^{(1)}$ gauge-invariant. Viceversa, without adding the counterterm $-B_e \wedge B_m/(2\pi)$ we would have an action which is $U(1)_m^{(1)}$, but not $U(1)_e^{(1)}$, gauge-invariant. There is no possible choice of counterterms to have both symmetries unbroken. We then have a mixed 't Hooft anomaly between $U(1)_e^{(1)}$ and $U(1)_m^{(1)}$.

6.4.2 A \mathbb{Z}_2 anomaly in quantum mechanics

Consider a free particle moving on a circle.⁷ The Lagrangian reads

$$L = \frac{\dot{q}^2}{2m} + \theta \dot{q}, \quad (6.4.5)$$

where t is Minkowskian time, $q(t)$ is a dimensionless variable describing the motion of the particle, $q \sim q + 1$, and θ is a theta angle. The second term in (6.4.5) is a total derivative. Since $\int dt \dot{q} = \mathbb{Z}$, we see that $\theta \sim \theta + 2\pi$. For simplicity we set the mass parameter $m = 1$ in what follows. The momentum conjugate to q is $\Pi = \dot{q} + \theta$, and the Hamiltonian reads

$$H = \frac{1}{2}(\Pi - \theta)^2, \quad (6.4.6)$$

which has

$$E_n = 2\pi^2 \left(n - \frac{\theta}{2\pi} \right)^2, \quad \psi_n(q) = e^{2i\pi n q}, \quad n \in \mathbb{Z}, \quad (6.4.7)$$

as eigenvalues and normalized eigenfunctions. The Lagrangian (6.4.5) is invariant under a shift symmetry

$$q \rightarrow q + \frac{\alpha}{2\pi}, \quad (6.4.8)$$

with α a real constant parameter for any θ . Note that $\alpha \sim \alpha + 2\pi$ as q is defined on a circle. At $\theta = 0, \pi$, the Lagrangian is also invariant under a charge conjugation symmetry $C : q \rightarrow -q$. For any value of $\theta \neq \pi$ the ground state is unique. At $\theta = \pi$, instead, we get two degenerate vacua, with $n = 0$ and $n = 1$. We focus on the two cases $\theta = 0, \pi$ where C is unbroken. The operator U_α implementing the shift symmetry in the Hilbert space is $U_\alpha = \exp(i\alpha\Pi)$. So we have

$$U_\alpha |n\rangle = e^{i\alpha n} |n\rangle, \quad \theta = 0, \pi. \quad (6.4.9)$$

The action of C on $|n\rangle$ is different at $\theta = 0$ and at $\theta = \pi$. At $\theta = 0$, we have simply

$$C|n\rangle = |-n\rangle, \quad \theta = 0. \quad (6.4.10)$$

⁷This section largely follows appendix D of [42].

Since $\theta \rightarrow -\theta \sim \theta + 2\pi$, at $\theta = \pi$ we get

$$C|n\rangle = |-n+1\rangle, \quad \theta = \pi. \quad (6.4.11)$$

Consider now the combined action of C and $U_{\alpha=\pi}$. We have

$$\begin{aligned} U_{\pi}C|n\rangle &= (-1)^n|-n\rangle, & CU_{\pi}|n\rangle &= (-1)^n|-n\rangle, & \theta &= 0, \\ U_{\pi}C|n\rangle &= -(-1)^n|-n+1\rangle, & CU_{\pi}|n\rangle &= (-1)^n|-n+1\rangle, & \theta &= \pi, \end{aligned} \quad (6.4.12)$$

which imply

$$\begin{aligned} [U_{\pi}, C] &= 0, & \theta &= 0, \\ \{U_{\pi}, C\} &= 0, & \theta &= \pi. \end{aligned} \quad (6.4.13)$$

We see that while the $\mathbb{Z}_2 \times \mathbb{Z}_2$ symmetry generated by U_{π} and C acts linearly in the Hilbert space, with commuting generators, at $\theta = \pi$ the symmetry acts projectively with anti-commuting generators. We can identify the red minus sign in (6.4.12) as a \mathbb{Z}_2 mixed anomaly between U_{π} and C . The ground state degeneracy of the vacuum at $\theta = \pi$ can be explained as due to this anomaly, as a unique ground state cannot support an anomaly.

We verify the presence of the anomaly by gauging the shift symmetry (6.4.8). We replace the time derivative with a covariant one, $\dot{q} \rightarrow D_t q = \dot{q} + A/(2\pi)$, with $A \rightarrow A - \dot{\alpha}$. The gauged version of the Lagrangian (6.4.5) reads

$$L = \frac{1}{2}(D_t q)^2 + \theta D_t q + kA. \quad (6.4.14)$$

In (6.4.14) we have added a linear term in A . This term is not invariant, but it transforms as a total derivative. The action S is also in general not invariant, but it shifts as $S \rightarrow S + 2\pi kn$, where $n \in \mathbb{Z}$, because of the identification $\alpha \sim \alpha + 2\pi$. In the quantum theory S enters as $\exp(iS)$ in the path integral and hence the term kA is allowed as long as k is an integer. Let us verify charge conjugation symmetry at $\theta = 0, \pi$. We demand that $A \rightarrow -A$ under C , so that $D_t q \rightarrow -D_t q$. At $\theta = 0$ C is unbroken if we set $k = 0$. At $\theta = \pi$, we get a breaking term of the form $(k + 1/2)A$. Since k has to be an integer, there is no choice for which we can recover charge conjugation symmetry. We can also verify that demanding charge conjugation leads to a breaking of the shift symmetry. Introduce a chemical potential μ that couples to the charge operator Π and consider the partition function of the system

$$Z(\mu) = \text{tr} e^{-\beta H} e^{i\mu \Pi} = \sum_{n=-\infty}^{\infty} e^{-E_n \beta + i\mu n}, \quad Z(\mu) = Z(\mu + 2\pi), \quad (6.4.15)$$

where E_n are given in (6.4.7). Invariance under C implies $Z(-\mu) = Z(\mu)$, as $\Pi \rightarrow -\Pi$ under charge conjugation. Let us look at the ground state contribution to Z at $\theta = 0, \pi$. At $\theta = 0$ the

vacuum is given by the state $n = 0$ and it is invariant under C : $Z_{\text{vacuum}} = 1$. At $\theta = \pi$ we have

$$Z_{\text{vacuum}} = e^{-\beta \frac{\pi^2}{2}} (1 + e^{i\mu}), \quad (6.4.16)$$

and C is broken. We can insist in having an invariant vacuum and assign a different charge under Π to the two vacua, namely $+1/2$ and $-1/2$ instead of 1 and 0. We define

$$\tilde{Z}_{\text{vacuum}} = e^{-i\frac{\mu}{2}} Z_{\text{vacuum}} = e^{-\beta \frac{\pi^2}{2}} (e^{-i\frac{\mu}{2}} + e^{i\frac{\mu}{2}}). \quad (6.4.17)$$

The new vacuum partition function is C -invariant: $\tilde{Z}_{\text{vacuum}}(-\mu) = \tilde{Z}_{\text{vacuum}}(\mu)$, but at the expense of breaking the shift symmetry, since we now have $\tilde{Z}_{\text{vacuum}}(\mu + 2\pi) = -\tilde{Z}_{\text{vacuum}}(\mu)$. We see again that there is no way to keep both symmetries manifest at the same time.

The presence of an anomaly in quantum mechanics has striking consequences. It is usually assumed that in quantum mechanics the presence of tunnelling forbids the possibility of having persistent degeneracies in the Hilbert space, i.e. possibly classical degeneracies are expected to be removed by quantum effects. We have seen in chapter 5 that in Euclidean space instantons are the configurations which are responsible for that. The \mathbb{Z}_2 anomaly above implies that the vacuum degeneracy should be robust under deformations that do not break charge conjugation and the \mathbb{Z}_2 shift $q \rightarrow q + 1/2$. For example, adding to the system a potential

$$V\left(q + \frac{1}{2}\right) = V(q), \quad V(-q) = V(q) \quad (6.4.18)$$

will not lift the two-fold degeneracy of the vacuum at $\theta = \pi$, since the anomaly is invariant under smooth deformations. This explains that the result of point (b) in the assignment 5.2.64 was not accidental, but had a deeper explanation in terms of this anomaly.

6.4.3 't Hooft anomalies and charge fractionalization

We have seen that insisting in having unbroken charge conjugation in the quantum mechanical model of section 6.4.2 leads to a charge assignment $\pm 1/2$ to the two vacua. This set-up is reminiscent of the charge fractionalization effect discussed in section 4.6. We have found there that a consistent $U(1)_V$ charge assignment of the two kinks states is $Q = \pm 1/2$. That choice came out by the implicit assumption of unbroken charge conjugation symmetry, used in the argument to show that positive and negative energy levels move symmetrically as the background is varied. We denote by $|-1/2\rangle$ and $|1/2\rangle$ the two kink ground states with $Q = -1/2$ and $Q = 1/2$ respectively. The analogue of the shift symmetry operator Π is played by the charge operator Q associated to the $U(1)_V$ symmetry (4.6.3). Let us denote by $U_\alpha = \exp(i\alpha Q)$ the topological operator which implements the $U(1)_V$ transformation (4.6.3). Charge conjugation, by definition, acts on the charge operator as

$$CQC^{-1} = -Q. \quad (6.4.19)$$

Under C the two kink states transform as

$$C|\pm \frac{1}{2}\rangle = |\mp \frac{1}{2}\rangle. \quad (6.4.20)$$

Let us see the effect of C and $U_{\alpha=\pi}$ in the Hilbert space of the theory. In the topologically trivial sector the vacuum has $Q = 0$ and is invariant under C . On an arbitrary fermion particle state with $Q = n$ we have

$$U_{\pi}C|n\rangle = e^{-i\pi n}| - n\rangle, \quad CU_{\pi}|n\rangle = e^{i\pi n}| - n\rangle, \quad (\text{vacuum sector}). \quad (6.4.21)$$

In the topologically non-trivial kink sector an arbitrary n -fermion particle state has half-integer $U(1)_V$ charge because of the ground state charge assignment. Let us denote by $|n + 1/2\rangle$ such a state. The kink ground states correspond to $n = 0$ and $n = -1$. For a general state we have

$$U_{\pi}C|n + \frac{1}{2}\rangle = e^{-i\pi(n + \frac{1}{2})}| - n - \frac{1}{2}\rangle, \quad CU_{\pi}|n + \frac{1}{2}\rangle = e^{i\pi(n + \frac{1}{2})}| - n - \frac{1}{2}\rangle, \quad (\text{kink sector}). \quad (6.4.22)$$

Eqs.(6.4.21) and (6.4.22) imply

$$\begin{aligned} [U_{\pi}, C] &= 0, & (\text{vacuum sector}), \\ \{U_{\pi}, C\} &= 0, & (\text{kink sector}). \end{aligned} \quad (6.4.23)$$

Note the similarity of (6.4.23) with (6.4.13), where $\theta = 0$ and $\theta = \pi$ corresponds respectively to the trivial and kink sector. Like in the quantum mechanical model, U_{π} and C are realized projectively in the kink sector Hilbert space. This is an indication of a \mathbb{Z}_2 't Hooft anomaly between the two symmetries, responsible eventually for the charge fractionalization effect.

6.4.4 $SU(N)$ Yang-Mills theory at $\theta = \pi$

Pure Yang-Mills theory is expected to confine for every value of θ . We would then expect that, for any θ , the vacuum is gapped and unique. In this section we will show by an anomaly argument that this expectation cannot be right, because of an anomaly occurring at $\theta = \pi$. Before discussing this anomaly it is necessary to elaborate a bit more on the different global properties between $SU(N)$ and $PSU(N)$ gauge theories. In particular, the key point (which we will not prove) necessary for our considerations is that instantons in $PSU(N)$ generally satisfy the following condition:

$$\frac{1}{8\pi^2} \int_X \text{tr} F \wedge F = \left(n + \frac{q}{N} \right), \quad n \in \mathbb{Z}, \quad q = 0 \dots N - 1. \quad (6.4.24)$$

With respect to the $SU(N)$ case (5.2.15), we have the possibility of having instanton with fractional value q/N .⁸ The presence of such instantons imply that the range θ in $PSU(N)$ is

⁸This is related to the presence of topologically stable \mathbb{Z}_N magnetic monopoles.

extended by a factor of N :

$$0 \leq \theta \leq 2\pi N, \quad PSU(N). \quad (6.4.25)$$

Under time reversal symmetry T , the term $F \wedge F$ changes sign, so

$$T: \theta \rightarrow -\theta. \quad (6.4.26)$$

Time-reversal symmetry is then explicitly broken by a θ term, except at the values $\theta = 0, \pi$ for $SU(N)$ and $\theta = 0, \pi N$ for $PSU(N)$.

By definition, $SU(N)$ and $PSU(N)$ gauge theories differ by the different global group that is gauged. In particular, gauge transformations that are related by an element of the center are different in $SU(N)$, but are identified as the same transformation in $PSU(N)$. The offset can be compensated by gauging the $\mathbb{Z}_N^{(1)}$ one-form symmetry. In $4d$ Yang-Mills theory it turns out that a $PSU(N)$ theory can be interpreted as a $SU(N)$ gauge theory where the electric $\mathbb{Z}_N^{(1)}$ symmetry is gauged. Wilson lines with $n \neq 0$ are projected out, and reproduce the result that only these are allowed in $PSU(N)$ theories. In $4d$ the dual quantum symmetry is still a one-form symmetry as $d - p - 2 = 1$ and it is identified with the magnetic $\mathbb{Z}_N^{(1)}$ symmetry. The twisted states (charged under $\mathbb{Z}_N^{(1)}$) are the magnetic sources defining 't Hooft lines, stable states in the Hilbert space.

We are now ready to argue that pure $SU(N)$ Yang-Mills theory at $\theta = \pi$ has a mixed \mathbb{Z}_2 't Hooft anomaly which involves time reversal symmetry and the electric one-form symmetry $\mathbb{Z}_N^{(1)}$.⁹ We detect the anomaly by checking that if we gauge $\mathbb{Z}_N^{(1)}$, time reversal T gets broken. The basic argument is very simple. We refer the reader to [42] for a more formal treatment and further details. At $\theta = \pi$ time reversal T is unbroken because

$$\pi \rightarrow -\pi \cong \pi, \quad SU(N). \quad (6.4.27)$$

When we gauge $\mathbb{Z}_N^{(1)}$, however, we get a $PSU(N)$ gauge theory, where the range of θ changes. In this theory at the point $\theta = \pi$ time reversal is explicitly broken because now

$$\pi \rightarrow -\pi \cong 2\pi N - \pi \neq \pi, \quad PSU(N). \quad (6.4.28)$$

We interpret this as a mixed 't Hooft anomaly between time-reversal symmetry T and $\mathbb{Z}_N^{(1)}$. The presence of such anomaly allows us to firmly conclude that the vacuum in Yang-Mills theory at $\theta = \pi$ cannot be trivially gapped. The anomaly does not allow us to predict what precisely happens. A natural and minimal hypothesis consistent with the anomaly is to assume that time reversal symmetry gets spontaneously broken and two degenerate vacua appear.

⁹The anomaly is at $\theta = \pi$ assuming that no anomaly occurs at $\theta = 0$.

Bibliography

- [1] J. L. Cardy, *Scaling and renormalization in statistical physics*. Cambridge lecture notes in physics. Cambridge Univ. Press, Cambridge, 1996.
- [2] E. Witten, *Baryons in the $1/n$ Expansion*, *Nucl. Phys. B* **160** (1979) 57–115.
- [3] S. Coleman, *Aspects of Symmetry: Selected Erice Lectures*. Cambridge University Press, 1985.
- [4] V. A. Rubakov, *Classical theory of gauge fields*. Princeton University Press, Princeton, New Jersey, 5, 2002.
- [5] M. Shifman, *Advanced Topics in Quantum Field Theory*. Cambridge University Press, 4, 2022.
- [6] N. S. Manton and P. Sutcliffe, *Topological solitons*. Cambridge Monographs on Mathematical Physics. Cambridge University Press, 2004.
- [7] D. Gaiotto, A. Kapustin, N. Seiberg, and B. Willett, *Generalized Global Symmetries*, *JHEP* **02** (2015) 172, [[arXiv:1412.5148](https://arxiv.org/abs/1412.5148)].
- [8] T. D. Brennan and S. Hong, *Introduction to Generalized Global Symmetries in QFT and Particle Physics*, [arXiv:2306.00912](https://arxiv.org/abs/2306.00912).
- [9] J. M. Maldacena, *The Large N limit of superconformal field theories and supergravity*, *Adv. Theor. Math. Phys.* **2** (1998) 231–252, [[hep-th/9711200](https://arxiv.org/abs/hep-th/9711200)].
- [10] E. Witten, *Anti-de Sitter space and holography*, *Adv. Theor. Math. Phys.* **2** (1998) 253–291, [[hep-th/9802150](https://arxiv.org/abs/hep-th/9802150)].
- [11] S. S. Gubser, I. R. Klebanov, and A. M. Polyakov, *Gauge theory correlators from noncritical string theory*, *Phys. Lett. B* **428** (1998) 105–114, [[hep-th/9802109](https://arxiv.org/abs/hep-th/9802109)].
- [12] G. 't Hooft, *A Planar Diagram Theory for Strong Interactions*, *Nucl. Phys. B* **72** (1974) 461.
- [13] M. Serone, *Notes on Quantum Field Theory I*, 2022.
https://people.sissa.it/~serone/QFT_Review_Aug17_2022.pdf.

- [14] D. J. Gross and A. Neveu, *Dynamical Symmetry Breaking in Asymptotically Free Field Theories*, *Phys. Rev. D* **10** (1974) 3235.
- [15] N. D. Mermin and H. Wagner, *Absence of ferromagnetism or antiferromagnetism in one-dimensional or two-dimensional isotropic Heisenberg models*, *Phys. Rev. Lett.* **17** (1966) 1133–1136.
- [16] P. C. Hohenberg, *Existence of Long-Range Order in One and Two Dimensions*, *Phys. Rev.* **158** (1967) 383–386.
- [17] S. R. Coleman, *There are no Goldstone bosons in two-dimensions*, *Commun. Math. Phys.* **31** (1973) 259–264.
- [18] M. Nakahara, *Geometry, Topology and Physics, Second Edition*. Graduate student series in physics. Taylor & Francis, 2003.
- [19] G. H. Derrick, *Comments on nonlinear wave equations as models for elementary particles*, *J. Math. Phys.* **5** (1964) 1252–1254.
- [20] H. B. Nielsen and P. Olesen, *Vortex Line Models for Dual Strings*, *Nucl. Phys. B* **61** (1973) 45–61.
- [21] G. 't Hooft, *Magnetic Monopoles in Unified Gauge Theories*, *Nucl. Phys. B* **79** (1974) 276–284.
- [22] A. M. Polyakov, *Particle Spectrum in Quantum Field Theory*, *JETP Lett.* **20** (1974) 194–195.
- [23] P. A. M. Dirac, *Quantised singularities in the electromagnetic field*, *Proc. Roy. Soc. Lond. A* **133** (1931), no. 821 60–72.
- [24] B. Julia and A. Zee, *Poles with Both Magnetic and Electric Charges in Nonabelian Gauge Theory*, *Phys. Rev. D* **11** (1975) 2227–2232.
- [25] M. K. Prasad and C. M. Sommerfield, *Exact classical solution for the 't hooft monopole and the julia-zee dyon*, *Phys. Rev. Lett.* **35** (Sep, 1975) 760–762.
- [26] P. Goddard, J. Nuyts, and D. I. Olive, *Gauge Theories and Magnetic Charge*, *Nucl. Phys. B* **125** (1977) 1–28.
- [27] M. F. Atiyah and I. M. Singer, *The index of elliptic operators on compact manifolds*, *Bulletin of the American Mathematical Society* **69** (1963), no. 3 422 – 433.
- [28] E. Witten, *Analytic Continuation Of Chern-Simons Theory*, *AMS/IP Stud. Adv. Math.* **50** (2011) 347–446, [[arXiv:1001.2933](https://arxiv.org/abs/1001.2933)].

- [29] A. A. Belavin, A. M. Polyakov, A. S. Schwartz, and Y. S. Tyupkin, *Pseudoparticle Solutions of the Yang-Mills Equations*, *Phys. Lett. B* **59** (1975) 85–87.
- [30] G. 't Hooft, *Computation of the Quantum Effects Due to a Four-Dimensional Pseudoparticle*, *Phys. Rev. D* **14** (1976) 3432–3450. [Erratum: *Phys.Rev.D* 18, 2199 (1978)].
- [31] E. Witten, *An $SU(2)$ Anomaly*, *Phys. Lett. B* **117** (1982) 324–328.
- [32] J. S. Schwinger, *Sources and magnetic charge*, *Phys. Rev.* **173** (1968) 1536–1544.
- [33] D. Zwanziger, *Quantum field theory of particles with both electric and magnetic charges*, *Phys. Rev.* **176** (1968) 1489–1495.
- [34] E. Witten, *Dyons of Charge e theta/2 pi*, *Phys. Lett. B* **86** (1979) 283–287.
- [35] S. R. Coleman, *The Fate of the False Vacuum. 1. Semiclassical Theory*, *Phys. Rev. D* **15** (1977) 2929–2936. [Erratum: *Phys.Rev.D* 16, 1248 (1977)].
- [36] C. G. Callan, Jr. and S. R. Coleman, *The Fate of the False Vacuum. 2. First Quantum Corrections*, *Phys. Rev. D* **16** (1977) 1762–1768.
- [37] S. R. Coleman and F. De Luccia, *Gravitational Effects on and of Vacuum Decay*, *Phys. Rev. D* **21** (1980) 3305.
- [38] H. Arason, D. J. Castano, B. Keszthelyi, S. Mikaelian, E. J. Piard, P. Ramond, and B. D. Wright, *Renormalization group study of the standard model and its extensions. 1. The Standard model*, *Phys. Rev. D* **46** (1992) 3945–3965.
- [39] G. Degrandi, S. Di Vita, J. Elias-Miro, J. R. Espinosa, G. F. Giudice, G. Isidori, and A. Strumia, *Higgs mass and vacuum stability in the Standard Model at NNLO*, *JHEP* **08** (2012) 098, [[arXiv:1205.6497](https://arxiv.org/abs/1205.6497)].
- [40] N. Seiberg and E. Witten, *Electric - magnetic duality, monopole condensation, and confinement in $N=2$ supersymmetric Yang-Mills theory*, *Nucl. Phys. B* **426** (1994) 19–52, [[hep-th/9407087](https://arxiv.org/abs/hep-th/9407087)]. [Erratum: *Nucl.Phys.B* 430, 485–486 (1994)].
- [41] C. Vafa and E. Witten, *Restrictions on Symmetry Breaking in Vector-Like Gauge Theories*, *Nucl. Phys. B* **234** (1984) 173–188.
- [42] D. Gaiotto, A. Kapustin, Z. Komargodski, and N. Seiberg, *Theta, Time Reversal, and Temperature*, *JHEP* **05** (2017) 091, [[arXiv:1703.00501](https://arxiv.org/abs/1703.00501)].